

September 2020

NEW MEXICO OZONE ATTAINMENT INITIATIVE PHOTOCHEMICAL MODELING STUDY – 2014 MODELING PLATFORM DEVELOPMENT AND MODEL EVALUATION



RAMBOLL



NEW MEXICO OZONE ATTAINMENT INITIATIVE PHOTOCHEMICAL MODELING STUDY – 2014 MODELING PLATFORM DEVELOPMENT AND MODEL EVALUATION

Project name **New Mexico Ozone Attainment Initiative Photochemical Modeling Study**
Project no. **1690017454**
Recipient **New Mexico Environmental Division**
Document type **Technical Report**
Version **V3.0**
Date **September 2020**
Prepared by **Ralph Morris, Marco Rodriguez, Tejas Shah, Jeremiah Johnson, Jung Chien,
Pradeepa Vennam and Fiona Jiang, Ramboll Environment and Health**

Tom Moore and Mary Uhl, Western States Air Resources Council

Ramboll
7250 Redwood Blvd.
Suite 105
Novato, CA 94945

T +1 415 899 0700
www.ramboll.com

CONTENTS

ACRONYMS and ABBREVIATIONS		viii
1.	INTRODUCTION	1
1.1	NM OAI Project Genesis	1
1.2	Conceptual Model for High Ozone Concentrations in New Mexico	3
1.2.1	Southern New Mexico	3
1.2.2	Bernalillo County and Vicinity	7
1.2.3	Northern New Mexico	8
1.3	Overview of NM OAI Study Modeling Approach	10
1.3.1	WRAP-WAQS 2014 PGM Platform Development Study	11
1.3.2	EPA 2016v1 Modeling Platform	12
1.3.3	Episode Selection	13
1.3.4	Model Selection	13
1.3.5	Domain Selection	14
1.3.6	Base and Future Year Emissions Data	16
1.3.7	Initial and Boundary Conditions Development	16
1.3.8	Diagnostic Sensitivity Analyses	16
1.3.9	Model Performance Evaluation	16
1.3.10	Future Year Base and Control Strategy Modeling	17
1.3.11	Future Year Source Apportionment Modeling	17
2.	2014 WRF METEOROLOGICAL MODELING	18
2.1	WRF Meteorological Model	18
2.2	WRF Horizontal Modeling Domain	18
2.3	WRF Model Configuration	19
2.3.1	Model Vertical Resolution	20
2.3.2	Vertical Coordinate	20
2.3.3	Topographic Inputs	22
2.3.4	Vegetation Type and Land Use Inputs	22
2.3.5	Atmospheric Data Inputs	22
2.3.6	Time Integration	23
2.3.7	Diffusion Options	23
2.3.8	Lateral Boundary Conditions	24
2.3.9	Top and Bottom Boundary Conditions	24
2.3.10	Sea Surface Temperature Inputs	24
2.3.11	Four Dimensional Data Assimilation (FDDA)	24
2.3.12	New Lightning Data Assimilation	24
2.3.13	PBL and LSM Physics Options	24
2.3.14	Remaining WRF Physics Options	25
2.3.15	Application Methodology	26
2.4	WRF Model Evaluation	26
2.4.1	Quantitative Evaluation Using METSTAT	26
2.4.2	Qualitative Evaluations Using PRISM Data	37
2.4.3	Conclusions of 2014 WRF Model Performance	40

3.	BOUNDARY CONDITION INPUTS	41
3.1	WRAP 2014 GEOS-Chem Modeling	41
3.2	2014 GEOS-Chem Model Evaluation	43
4.	2014 EMISSION INPUTS	44
4.1	Available Emissions Inventory Datasets	44
4.2	Development of CAMx Emission Inputs	44
4.2.1	Day-Specific On-Road Mobile Source Emissions	44
4.2.2	Point Source Emissions	45
4.2.3	Area and Non-Road Source Emissions	45
4.2.4	Episodic Biogenic Emissions	45
4.2.5	Wildfires, Prescribed Burns, Agricultural Burns	46
4.2.6	Other Natural Emissions	46
4.2.7	QA/QC of Emissions Processing and Emissions Merging	46
4.2.8	Use of the Plume-in-Grid (PiG) Subgrid-Scale Plume Treatment	47
4.2.9	QA/QC of Model-Ready Emissions	47
4.2.10	Summary of Emissions for 4-km New Mexico Domain	48
5.	DIAGNOSTIC SENSITIVITY TESTS	54
5.1	WRF-CAMx Processing of 2014 WRF Output	54
5.1.1	Treatment of Minimum Kv	54
5.1.2	Layer Collapsing Strategy	54
5.2	CAMx Meteorological Diagnostic Sensitivity Tests	56
5.3	Summary CAMx Diagnostic Sensitivity Tests	63
6.	FINAL MODEL BASE CASE CONFIGURATION	64
6.1	Meteorological Inputs	64
6.2	Emission Inputs	64
6.3	Photochemical Model Inputs	64
6.3.1	PGM Science Configuration and Input Configuration	64
7.	2014 BASE CASE MODELING AND MODEL PERFORMANCE EVALUATION	67
7.1	2014 Base Case Modeling	67
7.2	EPA Model Performance Evaluation Recommendations	67
7.2.1	Overview of EPA Model Performance Evaluation Recommendations	67
7.3	Overview of Evaluation of CAMx 2014 Base Case Procedures	68
7.3.1	Photochemical Model Evaluation Methodology	68
7.3.2	Model Performance Goals and Benchmarks	68
7.3.3	Available Aerometric Data for the Evaluations	69
7.3.4	Atmospheric Model Evaluation Tool (AMET)	69
7.4	Ozone Evaluation Across the 4-km New Mexico Domain	70
7.5	Ozone Evaluation Across New Mexico	71
7.6	Ozone Evaluation in New Mexico Subregions	74
7.7	Ozone Evaluation at Individual New Mexico Monitoring Sites	76
7.8	Ozone Performance Related to Future Year Ozone Projections	83
7.8.1	Bloomfield Top 10 Ozone Performance	84

7.8.2	Desert View Top 10 Ozone Performance	86
7.8.3	Carlsbad Top 10 Ozone Performance	87
8.	SUMMARY AND CONCLUSIONS	88
9.	REFERENCES	90

APPENDIX

Appendix A Time Series of Predicted and Observed MDA8 Ozone Concentrations at Sites in New Mexico

TABLE OF TABLES

Table 1-1.	Lambert Conformal Conic (LCC) projection parameters for the NM OAI Study 36/12/4 modeling domains.	15
Table 1-2.	Grid definitions for CAMx NM OAI Study 2014 36/12/4-km modeling domains.	15
Table 2-1.	WRF 36 level vertical layer structure for the NM OAI study. This is the same WRF layer structure as used in WAQS 2011/2014/2016 and EPA 2016 WRF modeling.	21
Table 2-2.	NM OAI Study 2014 WRF model configuration and comparison with the WRF configuration used in the WRAP-WAQS 2014 and EPA 2014/2015/2016 WRF modeling.	25
Table 2-3.	Meteorological model performance benchmarks for simple and complex conditions.	29
Table 3-1.	2014 GEOS-Chem simulation model configuration used by WRAP whose output is used to define the 2014 day-specific diurnally varying BC inputs for the NM OAI Study photochemical modeling.	41
Table 4-1.	2014 base case biogenic emissions summary by month (in short tons per day) for the 4-km New Mexico domain.	46
Table 4-2.	New Mexico 4-km domain emissions processing categories.	49
Table 4-3.	2014 base case anthropogenic emissions summary (episode average short tons per day) by source category for the 4-km New Mexico domain.	50
Table 5-1.	WRF to CAMx vertical layer collapsing strategy used in the NM OAI Study.	55
Table 6-1.	Final CAMx model configuration for the NM OAI Study.	66
Table 7-1.	Recommended benchmarks for photochemical model statistics (Source: Emery et al., 2016).	69

Table 7-2.	AQS monitoring sites categorized into subregions of southern New Mexico (orange), Bernalillo County (yellow) and southern New Mexico (blue).	75
Table 7-3.	Region specific NMB and NME values for MDA8 Ozone and MDA8 Ozone when Observed Value is above 60 ppb.	75
Table 7-4.	CAMx 2014 base case model performance statistics for MDA8 Ozone concentrations by monitoring site for summer (May15-Aug) modeling period.	77
Table 7-5.	2014 Base Case model performance statistics of MDA8 Ozone with an observed ozone 60 ppb cut-off by monitoring site for summer (May 15-Aug) modeling period.	78
Table 7-6.	Predicted and observed MDA8 ozone concentrations (ppb) at Bloomfield for CAMx 2014 base case for modeled ranked 36 highest MDA8 ozone concentrations.	85
Table 7-7.	Predicted and observed MDA8 ozone concentrations (ppb) at Desert View for CAMx 2014 base case for modeled ranked 36 highest MDA8 ozone concentrations.	86
Table 7-8.	Predicted and observed MDA8 ozone concentrations (ppb) at Carlsbad for CAMx 2014 base case for modeled ranked 36 highest MDA8 ozone concentrations.	87

TABLE OF FIGURES

Figure 1-1.	Trends in observed ozone DVs between 2013 and 2018 at 7 monitoring sites in New Mexico (Source: https://www.env.nm.gov/air-quality/wp-content/uploads/sites/2/2019/10/OAI_Presentation_09262019.pdf).	2
Figure 1-2.	7 counties in New Mexico under the jurisdiction of the NMED whose observed 2016-2018 ozone DVs are at or exceed 95% of the 2015 ozone NAAQS (70 ppb) (Source: https://www.env.nm.gov/air-quality/wp-content/uploads/sites/2/2019/10/OAI_Presentation_09262019.pdf).	2
Figure 1-3.	Contributions of geographic regions (including Boundary Conditions) to the 2011 and 2025 ozone Design Values at Desert View monitoring site in Dona Ana County in southern New Mexico (left) and 12/4-km modeling domain and definition of source regions (right).	4
Figure 1-4.	Contributions of Source Sector emissions within the 12/4-km modeling domain to the 2011 and 2025 ozone Design	

	Value at Desert View monitoring site (top) and top ten Source Group contributions (bottom).	5
Figure 1-5.	Contributions of major Source Sectors in New Mexico to 2011 (top) and 2025 (bottom) ozone DVs at nine monitoring sites in Southwestern New Mexico.	6
Figure 1-6.	Contributions to ozone in Albuquerque during the June and July 2017 modeling episodes.	7
Figure 1-7.	Linear regression of the annual 4 th highest MDA8 ozone concentrations and mean July through August NCEP/NCAR Reanalysis 500 hPa (or 500 mb) heights for the DM/NFR NAA region at the Rocky Flats North (RFNO) monitoring site for the years 1995 to 2018.	9
Figure 1-8.	Correlation between 500 hPa heights and elevated ozone concentrations for monitoring sites in the western U.S.	10
Figure 1-9.	36-km continental U.S. (36US1) and 12-km western U.S. (12WUS2) modeling domains used in the WRAP-WAQS CAMx 2014v2 modeling platform.	12
Figure 1-10.	NM OAI Study 2014 36/12/4-km PGM and emissions modeling domains.	14
Figure 1-11.	4-km New Mexico modeling domain for PGM and emissions modeling, with locations of New Mexico ozone monitors that were operating during some portion of 2014.	15
Figure 2-1.	WRF 36-km (outer extent), 12-km (d02) and 4-km (d03) modeling domains used in the NM OAI Study.	19
Figure 2-2.	Cross-sections of layer interface heights over the Rocky Mountains for the eta (left panel) and hybrid (right panel) vertical coordinates for the WRF-Based Rapid Refresh (RAP) model. Adapted from Park et al., (2018).	22
Figure 2-3.	Soccer plot comparing WRF/NAM (top) and WRF/ERA5 (bottom) surface wind speed (m/s) model performance against the Simple and Complex Benchmarks for monthly RMSE (y-axis) and Mean Bias (x-axis).	31
Figure 2-4.	Soccer plot comparing WRF/NAM (top) and WRF/ERA5 (bottom) surface wind direction (degrees) model performance against the Simple and Complex Benchmarks for monthly RMSE (y-axis) and Mean Bias (x-axis).	32
Figure 2-5.	Soccer plot comparing WRF/NAM (top) and WRF/ERA5 (bottom) surface temperature (K) model performance against the Simple and Complex Benchmarks for monthly RMSE (y-axis) and Mean Bias (x-axis).	33

Figure 2-6.	Soccer plot comparing WRF/NAM (top) and WRF/ERA5 (bottom) surface humidity (g/kg) model performance against the Simple and Complex Benchmarks for monthly RMSE (y-axis) and Mean Bias (x-axis).	34
Figure 2-7.	Time series plot of predicted and observed (black) daily humidity (g/kg) at Las Cruces International Airport for the WRF/ERA5 (red) and WRF/NAM (blue) simulations.	35
Figure 2-8.	Soccer plot comparing WRF/NAM (top) and WRF/ERA5 (bottom) surface humidity (g/kg) model performance at Las Cruces International Airport against the Simple and Complex Benchmarks for monthly RMSE (y-axis) and Mean Bias (x-axis).	36
Figure 2-9.	May monthly precipitation amounts from PRISM based on observations (left) and predicted by WRF/NAM (middle) and WRF/ERA5 (right).	38
Figure 2-10.	June monthly precipitation amounts from PRISM based on observations (left) and predicted by WRF/NAM (middle) and WRF/ERA5 (right).	38
Figure 2-11.	July monthly precipitation amounts from PRISM based on observations (left) and predicted by WRF/NAM (middle) and WRF/ERA5 (right).	39
Figure 2-12.	June monthly precipitation amounts from PRISM based on observations (left) and predicted by WRF/NAM (middle) and WRF/ERA5 (right).	39
Figure 4-1.	New Mexico 2014 base case anthropogenic NO _x and VOC emissions by source category.	51
Figure 4-2.	Spatial distribution of the non-point (top) and point (bottom) source oil and gas NO _x (left) and VOC (right) emissions (episode avg tons per day) for New Mexico 4-km domain.	52
Figure 4-3.	Spatial distribution of on-road (top), rail (middle) and non-point/non-road equipment (bottom) NO _x (left) and VOC (right) emissions (episode avg tons per day) for New Mexico 4-km domain.	53
Figure 5-1.	Comparison of sensitivity tests NMB with 60 ppb cutoff spatial plots over NM.	57
Figure 7-1.	Scatter plot of predicted and observed MDA8 ozone across the AQS and CASTNET monitoring sites within the 4-km New Mexico domain during the modeling period (May 15-Aug 31, 2014) for the CAMx 2014 base case simulations.	70

- Figure 7-2. Spatial distribution of CAMx 2014 base case simulation period (May15-Aug 31) site-specific Normalized Mean Bias within the 4-km domain for MDA8 O3 (left) and MDA8 O3 above 60ppb cut-off (right). 71
- Figure 7-3. Scatter plots of predicted and observed MDA8 ozone (left) and MDA8 ozone when observed value is above 60 ppb cut-off (right) across the AQS monitoring sites in New Mexico during modeling period (May15-Aug 31) for the CAMx 2014 base case simulations. 72
- Figure 7-4. Soccer plots of MDA8 ozone (left) and MDA8 ozone when observed value is above a 60 ppb cut-off (right) with monthly average NMB and NME values across sites in New Mexico. The dashed lines represents the performance goals and criteria. 73
- Figure 7-5. Spatial distribution of site-specific Normalized Mean Bias for sites in New Mexico and the CAMx 2014 May-August base case simulation for all MDA8 ozone data (left) and MDA8 ozone with observed value above a 60 ppb cut-off (right). 73
- Figure 7-6. Time series of predicted and observed MDA8 ozone concentrations (ppb; top) and daily bias (ppb; bottom) at Bloomfield monitoring site (Site ID: 350450009). 79
- Figure 7-7. Time series of predicted and observed MDA8 ozone concentrations (ppb; top) and daily bias (ppb; bottom) at Coyote Ranger monitoring site (Site ID: 350390026). 80
- Figure 7-8. Time series of predicted and observed MDA8 ozone concentrations (ppb; top) and daily bias (ppb; bottom) at South Valley monitoring site (Site ID: 350010029). 81
- Figure 7-9. Time series of predicted and observed MDA8 ozone concentrations (ppb; top) and daily bias (ppb; bottom) at Desert View monitoring site (Site ID: 350130021). 82
- Figure 7-10. Time series of predicted and observed MDA8 ozone concentrations (ppb; top) and daily bias (ppb; bottom) at Carlsbad monitoring site (Site ID: 350151005). 83

ACRONYMS AND ABBREVIATIONS

3SAQS	Three-State Air Quality Study
AIRS	Aerometric Information Retrieval System
AMET	Atmospheric Model Evaluation Tool
APCA	Anthropogenic Precursor Culpability Assessment
AQ	Air Quality
AQS	Air Quality System
BC	Boundary Condition
BLM	Bureau of Land Management
CAMx	Comprehensive Air-quality Model with extensions
CARB	California Air Resources Board
CASTNet	Clean Air Status and Trends Network
CB6r2	Carbon Bond mechanism version 6, revision 2
CMAQ	Community Multiscale Air Quality modeling system
CONUS	Continental United States
CPC	Center for Prediction of Climate
CSAPR	Cross State Air Pollution Rule
CSN	Chemical Speciation Network
EC	Elemental Carbon Fine Particulate Matter
ECMWF	European Center for Medium Range Weather Forecasting
EGU	Electrical Generating Units
EIS	Environmental Impact Statement
EPA	Environmental Protection Agency
ERA5	ECMWF global hourly meteorological forecasts at 30-km
FB	Fractional Bias
FE	Fractional Error
FRM	Federal Reference Method
GCM	Global Chemistry Model
GEOS-Chem	Goddard Earth Observing System (GEOS) global chemistry model
GIRAS	Geographic Information Retrieval and Analysis System
IMPROVE	Interagency Monitoring of PROtected Visual Environments
IWDW	Intermountain West Data Warehouse
LCC	Lambert Conformal Conic projection
LSM	Land Surface Model
MADIS	Meteorological Assimilation Data Ingest System
MATS	Modeled Attainment Test Software
MCIP	Meteorology-Chemistry Interface Processor
MEGAN	Model of Emissions of Gases and Aerosols in Nature
MNGE	Mean Normalized Gross Error
MNB	Mean Normalized Bias
MNE	Mean Normalized Error
MOVES	Motor Vehicle Emissions Simulator
MOZART	Model for OZone And Related chemical Tracers
MPE	Model Performance Evaluation
MSKF	Multi-Scale Kain-Fritsch Cumulus Parameterization
NAAQS	National Ambient Air Quality Standard

NAM	North American Mesoscale Forecast System
NCAR	National Center for Atmospheric Research
NCEP	National Center for Environmental Prediction
NCDC	National Climatic Data Center
NEI	National Emissions Inventory
NEPA	National Environmental Policy Act
NH ₄	Ammonium Fine Particulate Matter
NMB	Normalized Mean Bias
NME	Normalized Mean Error
NMED	New Mexico Environmental Division
NO ₂	Nitrogen Dioxide
NO ₃	Nitrate Fine Particulate Matter
NOAA	National Oceanic and Atmospheric Administration
OA	Organic Aerosol Fine Particulate Matter
OAI	Ozone Attainment Initiative
OC	Organic Carbon Fine Particulate Matter
OSAT	Ozone Source Apportionment Technology
PAVE	Package for Analysis and Visualization
PBL	Planetary Boundary Layer
PGM	Photochemical Grid Model
PM	Particulate Matter
PPB	Parts Per Billion
PPM	Piecewise Parabolic Method
QA	Quality Assurance
QC	Quality Control
RMP	Resource Management Plan
RRF	Relative Response Factor
SCC	Source Classification Code
SIP	State Implementation Plan
SMOKE	Sparse Matrix Kernel Emissions modeling system
SNMOS	Southern New Mexico Ozone Study
SOA	Secondary Organic Aerosol
SO ₂	Sulfur Dioxide
SO ₄	Sulfate Fine Particulate Matter
TCEQ	Texas Commission on Environmental Quality
UNC-IE	University of North Carolina Institute for the Environment
USFS	United States Forest Service
VERDI	Visualization Environment for Rich Data Interpretation
VMT	Vehicle Miles Traveled
WBD	Wind Blown Dust model
WAQS	Western Air Quality Study
WESTAR	Western States Air Resources Council
WestJumpAQMS	West-Wide Jump-Start Air Quality Modeling Study
WESTUS	Western United States
WRAP	Western Regional Air Partnership
WGA	Western Governors' Association
WRF	Weather Research Forecast model

1. INTRODUCTION

This document presents the development and evaluation of a photochemical grid model (PGM) modeling platform for the New Mexico (NM) Ozone Attainment Initiative (OAI) Photochemical Modeling Study (“NM OAI Study”). The New Mexico Environmental Division (NMED) has contracted with a team consisting of Western States Air Resources Council (WESTAR) and Ramboll US Corporation to conduct the NM OAI Study. The NM OAI Study leverages the 2014 PGM modeling platform developed by the Western Regional Air Partnership (WRAP) in the Western Air Quality Study (WAQS) and enhances it by adding a 4-km grid resolution modeling domain covering New Mexico and adjacent regions. Future year modeling, source apportionment and control measure evaluation are planned to assist the NMED in ozone air quality planning for the state.

1.1 NM OAI Project Genesis

The NMED Air Quality Bureau has authority over air quality management activities throughout the state of New Mexico, with the exception Bernalillo County and Tribal Lands. The City of Albuquerque/Air Quality Division has authority in Bernalillo County and, except for where Tribal Implementation Plans have been approved, EPA oversees air quality issues in Tribal Lands. The New Mexico Air Quality Control Act (NMAQCA) requires the NMED to develop a plan to address elevated ozone levels when air quality is within 95% of the ozone NAAQS (74-3-5.3, NMSA 1978¹). The ozone NAAQS was revised in 2015 with a threshold of 0.070 ppm (70 ppb) with the relevant metric being the ozone Design Value (DV) that is expressed as the three-year average of the fourth highest Maximum Daily Average 8-hour (MDA8) ozone concentrations. Figure 1-1 displays the trends in observed ozone DVs at 8 New Mexico monitoring sites from 2013 to 2018 and compares them with the 70 ppb 2015 ozone NAAQS (red line) and 95% of the 70 ppb NAAQS (i.e., ≥ 67 ppb; black line). This results in 7² counties in New Mexico under NMED jurisdiction with measured 2016-2018 ozone DVs at or exceeding 95% of the 70 ppb ozone NAAQS, as shown in Figure 1-1.

¹ <https://law.justia.com/codes/new-mexico/2017/chapter-74/article-2/section-74-2-5.3/>

² 8 total counties in New Mexico if you also include Bernalillo County whose air quality is under the jurisdiction of the City of Albuquerque.

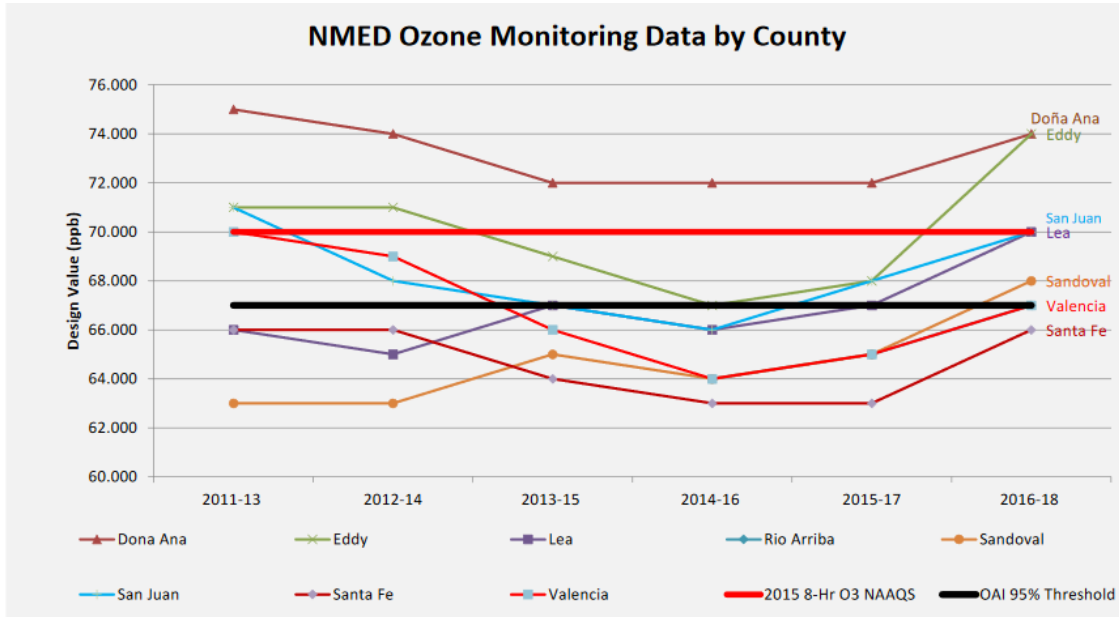
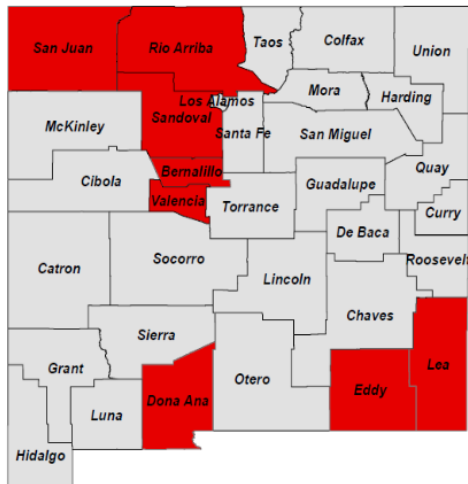


Figure 1-1. Trends in observed ozone DVs between 2013 and 2018 at 7 monitoring sites in New Mexico (Source: https://www.env.nm.gov/air-quality/wp-content/uploads/sites/2/2019/10/OAI_Presentation_09262019.pdf).



*Parallel planning is occurring for Bernalillo County through the Albuquerque/Bernalillo County Department of Environmental Health

- Counties within 95% of the standard:
 - San Juan (Navajo Lake, 70 ppb)
 - Doña Ana (several monitors, 74 ppb)
 - Eddy (Carlsbad, 74 ppb)
 - Lea (Hobbs, 70 ppb)
 - Rio Arriba (Coyote, 67 ppb)
 - Sandoval (Bernalillo, 68 ppb)
 - Valencia (Los Lunas, 67 ppb)

1

Figure 1-2. 7 counties in New Mexico under the jurisdiction of the NMED whose observed 2016-2018 ozone DVs are at or exceed 95% of the 2015 ozone NAAQS (70 ppb) (Source: https://www.env.nm.gov/air-quality/wp-content/uploads/sites/2/2019/10/OAI_Presentation_09262019.pdf).

To address the high observed ozone concentrations in New Mexico, the NMED has embarked on an Ozone Attainment Initiative (OAI³) to protect the ozone attainment status of the state and ensure health and welfare of the residents of the state for future generations. The OAI was initiated in Spring 2018. As part of the OAI, NMED released a Request for Proposal (RFP#20 667 4040 0001) for the NM OAI Study and the NM OAI Study PGM modeling was awarded to a contracting team of WESTAR and Ramboll. .

1.2 Conceptual Model for High Ozone Concentrations in New Mexico

There are three interrelated but distinct Conceptual Models of ozone formation within New Mexico: southern New Mexico, Bernalillo County and surrounding areas, and northern New Mexico. All three regions share the attribute that ozone transport dominates ozone concentrations on all days. Days with the highest local ozone formation are typically hot summer days with slow winds and without an excessive amount of precipitation (summer monsoon).

1.2.1 Southern New Mexico

Ozone at monitoring sites in southern New Mexico, including Dona Ana, Eddy and Lea Counties, is dominated by ozone transport from outside of New Mexico. This transport includes long-range transport from the remainder of U.S. and global sources (e.g., Central America and Asia) as well as medium-range transport from Texas and Mexico. Current year on-road mobile source emissions tend to be the largest contributing Source Sector within southern New Mexico and nearby areas, with non-road mobile and O&G sources also contributing. With the exception of emissions from Mexico, the contributions of Electrical Generating Units (EGU) and other large industrial point sources tends to be smaller than the other Source Sectors.

The Southern New Mexico Ozone Study (SNMOS⁴) conducted CAMx ozone modeling for a 2011 base and 2025 future year using a 12/4-km modeling domain, as shown in the right panel of Figure 1-3. SNMOS found that a vast majority of ozone in southern New Mexico is due to ozone transport from outside of New Mexico. For example, the left panel in Figure 1-3 displays the 2011 and 2025 ozone contributions to the ozone Design Value (DV) at the Desert View monitoring site in Dona Ana County by geographic regions within the 12/4-km PGM modeling domain shown in the right panel in Figure 1-3. Only 3 percent of the 2011 ozone DV at the Desert View monitor in Dona Ana County is due to anthropogenic emissions from New Mexico, and New Mexico emissions contribute less than 2 percent of the projected 2025 ozone DV at Desert View (not shown).

³ <https://www.env.nm.gov/air-quality/o3-initiative/>

⁴ <https://www.wrapair2.org/SNMOS.aspx>

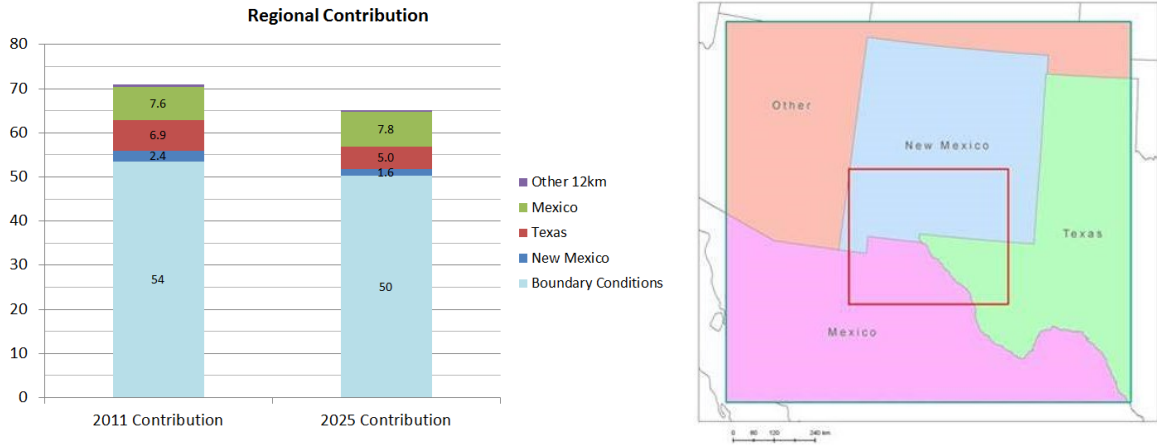


Figure 1-3. Contributions of geographic regions (including Boundary Conditions) to the 2011 and 2025 ozone Design Values at Desert View monitoring site in Dona Ana County in southern New Mexico (left) and 12/4-km modeling domain and definition of source regions (right).

The SNMOS 2011 and 2025 ozone source apportionment modeling also obtained contributions by Source Sector in addition to the four Source Regions depicted in the right panel of Figure 1-3. Figure 1-4 displays the Source Sector contributions to the 2011 and 2025 ozone DV at the Desert View monitor as well as the 10 highest Source Groups (i.e., Source Sector emissions from Source Regions) contributions. On-road mobile sources has the highest contribution to ozone DVs in both 2011 and 2025 (Figure 1-4, top panel), but that is mainly due to on-road mobile source emissions in Texas and Mexico that are the two highest contributing Source Groups (Figure 1-4, bottom panel).

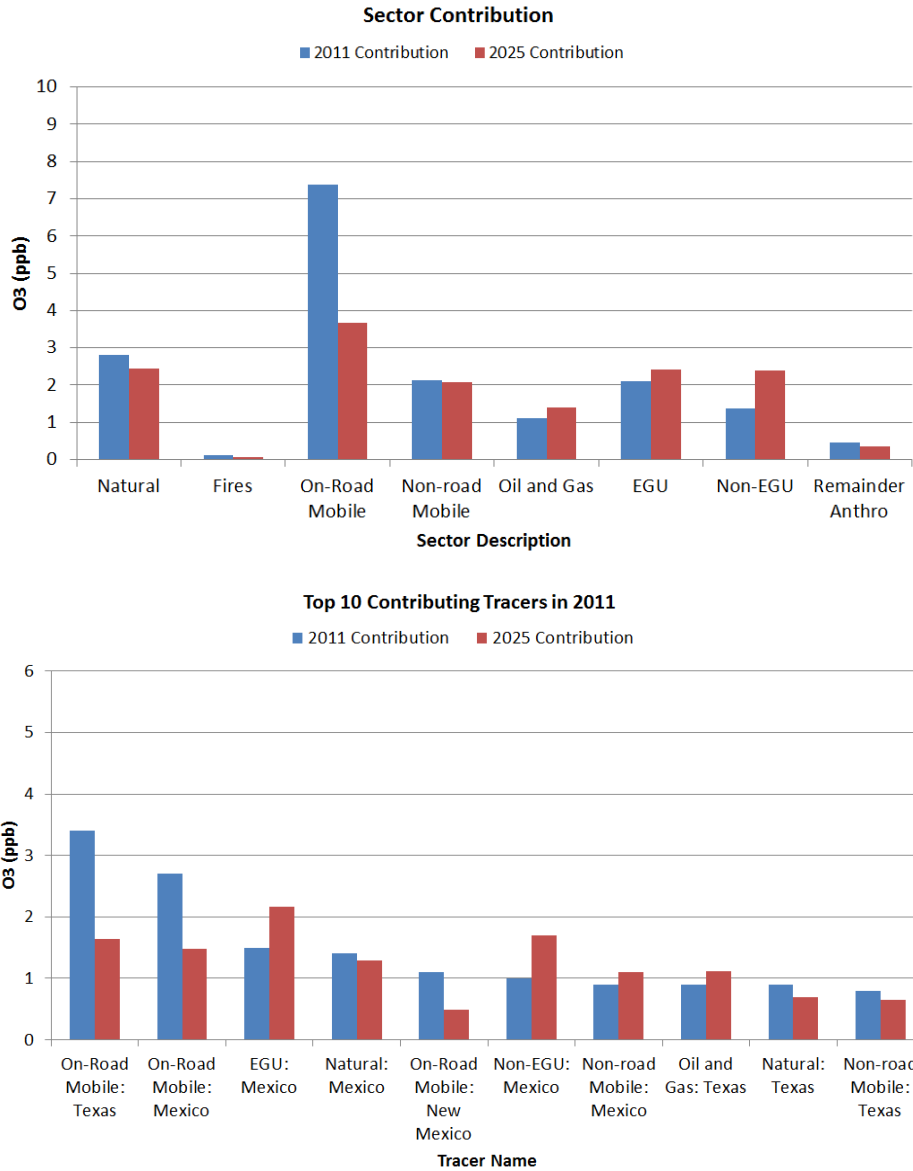


Figure 1-4. Contributions of Source Sector emissions within the 12/4-km modeling domain to the 2011 and 2025 ozone Design Value at Desert View monitoring site (top) and top ten Source Group contributions (bottom).

Figure 1-5 examines the contributions of emissions from New Mexico to 2011 and 2025 ozone DVs at nine monitoring sites in southern New Mexico. With one exception, on-road mobile source emissions are the largest contributing Source Sector in New Mexico to 2011 ozone DVs in southern New Mexico with the on-road mobile contribution at the Solano monitoring site being higher than the others. The one exception is the furthest east Carlsbad monitoring site in Eddy County where O&G emissions are the largest contributing Source Sector in New Mexico due to being within the Permian Basin O&G development region. Although on-road mobile source emissions are the largest

contributor in 2011, it is also the Source Sector whose New Mexico ozone contribution is reduced the most in 2025, by over a factor of two. This is in contrast to O&G whose contribution at the Carlsbad monitoring site is projected to increase between 2011 and 2025, although future year projections of O&G emissions are highly uncertain. In any event, by 2025 the SNMOS estimate that on-road mobile, non-road mobile and O&G Source Sectors in New Mexico will contribute the most, with New Mexico EGU and non-EGU point sources and other anthropogenic emission Source Sectors having relatively lower ozone contributions.

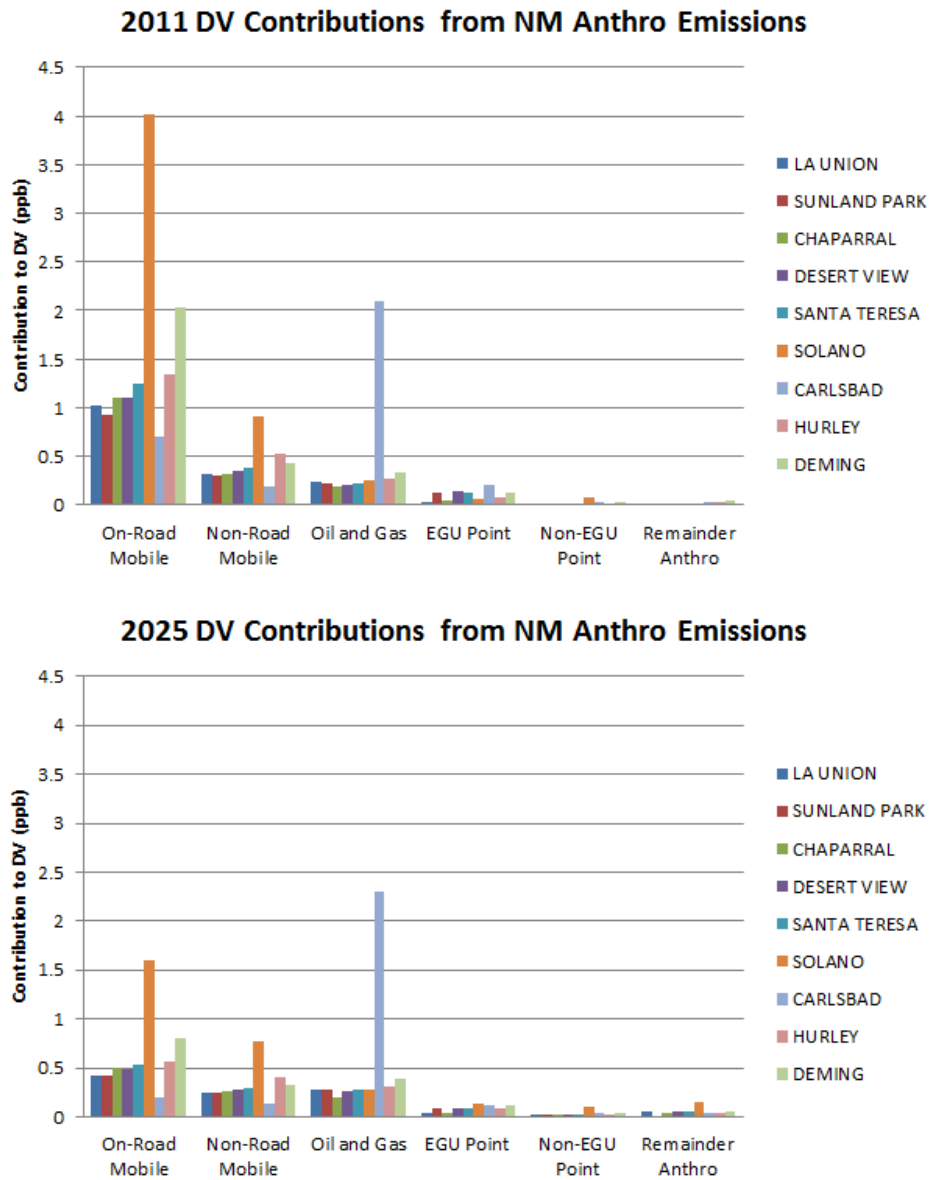


Figure 1-5. Contributions of major Source Sectors in New Mexico to 2011 (top) and 2025 (bottom) ozone DVs at nine monitoring sites in Southwestern New Mexico.

1.2.2 Bernalillo County and Vicinity

High ozone in Bernalillo County and nearby areas is dominated by ozone transport and shares some of same ozone Conceptual Model attributes as northern New Mexico, with the addition of local contributions from a major city (Albuquerque). The City of Albuquerque conducted an ozone modeling study⁵ for two episodes in 2017: June 12-16, 2017 and July 3-14, 2017. The purpose of the study was to better understand the source of high ozone concentrations in Bernalillo County and what types of control strategies, if needed, would be most effective at reducing ozone concentrations in the County. Ozone source apportionment was performed to determine the geographic regions that contributed to elevated ozone concentrations in Albuquerque. Figure 1-6 displays the contributions to ozone concentrations in Albuquerque for the June and July episodes. Anthropogenic emissions from New Mexico contributed 14% and 24% to ozone in Albuquerque during the, respectively, June and July 2017 episodes. And anthropogenic emissions from Bernalillo County accounted for up to 75% of the New Mexico contribution. But sources other than New Mexico anthropogenic emissions (e.g., natural sources and sources outside of New Mexico) were the largest contributor accounting for 86% and 76% of the ozone during the, respectively, June and July episodes.

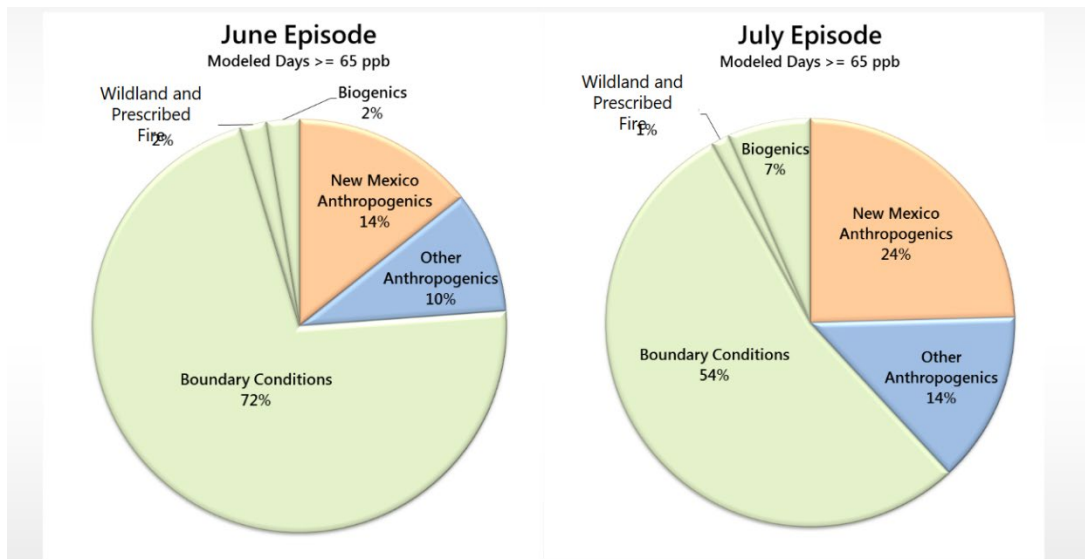


Figure 1-6. Contributions to ozone in Albuquerque during the June and July 2017 modeling episodes.

Although only two short episodes were modeled so any conclusions are limited to those conditions, the City of Albuquerque Ozone Modeling Study concluded as follows:

- Transport from outside of New Mexico is always important and accounts for over half of the ozone in Albuquerque.

⁵ <https://www.cabq.gov/airquality/documents/06-ken-craig-sonoma-technology-inc-ozone-modeling-presentation-10-17-2018-aqcb-meeting.pdf>

- Local emissions in Albuquerque and Bernalillo County are also important with half of the locally generated ozone due to on-road mobile sources in 2017.
- On high ozone days for the two modeled episodes, contributions from major power plants in northern New Mexico were small at sites in Albuquerque.
- Impacts from man-made emissions in western states, including California, are non-negligible.
- Ozone contributions from wildfire smoke were important for both episodes.
- As on-road mobile source emissions are reduced, emissions from non-road and non-mobile sources are becoming increasingly more important.
- NO_x emission controls are more effective at reducing high ozone concentrations in Albuquerque than VOC controls.
- Ozone in Albuquerque is sensitive to emissions from O&G sources throughout New Mexico.

1.2.3 Northern New Mexico

The Four Corners Air Quality Task Force (FCAQTF) conducted a comprehensive modeling study of the region and found, although there are significant contributions due to local power plants and O&G production in the San Juan Basin, ozone transport was by far the largest contributor. The FCAQTF identified numerous local control measures that could help mitigate elevated ozone concentrations in the region.

Reddy and Pfister (2016) and CDPHE and RAQC (2016c) analyzed meteorological factors that contributed to the interannual variability in midsummer ozone concentrations focusing mainly on Utah and Colorado that is also relevant to northern New Mexico. Reddy and Pfister analyzed ozone and meteorology for July during 1995-2013 and found several meteorological variables that were able to explain the years with higher ozone formation conditions. The most powerful meteorological variable for describing high ozone formation potential conditions (i.e. ozone conducive conditions) was the height of the 500 hPa⁶ pressure level. The Denver 2017 ozone SIP modeling study (CDPHE and RAQC, 2016c) extended the analysis to include more recent years and for summer-average conditions. Figure 1-7 shows the relationship between summer-average 500 hPa heights and summer-average ozone at the Rocky Flats North (RFNO) monitoring site northwest of downtown Denver and the years 1995-2018 that shows years with higher 500 hPa heights tend to have higher ozone, and vice versa.

Figure 1-8 displays the correlation between elevated ozone concentrations and 500 hPa heights in the western U.S. Some of the sites in New Mexico are also weakly to moderately correlated to the 500 hPa heights, like the sites in Denver and Utah. Elevated ozone at sites in northern New Mexico show less correlation with 500 hPa heights as it is believed that the large point source NO_x and oil and gas NO_x and VOC emissions in the region swamp the signal. But the presence of a large high pressure over the region, which results in slow winds and hot temperatures, is correlated with high ozone concentrations in northern New Mexico.

⁶ hPa is 100 Pa where Pa is short for Pascal that is a unit of pressure where 500 hPa = 500 mb.

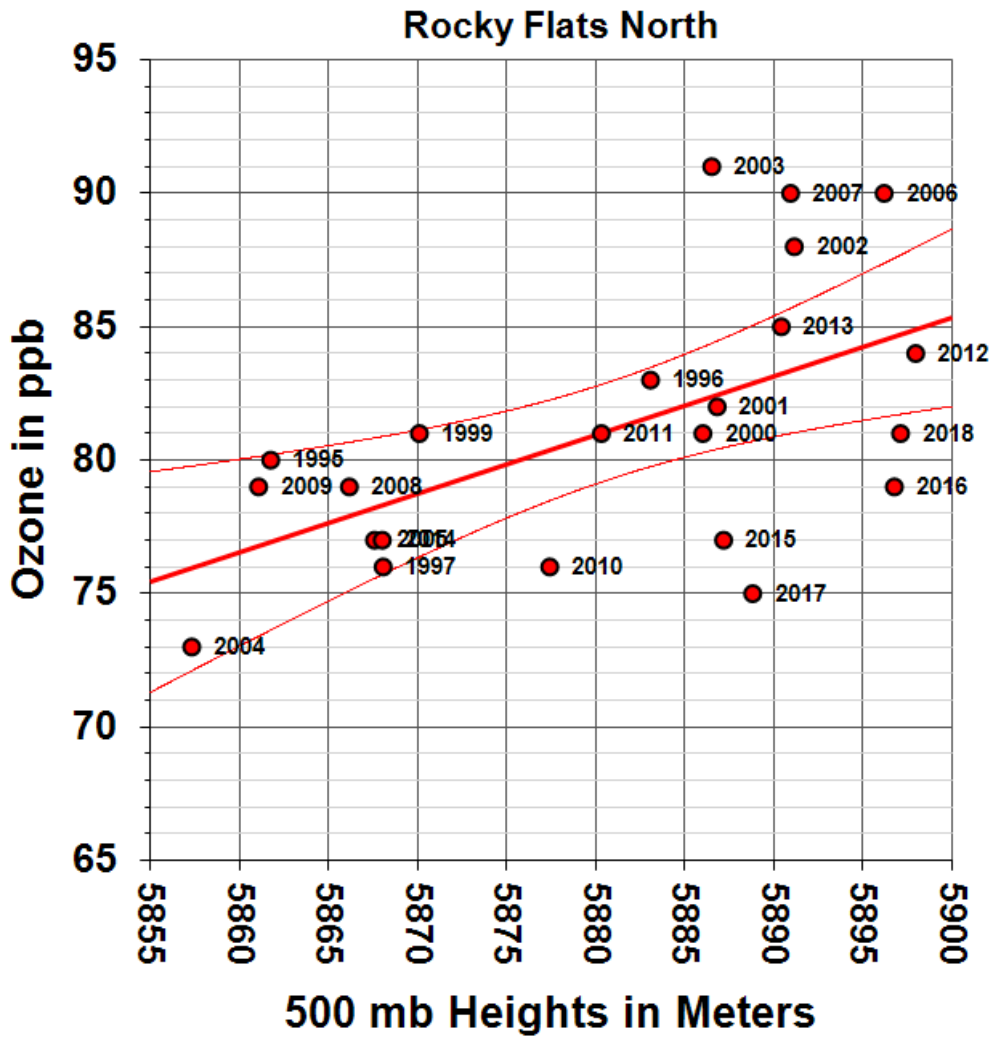


Figure 1-7. Linear regression of the annual 4th highest MDA8 ozone concentrations and mean July through August NCEP/NCAR Reanalysis 500 hPa (or 500 mb) heights for the DM/NFR NAA region at the Rocky Flats North (RFNO) monitoring site for the years 1995 to 2018.

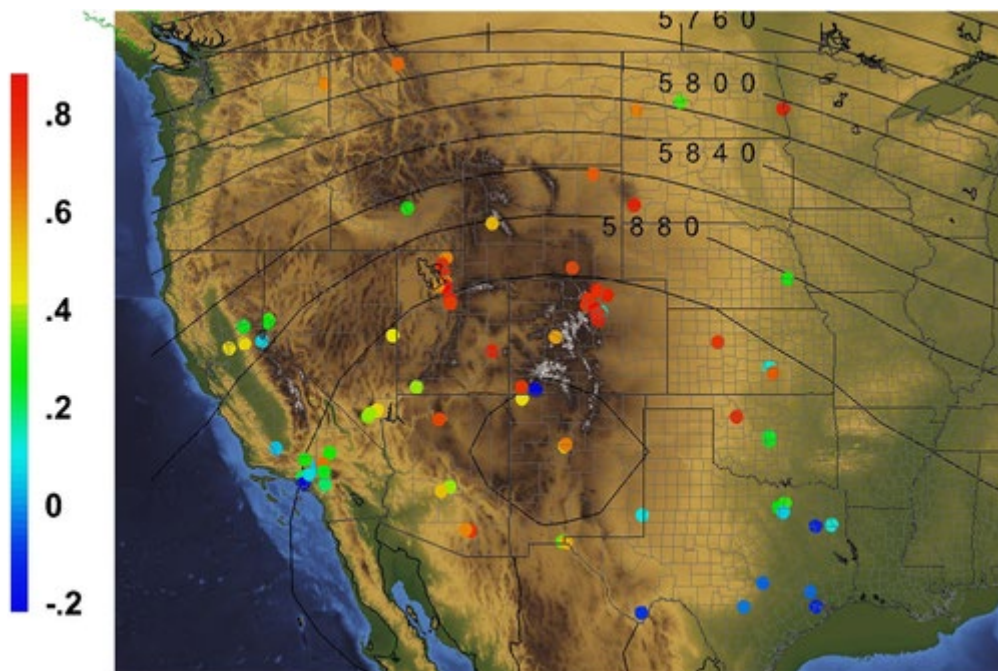


Figure 1-8. Correlation between 500 hPa heights and elevated ozone concentrations for monitoring sites in the western U.S.⁷

1.3 Overview of NM OAI Study Modeling Approach

The procedures used for the NM OAI Study photochemical modeling were described in a detailed Modeling Protocol dated May 19, 2020 (Ramboll and WESTAR, 2020a⁸). A description of the tasks and schedule for completing the NM OAI Study is contained in a Work Plan (Ramboll and WESTAR, 2020b⁹) with presentations, results and reports posted to the NM OAI Study webpage¹⁰ as they are produced.

The NM OAI Study is conducting PGM modeling by enhancing the WRAP-WAQS 2014v2 36/12-km PGM modeling platform¹¹ with the addition of a new 4-km grid resolution domain covering New Mexico and surrounding areas, especially the oil and gas (O&G) production regions in the Permian and San Juan Basins. The NM OAI Study PGM modeling is performing 2014 base year modeling and model performance evaluation. Future year modeling will also be conducted. The NM OAI Study PGM modeling is being conducted in accordance with EPA’s guidance for ozone State Implementation Plan (SIP) attainment demonstration modeling (EPA, 2018d).

⁷ <https://agupubs.onlinelibrary.wiley.com/cms/asset/192a6975-cd1c-4bce-a20a-a2a049ca4df6/jgrd52767-fig-0001-m.png>

⁸ https://www.wrapair2.org/pdf/NM_OAI_Modeling_Protocol_v5.pdf

⁹ https://www.wrapair2.org/pdf/NM_OAI_Work_Plan_v2.pdf

¹⁰ <https://www.wrapair2.org/NMOAI.aspx>

¹¹ <http://views.cira.colostate.edu/wiki#WAQS-2014-Modeling-Platform>

The two main studies that the NM OAI Study modeling is leveraging off of to cost-effectively develop a PGM modeling platform for analyzing ozone issues in New Mexico are discussed below.

1.3.1 WRAP-WAQS 2014 PGM Platform Development Study

The WRAP-WAQS developed an annual 2014 PGM modeling platform to address air quality issues in the western states. The initial use of the WRAP-WAQS 2014 PGM modeling platform is to address the western state technical needs for their Regional Haze SIPs that are scheduled to be submitted to EPA by July 2021. But the platform is designed so it can be used to address visibility, ozone, particulate matter, deposition and other air quality and air quality related values issues in the western states.

An initial WRAP-WAQS 2014v1 PGM modeling platform was developed in 2019 for the CAMx and CMAQ PGMs that is documented in a webpage¹² on the Intermountain West Data Warehouse (IWDW). Additional diagnostic sensitivity tests were conducted to address several model performance issues culminating in the WRAP-WAQS 2014v2 36/12-km CAMx modeling database that was used as the starting point for the NM OAI Study CAMx summer of 2014 36/12/4-km modeling database. The develop of the WRAP-WAQS 2014v2 PGM database and model performance evaluation is available in a webpage¹³ on the IWDW.

The WRAP-WAQS 2014v2 CAMx platform used a 36/12-km grid resolution domains structure as shown in Figure 1-9. Meteorological inputs were based on the WAQS 2014 36/12/4-km WRF meteorological model simulation (Bowden, Talgo and Adelman, 2016¹⁴). The 2014 emissions were based on the 2014 National Emissions Inventory (2014NEI¹⁵) with updates from western states¹⁶. Boundary Condition (BC) inputs were based on a WRAP 2014 GEOS-Chem model simulation.

Because the NM OAI Study requires a 4-km modeling domain for New Mexico, new summer of 2014 36/12/4-km WRF meteorological modeling was conducted that was used to develop 36/12/4-km meteorological inputs for CAMx. The NM OAI Study defined their 36/12-km domains to match WRAP-WAQS 2014v2 36/12-km domains so the WRAP-WAQS 2014v2 36/12-km emission and some other inputs (e.g., BCs) can be directly used in the NM OAI Study PGM modeling.

¹² http://views.cira.colostate.edu/iwdw/docs/waqs_2014v1_shakeout_study.aspx

¹³ https://views.cira.colostate.edu/iwdw/docs/WRAP_WAQS_2014v2_MPE.aspx

¹⁴ http://views.cira.colostate.edu/wiki/Attachments/Modeling/WAQS_2014_WRF_MPE_January2016.pdf

¹⁵ <https://www.epa.gov/air-emissions-inventories/2014-national-emissions-inventory-nei-data>

¹⁶

https://www.wrapair2.org/pdf/WRAP%20Regional%20Haze%20SIP%20Emissions%20Inventory%20Review%20Documentation_for_Docket%20Feb2019.pdf

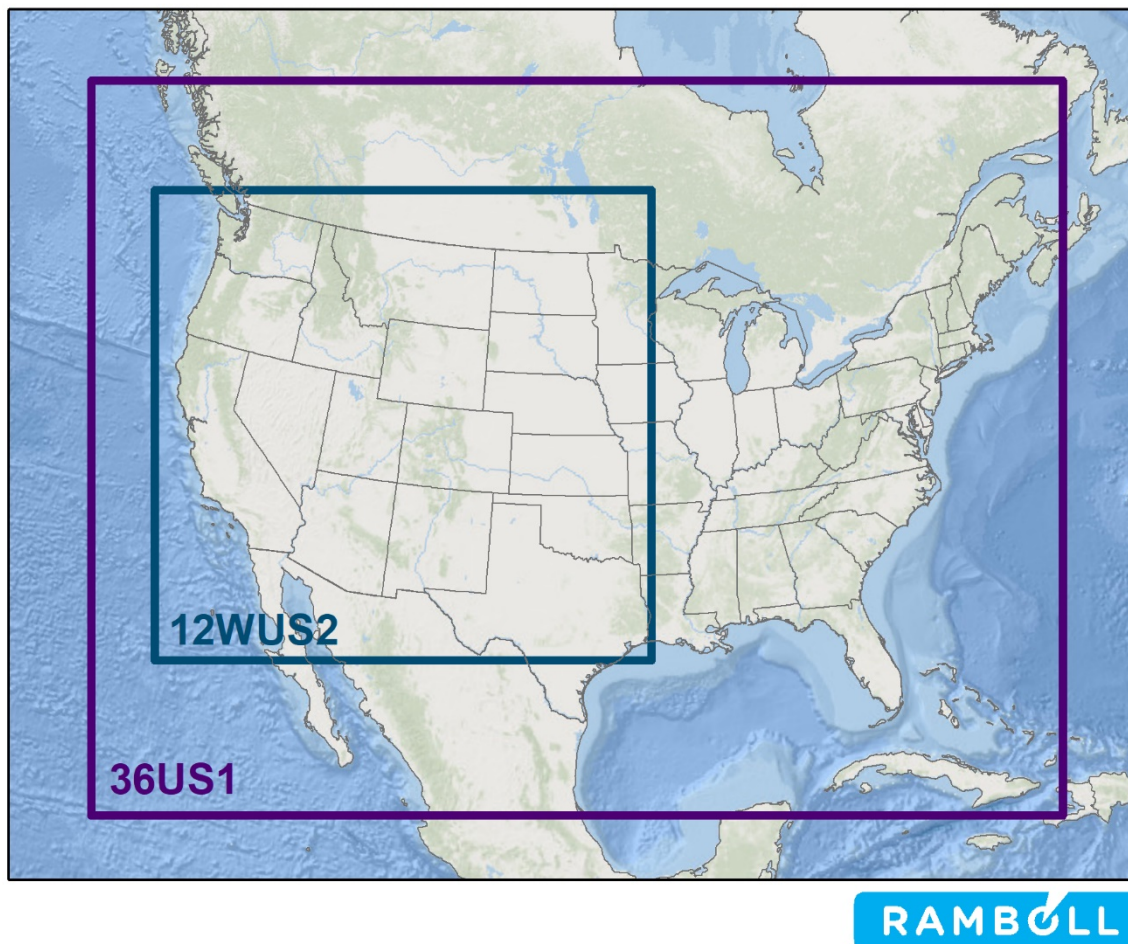


Figure 1-9. 36-km continental U.S. (36US1) and 12-km western U.S. (12WUS2) modeling domains used in the WRAP-WAQS CAMx 2014v2 modeling platform.

1.3.2 EPA 2016v1 Modeling Platform

The EPA, Multi-Jurisdictional Organizations (MJOs), and states conducted a collaborative national 2016 emissions modeling platform¹⁷ (2016 EMP) study to develop a 2016 emissions inventory of comparable quality to the NEI. Separately, EPA developed a 2016 PGM modeling platform that used a 12-km grid resolution continental U.S. domain and an expanded 36-km grid resolution 36US3 domain. EPA has released several versions of their 2016 36/12-km PGM modeling platform with version 1 being the latest version (2016v1).

EPA's 2016v1¹⁸ PGM modeling platform uses the 2016 EMP version 1 emissions¹⁹ from the EPA/MJO/states emissions collaborative study (called 2016fh). It was released in

¹⁷ <http://views.cira.colostate.edu/wiki/wiki/9169>

¹⁸ <https://www.epa.gov/air-emissions-modeling/2016v1-platform>

¹⁹ <http://views.cira.colostate.edu/wiki/wiki/10202>

October 2019 with future year emissions for 2023 and 2028 (2023fh and 2028fh inventories). Since the release of the EPA 2016v1 modeling platform in October 2019, there have been several updates to the emissions, as follows:

1. Updates to 2023 and 2028 EGU emissions to address the accidental dropping of NO_x and SO₂ emissions for a few EGU sources (January 2020). EPA found that source/hour where the heat input, steam load, and gross load are all zero in the hourly CEMs data, SMOKE will set all emissions to zero for that source/hour, even if the CEMs NO_x or SO₂ for that source/hour is not zero.²⁰
2. The 2023 and 2028 Commercial Marine Vessel (CMV) emissions were updated to address hoteling and to match the 2016 days-of-week (February 2020).²¹
3. The WRAP 2016 and 2023 O&G emissions were added as an option to EPA's 2016 and 2023 O&G estimates (April 2020). This resulted in double counting as EPA incorrectly had O&G emissions in files that were not supposed to include O&G emissions (i.e., non-EGU point) so corrections have to be made if the WRAP 2023 O&G emissions are used.
4. New 2016, 2023 and 2028 airport emissions for all airports to correct an error that resulted in airport emissions that are a little more than half of the airport emissions in the initial release of the 2016v1 inventories.
5. The SMOKE processing of the 2016 EGU emissions dropped some EGUs as duplicates when they were not. This appears to be a minor issues for EGUs in the western states (August 2020).

The NM OAI Study plans to use the EPA 2016v1 emission projections in their future year modeling.

1.3.3 Episode Selection

The May-August 2014 modeling period was selected as it has a high quality emissions inventory with western state updates and has a PGM platform already developed from the WRAP-WAQS regional haze modeling that can be leveraged for the NM OAI Study. Details on the episode selection are contained in Chapter 3 of the NM OAI Study Modeling Protocol (Ramboll and WESTAR, 2020a).

1.3.4 Model Selection

Details on the rationale for model selection are provided in Chapter 2 of the NM OAI Study Modeling Protocol (Ramboll and WESTAR, 2020a). The Weather Research Forecast (WRF) prognostic meteorological model was selected. Emissions modeling will be performed using the Sparse Matrix Operator Kernel Emissions (SMOKE) model for most source categories. The Model of Emissions of Gases and Aerosols from Nature (MEGAN v3.1) will be used for biogenic emissions. There are special processors for fires, windblown dust (WBD), lightning NO_x (LNO_x) and oceanic sea salt (NaCl) and Dimethyl Sulfide (DMS) emissions that were used. The 2014 version of the Motor Vehicle Emissions Simulator (MOVES2014b) on-road mobile source emissions model

²⁰ ftp://newftp.epa.gov/Air/emismod/2016/v1/2023fh1_2028fh1_addendum/README_2023fh1_2028fh1_ptegu_addendum.txt

²¹ <http://views.cira.colostate.edu/wiki/wiki/11205>

will be used with SMOKE-MOVES and WRF meteorological data to generate on-road mobile source emissions for the 4-km New Mexico modeling domain.

The Comprehensive Air-quality Model with extensions (CAMx) photochemical grid model (PGM) was used because it supports two-way grid nesting, was used in the WRAP-WAQS regional haze modeling, contains a well-validated ozone source apportionment tool and has a rich and successful history of application to the region.

1.3.5 Domain Selection

The NM OAI Study modeling is using the same 36-km 36US and 12-km 12WUS2 domains as used in the WRAP-WAQS 2014 modeling platform (Figure 1-9). A new 4-km New Mexico domain was added to the 36/12-km domain structure. Figure 1-10 displays the 36/12/4-km domain structure with Figure 1-11 showing the 4-km New Mexico domain. New WRF 2014 36/12/4-km meteorological modeling was conducted to generate finer scale 4-km meteorological conditions for the New Mexico domain and consistent meteorology among the 36/12/4-km domains. The domains use a Lambert Conformal Conic (LCC) projection using the parameters given in Table 1-1 with the definitions of the extent of the 36/12/4-km domains given in Table 1-2. CAMx will be run using the 36/12/4-km domain structure shown in Figure 1-10 using two-way interactive grid nesting.

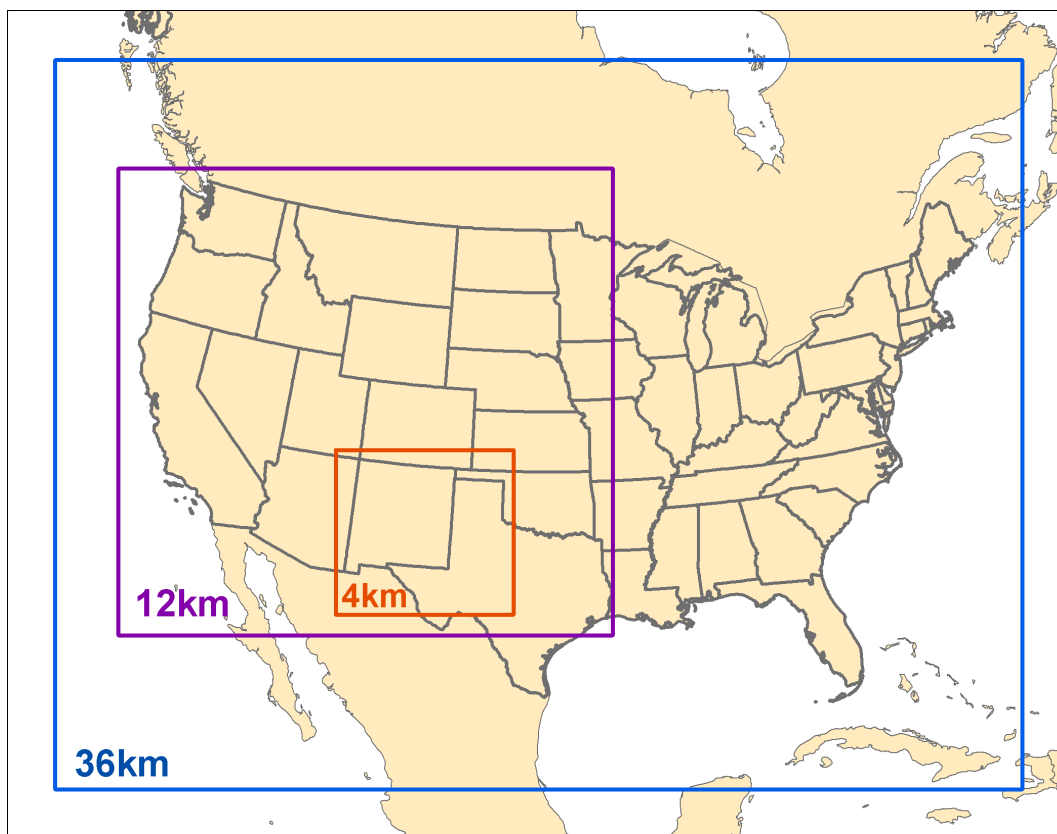


Figure 1-10. NM OAI Study 2014 36/12/4-km PGM and emissions modeling domains.

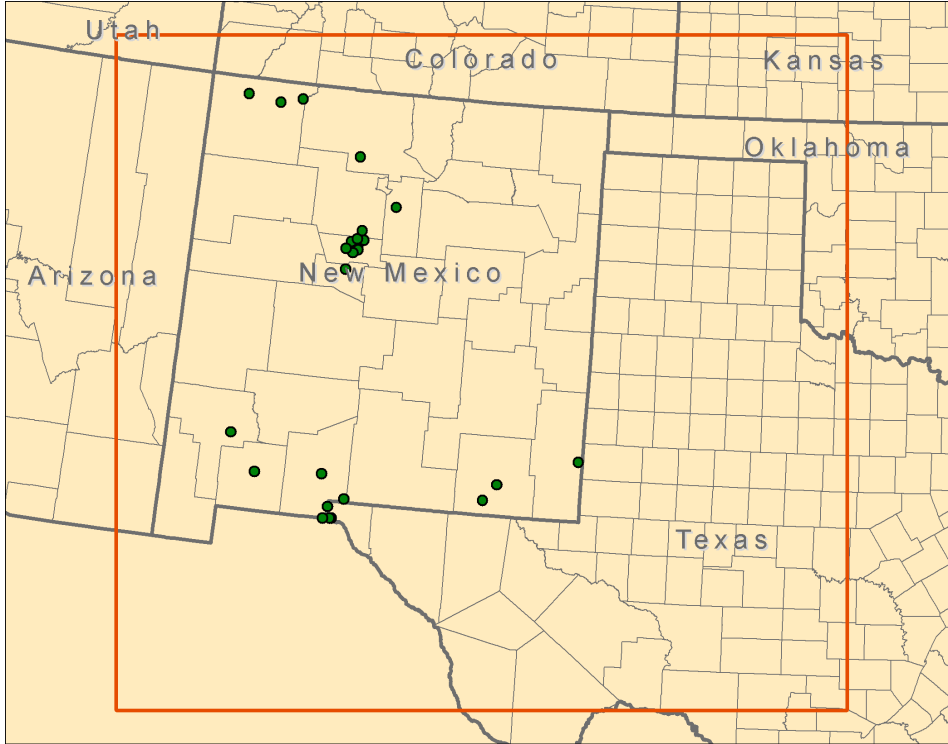


Figure 1-11. 4-km New Mexico modeling domain for PGM and emissions modeling, with locations of New Mexico ozone monitors that were operating during some portion of 2014.

Table 1-1. Lambert Conformal Conic (LCC) projection parameters for the NM OAI Study 36/12/4 modeling domains.

Parameter	Value
Projection	Lambert-Conformal
1st True Latitude	33 degrees N
2nd True Latitude	45 degrees N
Central Longitude	-97 degrees W
Central Latitude	40 degrees N

Table 1-2. Grid definitions for CAMx NM OAI Study 2014 36/12/4-km modeling domains.

Grid	Origin (SW) (km)	Extent (NE) (km)	NX	NY
36-km	(-2736, -2088)	(2592, 1944)	148	112
12-km*	(-2388, -1236)	(336, 1344)	227	215
4-km*	(-1192, -1120)	(-212, -212)	245	227

*Definition includes outer row/column of buffer cells required by CAMx for nested domains

1.3.6 Base and Future Year Emissions Data

The 2014 base year emissions data were based on the WRAP-WAQS 2014v2 emissions that were in turn based on the 2014NEIv2 with updates from western states. New emissions were generated for natural emission sources (e.g., biogenic and LNOx). Future year emissions are based on the EPA 2016v1 modeling platform. The 2014, 2023 and 2028 emissions for New Mexico were reviewed by NMED and updated to address their comments.

1.3.7 Initial and Boundary Conditions Development

The first two-weeks of May were run on the 36/12/4-km domains to spin-up the model before the first high ozone day in New Mexico (68 ppb on May 17). This washes out the influence of the initial concentrations (IC) before elevated ozone concentrations occur in New Mexico.

Boundary conditions (BC) for the outer 36-km 36US domain were based on a 2014 simulation of the GEOS-Chem global chemistry model conducted by WRAP processed by the GC2CAMx converter. The result is day-specific diurnally varying BCs for the lateral boundaries around the 36-km 36US modeling domain. The top BC (TopCon) was based on a zero-gradient assumption where concentrations above the top of the model (above 50 mb, or ~19-km above sea level) are assumed to be the same as in the top vertical layer of CAMx.

Chapter 3 has more details on the development of the 2014 CAMx BC inputs. Because of uncertainties in international emissions and their projections, the 2014 BCs will be held constant for the future year modeling.

1.3.8 Diagnostic Sensitivity Analyses

The NM OAI Study conducted four diagnostic sensitivity tests for the CAMx 2014 36/12/4-km base case that compared the CAMx ozone performance for four alternative meteorological inputs. The NM OAI Study conducted two WRF 2014 36/12/4-km WRF simulations that used different analysis fields as input. The two 2014 36/12/4-km WRF outputs were processed with WRFCAMx using two different options for vertical turbulent exchange (i.e., vertical mixing) coefficients (Kv or Kz). This resulted in four different CAMx meteorological inputs that were evaluated using CAMx diagnostic sensitivity tests that are described in Chapter 5.

1.3.9 Model Performance Evaluation

The NM OAI Study CAMx 2014 36/12/4-km base case simulation Model Performance Evaluation (MPE) followed EPA's MPE recommendations in their ozone modeling guidance (EPA, 2018a) and other sources (e.g., Simon, Baker and Phillips, 2012; Emery et al., 2016). The CAMx 2014 36/12/4-km base case simulation MPE focuses on ozone model performance within the 4-km New Mexico domain, and especially within New Mexico. The CAMx 2014 MPE is presented in Chapter 7.

1.3.10 Future Year Base and Control Strategy Modeling

Future year modeling for ozone will be performed using the EPA 2016v1 platform 2028 emission projections. A CAMx future year 36/12/4-km base case simulation will be conducted and used to project future year ozone design values (DVs). The procedures to calculate projected ozone DVs will follow EPA's latest guidance (EPA, 2018d). These procedures use the modeling results in a relative fashion to scale the current year observed 8-hour ozone Design Values (DVCs) to project future year ozone Design Values (DVs). The scaling factors are called Relative Response Factors (RRFs) and are the ratio of the future-year to current-year modeling results for the 10 highest base year modeled MDA8 ozone days near the monitoring site. EPA has developed the Speciated Modeled Attainment Test (SMAT²²) tool that includes the recommended procedures in the latest EPA guidance for projecting ozone DVs.

The current NM OAI Study also plans to conduct future year emission reduction control strategy sensitivity modeling. The future year modeling will be discussed in a separate report at a later date.

1.3.11 Future Year Source Apportionment Modeling

The current NM OAI Study has plans to conduct future year ozone source apportionment modeling using the CAMx Anthropogenic Precursor Culpability Assessment (APCA) ozone source apportionment tool. The WRAP 2014 GEOS-Chem global chemistry base case, ZROW and NAT simulation will be processed to isolate the contributions of U.S. anthropogenic, International anthropogenic and natural sources to the BCs. Within New Mexico, contributions will be obtained for the major Source Sectors. A NM OAI Study future year ozone source apportionment plan will be developed and discussed with NMED prior to conducting the source apportionment modeling.

²² <https://www.epa.gov/scram/photochemical-modeling-tools>

2. 2014 WRF METEOROLOGICAL MODELING

The NM OAI Study conducted 2014 36/12/4-km WRF meteorological modeling to generate CAMx meteorological inputs for the summer of 2014 and the 36/12/4-km domain structure shown in Figure 1-10.

2.1 WRF Meteorological Model

The Weather Research and Forecasting (WRF) Model is a mesoscale numerical weather prediction system designed to serve both operational forecasting and atmospheric research needs (Skamarock, 2004; 2006; Skamarock et al., 2005; 2008; 2019). The Advanced Research WRF (ARW) version of WRF was used in the NM OAI Study.

This chapter describes the application and evaluation of the WRF meteorological model to generate 2014 36/12/4-km meteorological inputs for CAMx photochemical grid modeling. The WRF model contains separate modules to compute different physical processes, such as surface energy budgets and soil interactions, turbulence, cloud microphysics, and atmospheric radiation. Within WRF, the user has many options for selecting the different schemes for each type of physical process. The WRF Pre-processing System (WPS) generates the initial conditions (ICs) and boundary conditions (BCs) and analysis fields used by WRF, based on topographic datasets, land use information, and larger-scale atmospheric and oceanic models.

2.2 WRF Horizontal Modeling Domain

The PGM (CAMx) 2014 36/12/4-km modeling domains were shown in Figure 1-10 in the previous Chapter. The WRF 2014 36/12/4-km modeling domains are shown in Figure 2-1 and were defined slightly larger than the PGM 36/12/4-km domains so that any modeling artifacts that occur near the WRF boundaries as the BCs come into dynamic balance with the WRF numerical algorithms are not present in the PGM meteorological inputs.

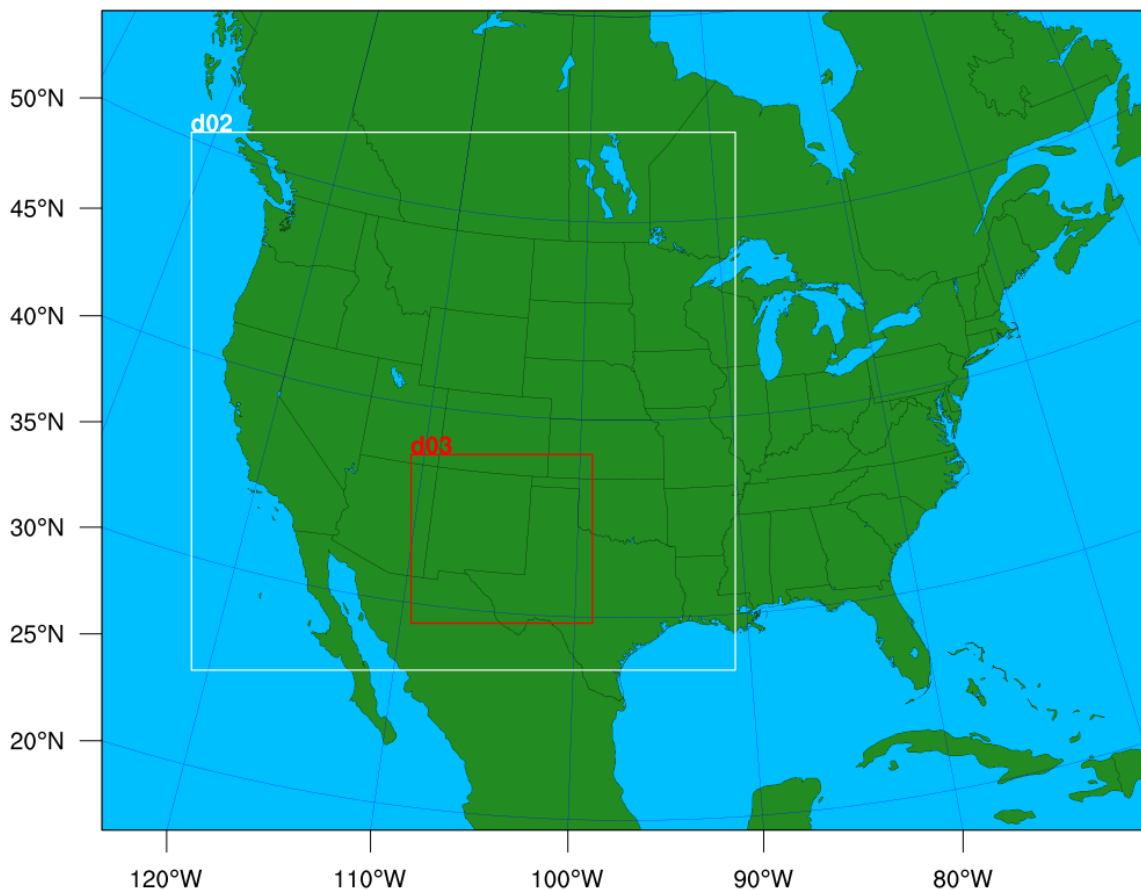


Figure 2-1. WRF 36-km (outer extent), 12-km (d02) and 4-km (d03) modeling domains used in the NM OAI Study.

2.3 WRF Model Configuration

WPS and WRF version 4.2 were used for this modeling analysis. Previous studies utilizing WRF at high resolution over New Mexico, such as the WRAP WestJumpAQMS, WAQS, SNMOS and EPA modeling platform development, have evaluated different configurations of WRF. Table 2-2 presented later in this section summarizes the WRF configurations used in the NM OAI Study and compares it to the WRF configuration used in the WRAP-WAQS 2014 and EPA 2014/2015/2016 WRF modeling. Preliminary analysis of WRAP-WAQS 2014 WRF 12 km model performance in New Mexico showed superior summertime precipitation performance compared to EPA’s 2014 WRF modeling.²³ Therefore, the NM OAI Study WRF application was set to match the WRF physics configuration options used by WRAP-WAQS 2014 WRF modeling, except where noted below.

The NM OAI Study 36/12-km WRF/PGM grid configuration (e.g., horizontal domains and vertical layer structure) was designed to be identical to the WRAP-WAQS 2014

²³ https://www.wrapair2.org/pdf/NM_OAI_Study_Webinar1_2020-05-28.pdf

WRF/PGM grid configuration in order to facilitate the use of data between the two studies.

2.3.1 Model Vertical Resolution

The WAQS 2011/2014 WRF modeling used 36 vertical levels (35 vertical layers) from the surface to a 50 mb (hPa) height (approximately 19-km above sea level). The EPA 2014, 2015 and 2016 WRF modeling also used 35 vertical layers up to a 50 mb height. Table 2-1 displays the 36-vertical layer structure used in the WRAP-WAQS 2011/2014 WRF modeling that was also adopted for the NM OAI Study WRF 2014 36/12/4-km modeling.

2.3.2 Vertical Coordinate

Since its inception, WRF has used the eta (sometimes called sigma or “terrain-following”) vertical coordinate system. One weakness of the eta coordinate is that variations in terrain (especially steep topography) can increase numerical errors in the model. To reduce these errors, Park et al., (2018) developed a hybrid sigma–pressure coordinate that is now included as the default vertical coordinate system for the WRF model (Skamarock et al., 2019).

Figure 2-2 shows vertical cross sections of layer interface heights over the Rocky Mountains during a strong near-surface wind event (Park et al., 2018). The left panel shows the results using the eta or terrain-following vertical coordinate and the right panel shows the same results but using the new hybrid vertical coordinate. The eta coordinate cross-sections show the influence of terrain extending high into the stratosphere. This is a representation of numerical noise and results in erroneous vertical motion in the model. Park et al., (2018) found that the simulation using the eta vertical coordinate produced high turbulence forecasts aloft which were not observed by pilots or soundings. In CAMx, erroneous vertical motion can help transport stratospheric ozone toward the surface. In contrast, the same simulation using the hybrid vertical coordinate produced lower turbulence forecasts that agreed more closely with observations. The hybrid vertical coordinate cross-sections show a gradual damping of terrain effects with increasing altitude until the layer interfaces are flat aloft. The purpose of using the hybrid vertical coordinate in the CAMx is to better represent ozone in the upper troposphere and lower stratosphere. Eliminating this source of numerical noise reduces spurious downward transport of stratospheric ozone.

For the NM OAI Study 2014 36/12/4-km WRF modeling, we used the new hybrid vertical coordinate system and a new version of the WRFCAMx processor that has been updated to use WRF’s hybrid vertical coordinate. The hybrid vertical coordinate system and use of 4-km New Mexico domain are the two biggest differences between the NM OAI Study and WRAP-WAQS 2014 WRF modeling. The WRAP-WAQS 2014 WRF/CAMx modeling did not use the hybrid vertical coordinate system in WRF because at the time it was not supported in the WRFCAMx processor.

Table 2-1. WRF 36 level vertical layer structure for the NM OAI study. This is the same WRF layer structure as used in WAQS 2011/2014/2016 and EPA 2016 WRF modeling.

WRF Layer	Sigma	Pressure (mb)	Height (m)	Thickness (m)
36	0.0000	50.00	19260	2055
35	0.0270	75.65	17205	1850
34	0.0600	107.00	15355	1725
33	0.1000	145.00	13630	1701
32	0.1500	192.50	11930	1389
31	0.2000	240.00	10541	1181
30	0.2500	287.50	9360	1032
29	0.3000	335.00	8328	920
28	0.3500	382.50	7408	832
27	0.4000	430.00	6576	760
26	0.4500	477.50	5816	701
25	0.5000	525.00	5115	652
24	0.5500	572.50	4463	609
23	0.6000	620.00	3854	461
22	0.6400	658.00	3393	440
21	0.6800	696.00	2954	421
20	0.7200	734.00	2533	403
19	0.7600	772.00	2130	388
18	0.8000	810.00	1742	373
17	0.8400	848.00	1369	271
16	0.8700	876.50	1098	177
15	0.8900	895.50	921	174
14	0.9100	914.50	747	171
13	0.9300	933.50	577	84
12	0.9400	943.00	492	84
11	0.9500	952.50	409	83
10	0.9600	962.00	326	82
9	0.9700	971.50	243	82
8	0.9800	981.00	162	41
7	0.9850	985.75	121	24
6	0.9880	988.60	97	24
5	0.9910	991.45	72	16
4	0.9930	993.35	56	16
3	0.9950	995.25	40	16
2	0.9970	997.15	24	12
1	0.9985	998.58	12	12
0	1.0000	1000.00	0	

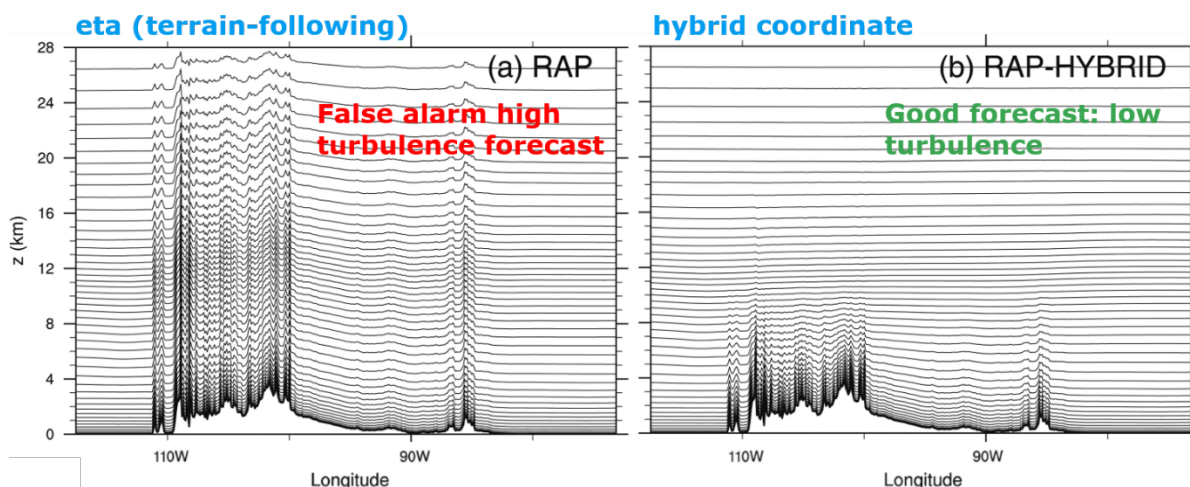


Figure 2-2. Cross-sections of layer interface heights over the Rocky Mountains for the eta (left panel) and hybrid (right panel) vertical coordinates for the WRF-Based Rapid Refresh (RAP) model. Adapted from Park et al., (2018).

2.3.3 Topographic Inputs

Topographic information for WRF was based on a combination of the standard WRF terrain databases and high-resolution terrain. The 36-km 36US domain used the 10-minute global data, the 12-km 12WUS2 domain used the 2-minute data, and the 4-km New Mexico domain used the 30 second data.

2.3.4 Vegetation Type and Land Use Inputs

Vegetation type and land use information used the United States Geological Survey (USGS) land use databases from the most recently released WRF databases provided with the WRF distribution. Standard WRF surface characteristics corresponding to each land use category was employed.

2.3.5 Atmospheric Data Inputs

WRF relies on other model or re-analysis output meteorological fields to provide initial and boundary conditions (IC/BC) and fields for the four-dimensional data assimilation (FDDA). FDDA refers to the nudging of the WRF meteorological fields to observed analysis fields so that the WRF meteorological fields better represent what was observed and prevent the model from drifting away from the observed meteorology. As seen in Table 2-2, both the WRAP-WAQS 2014 and EPA 2014/2015/2016 12-km WRF modeling used the 12-km resolution North American Mesoscale Forecast System (NAM²⁴) analysis fields for IC/BC and analysis nudging (i.e., FDDA).

The NM OAI Study applied WRF with two different analysis fields that were evaluated for their performance against meteorological variables as well as their effect on CAMx ozone model performance. Both the NAM and the ~30-km resolution European Center for Medium-Range Weather Forecasting (ECMWF) Re-Analysis (ERA5²⁵) dataset analysis

²⁴ <https://www.ncdc.noaa.gov/data-access/model-data/model-datasets/north-american-mesoscale-forecast-system-nam>

²⁵ <https://www.ecmwf.int/en/forecasts/datasets/archive-datasets/reanalysis-datasets/era5>

fields were used for IC/BC and FDDA in the two NM OAI Study WRF sensitivity simulations. We have found from previous work that the ERA-Interim (lower resolution predecessor to ERA5) dataset has lower humidity near the surface and higher humidity aloft leading to lower convective available potential energy (CAPE), which lowers overall precipitation rates, especially during the summer Monsoon season that is important for ozone modeling in New Mexico. Many WRF simulations of the southwest U.S. summer Monsoon have featured an over-prediction of summertime (convective) precipitation when the NAM analysis fields are used. The Southern New Mexico Ozone Study (SNMOS) conducted PGM ozone sensitivity modeling using meteorological fields based on WRF simulations using the NAM and ERA analysis fields and found that the PGM results using the WRF/ERA meteorological inputs produced superior ozone performance than when WRF/NAM inputs were used so the SNMOS ended up using the WRF/ERA meteorological inputs.²⁶

The ERA5 is a fairly new analysis fields product that has not been used in WRF modeling as extensively as the ERA fields. We conducted WRF and PGM sensitivity modeling using the NAM and ERA5 analysis fields to determine which configuration provides the best meteorological inputs and best ozone model performance. The ERA5 fields were objectively re-analyzed using meteorological observational data to the higher resolution for the 36-km and 12-km grid domains using the OBSGRID program. These fields are used both to initialize the model and used with analysis nudging FDDA (on the 36/12-km domains) to guide the model to better match the observations.

2.3.6 Time Integration

Third-order Runge-Kutta integration was used ($rk_ord = 3$). The maximum time step, defined for the outer-most domain (36 km) only, is set by evaluating the following equation:

$$dt = \frac{6dx}{F_{map}}$$

Where dx is the grid cell size in km, F_{map} is the maximum map factor (which can be found in the output from REAL.EXE), and dt is the resulting time-step in seconds. For the case of the 36 km RPO domain, $dx = 36$ and $F_{map} = 1.08$, so dt should be taken to be less than 200 seconds. Longer time steps risk CFL errors, associated with large values of vertical velocity, which tend to occur in areas of steep terrain (especially during stable conditions typical of winter). For this WRF run, adaptive time-stepping was used with a maximum timestep of 180s.

2.3.7 Diffusion Options

Horizontal Smagorinsky first-order closure ($km_opt=4$) with sixth-order numerical diffusion and suppressed up-gradient diffusion ($diff_6^{th}_opt=2$) was used.

²⁶ <https://www.wrapair2.org/SNMOS.aspx>

2.3.8 Lateral Boundary Conditions

Lateral boundary conditions was specified from the initialization dataset (i.e., either NAM or ERA5) on the 36-km WRF domain with continuous updates nested from each “parent” domain to its “child” domain, using one-way nesting (feedback=0).

2.3.9 Top and Bottom Boundary Conditions

The implicit Rayleigh dampening for the vertical velocity was used for the top boundary conditions. Consistent with the model application for non-idealized cases, the bottom boundary condition was selected as physical, not free-slip.

2.3.10 Sea Surface Temperature Inputs

The water temperature data for the WRF application was taken from the Fleet Numerical Meteorology and Oceanography Center (FNMOC)²⁷. The FNMOC product has horizontal resolution of about 9-km in the mid-latitudes but is produced *four* times per day using AVHRR satellite sensors and in-situ observations.

2.3.11 Four Dimensional Data Assimilation (FDDA)

Analysis nudging was used for winds, temperature, and humidity on the 36-km and 12-km domains. Both surface and aloft nudging was used but nudging for temperature and mixing ratio was not performed within the boundary layer. Observation nudging was not used, even on the 4-km domain.

2.3.12 New Lightning Data Assimilation

More recently, the assimilation of lightning data in WRF simulations has shown to improve the locations and amounts of convective precipitation. The use of lightning detection networks, such as the National Lightning Detection Network (NLDN), have been used in WRF simulations and used to force deep convection (thunderstorms) when lightning is observed and only allow shallow convection when lightning is not present. The use of the new lightning assimilation approach has been demonstrated to improve both WRF convective precipitation as well as PGM concentration and deposition performance (Heath et al., 2016). The new lightning data assimilation algorithms was not used in the NM OAI Study 2014 WRF modeling for several reasons: (1) it would have to be tested and evaluated and there is insufficient time in the schedule to conduct such diagnostic testing; (2) the NLDN data used to date with the WRF lightning assimilation is a commercial product that is expensive and not within the budget; (3) the implementation of the lightning detection data assimilation in WRF has a flaw that it doesn't distinguish between no lightning detects and missing data and suppresses convection in areas with missing data (e.g., over the Gulf of Mexico); and (4) the lightning detection data assimilation algorithm has not been implemented in the latest versions of WRF so its use would limit the use of other model options.

2.3.13 PBL and LSM Physics Options

As used in the WRAP-WAQS 2014 WRF modeling, the YSU Planetary Boundary Layer (PBL) and Noah Land Surface Model (LSM) physics options were used in the NM OAI

²⁷<https://www.usno.navy.mil/FNMOC>

Study 2014 36/12/4-km WRF modeling. Previous WRF sensitivity modeling for the intermountain west region found the YSU/Noah PBL/LSM schemes produces the most realistic meteorological fields. Note that EPA’s 2014/2015/2016 WRF modeling uses the ACM2 PBL and Pleim-Xiu (PX) LSM schemes (Table 2-2). The WRAP-WAQS tried to evaluate WRF using the ACM2/PX PBL/LSM and found it more difficult to implement and didn’t always run so that annual fields could not be generated. Furthermore, the PX LSM scheme requires each run segment of a WRF run soil moisture inputs to be initialized using the previous WRF run segment PX output so that an annual WRF simulations must be run in series. This contrasts with the Noah LSM scheme that initializes soil moisture based on observations with some spin-up time (typically 12-hours) that allows annual WRF runs to be performed using parallel run segments (e.g., 5.5 day run segments). Thus, annual WRF simulations using the YSU/NOAH PBL/LSM physics options can be completed much faster than when ACM2/PX is used.

2.3.14 Remaining WRF Physics Options

Table 2-2 lists the remaining WRF physics options for the NM OAI Study 2014 36/12/4-km WRF application. These are standard WRF physics options and consistent with the WRF options used in the WRAP-WAQS 2014 and EPA 2014/2015/2016 WRF modeling. Our comparison of 2014 WRAP-WAQS and 2014 EPA WRF modeling for summertime precipitation performance in New Mexico found that the WRAP-WAQS WRF meteorological model performance was better than EPA WRF for most variables. Therefore, we used the same microphysics and cumulus schemes for the NM OAI Study as used in 2014 WRAP-WAQS (Thompson and Multi-Scale Kain-Fritsch, respectively) and most of the same other physics options (Table 2-2).

Table 2-2. NM OAI Study 2014 WRF model configuration and comparison with the WRF configuration used in the WRAP-WAQS 2014 and EPA 2014/2015/2016 WRF modeling.

WRF Option	NM OAI Study	2014 WRAP-WAQS	2014 EPA
Horizontal Domains	36/12/4-km	36/12/4-km	12-km
Vertical Coordinate	Hybrid Sigma	Sigma	Sigma
Microphysics	Thompson	Thompson	Morrison 2
LW Radiation	RRTMG	RRTMG	RRTMG
SW Radiation	RRTMG	RRTMG	RRTMG
Sfc Layer Physics	MM5 similarity	MM5 similarity	MM5 similarity
LSM	Noah	Noah	Pleim-Xiu
PBL scheme	Yonsei University (YSU)	YSU	ACM2
Cumulus	36/12/4-km Multi-scale Kain Fritsch	36/12-km Multi-scale_Kain Fritsch; 4-km None	Kain-Fritsch
BC, IC Analysis Nudging Source	36/12-km NAM & ERA5	36/12-km NAM	12-km NAM
Analysis Nudging Grids	36/12-km	36/12-km	12-km
Obs Nudging	None	4-km	None
Sea Sfc Temp	FNMOG	FNMOG	FNMOG

2.3.15 Application Methodology

The WRF model was executed in 5.5-day blocks initialized at 12Z every five days. Model results were output every 60 minutes, split at twelve (12) hour intervals. Twelve (12) hours of spin-up is included in each 5-day block before the data is used in the subsequent evaluation and PGM meteorological inputs.

2.4 WRF Model Evaluation

Quantitative and qualitative evaluations of the NM OAI Study 2014 WRF 36/12/4-km simulation meteorological performance was conducted for both the WRF/NAM and WRF/ERA5 applications. The quantitative evaluations compare integrated surface hourly meteorological observations with WRF predictions matched by time and location and included the calculation of model performance statistical metrics that were compared against performance benchmarks. The qualitative evaluations compared time series plots of modeled wind speed and wind direction to the observations at specific sites. The qualitative evaluation also compared spatial plots of WRF precipitation estimates against spatial maps of precipitation analysis fields based on observations. The evaluation focuses on the meteorological model performance within the 4-km New Mexico domain.

2.4.1 Quantitative Evaluation Using METSTAT

A quantitative model performance evaluation of the NM OAI Study 2014 WRF modeling was conducted using the publicly available METSTAT software (Ramboll Environ, 2015) evaluation tool. Output from the WRF meteorological model was compared against meteorological observations for sites located in New Mexico. This was carried out both graphically and statistically to evaluate model performance for surface winds, temperatures and humidity. The purpose of these evaluations is to establish a first-order acceptance/rejection of the simulation in adequately replicating the weather phenomena in the study area. Thus, this approach screens for obvious model flaws and errors.

2.4.1.1 Quantitative Statistics

The quantitative analysis was conducted using METSTAT. Statistical measures calculated by METSTAT include observation and prediction means, prediction bias, and prediction error that are given as follows.

Mean Observation (M_o) is calculated using values from all sites for a given time period by Eq. (5-1):

$$M_o = \frac{1}{IJ} \sum_{j=1}^J \sum_{i=1}^I O_j^i \quad (5-1)$$

where O_j^i is the individual observed quantity at site i and time j , and the summations are over all sites (I) and over time periods (J).

Mean Prediction (M_p) is calculated from simulation results that are interpolated to each observation used to calculate the mean observation for a given time period by Eq. (5-2):

$$M_p = \frac{1}{IJ} \sum_{j=1}^J \sum_{i=1}^I P_j^i \quad (5-2)$$

where P_j^i is the individual predicted quantity at site i and time j . Note the predicted mean wind speed and mean resultant direction are derived from the vector-average (for east-west component u and north-south component v), from which the

Bias (B) is calculated as the mean difference in prediction-observation pairings with valid data within a given analysis region and for a given time period by Eq. **(5-3)**:

$$B = \frac{1}{IJ} \sum_{j=1}^J \sum_{i=1}^I (P_j^i - O_j^i) \quad (5-3)$$

Gross Error (E) is calculated as the mean *absolute* difference in prediction-observation pairings with valid data within a given analysis region and for a given time period by Eq. **(5-4)**:

$$E = \frac{1}{IJ} \sum_{j=1}^J \sum_{i=1}^I |P_j^i - O_j^i| \quad (5-4)$$

Note that the bias and gross error for winds are calculated from the predicted-observed residuals in speed and direction (not from vector components u and v). The direction error for a given prediction-observation pairing is limited to range from 0 to $\pm 180^\circ$.

Root Mean Square Error (RMSE) is calculated as the square root of the mean squared difference in prediction-observation pairings with valid data within a given analysis region and for a given time period by Eq **(5-5)**:

$$RMSE = \left[\frac{1}{IJ} \sum_{j=1}^J \sum_{i=1}^I (P_j^i - O_j^i)^2 \right]^{\frac{1}{2}} \quad (5-5)$$

The RMSE, as with the gross error, is a good overall measure of model performance. However, since large errors are weighted heavily (due to squaring), large errors in a small sub-region may produce a large RMSE even though the errors may be small and quite acceptable elsewhere.

2.4.1.2 METSTAT Processing

METSTAT was developed to calculate and graphically present statistics associated with temporally paired meteorological model predictions and observations. The horizontal analysis range can be given for an entire output grid, by a coordinate box, or as a list of specific site identifiers (such as WBAN or AIRS numbers), as labeled on the observational file. This allows for an evaluation at a single site, a subset of specific sites (e.g., within a state) or over an entire regional domain. The program then proceeds to calculate statistics for each hour and for each day of the time window.

The process involves statistical comparisons of model data from the WRF grid cells to observational measurements located with each grid cell. METSTAT evaluates wind speed and direction, air temperature, and air humidity using both bias and error statistics. METSTAT has been widely applied to WRF runs for many years, across many modeling domains. Using a consistent definition of the statistical quantities to be calculated and a consistent methodology for pairing observations in time, METSTAT allows for more straightforward comparisons between model applications in widely different regions and time periods.

2.4.1.3 Statistical Benchmarks

METSTAT calculates statistical performance metrics for bias, error and correlation for surface winds, temperature, and mixing ratio (i.e., water vapor or humidity). To evaluate the performance of a meteorological model simulation for air quality model applications, a number of performance benchmarks for comparison are typically used. Table 2-3 lists the meteorological model performance benchmarks for simple (Emery et al., 2001) and complex (Kemball-Cook et al., 2005) situations. The simple benchmarks were developed by analyzing well-performing meteorological model evaluation results for simple, mostly flat terrain conditions and simple meteorological conditions (e.g., stationary high pressure) that were mostly conducted to support air quality modeling studies (e.g., ozone SIP modeling). The complex benchmarks were developed during the Western Regional Air Partnership (WRAP) regional haze modeling and are performance benchmarks for more complex conditions, such as the complex terrain of the Rocky Mountains and Alaska (Kemball-Cook et al., 2005). McNally (2009) analyzed multiple annual runs that included complex terrain conditions and suggested an alternative set of benchmarks for temperature under more complex conditions. The purpose of the benchmarks is to understand how good or poor the results are relative to other model applications run for the U.S.

The NM OAI Study 2014 WRF application compared the WRF meteorological variables to the benchmarks as an indication of WRF model performance. These benchmarks include bias and error in temperature, wind direction and mixing ratio as well as the wind speed bias and Root Mean Squared Error (RMSE) between the models and databases.

Table 2-3. Meteorological model performance benchmarks for simple and complex conditions.

Parameter	Emery et al. (2001)	Kemball-Cook et al. (2005)	McNally (2009)	Resulting Criteria
Conditions	Simple	Complex	Complex	Complex
Temperature Bias	$\leq \pm 0.5$ K	$\leq \pm 2.0$ K	$\leq \pm 1.0$ K	$\leq \pm 1.0$ K
Temperature Error	≤ 2.0 K	≤ 3.5 K	≤ 3.0 K	≤ 3.0 K
Temperature IOA	≥ 0.8	(not addressed)	(not addressed)	≥ 0.8
Humidity Bias	$\leq \pm 1.0$ g/kg	$\leq \pm 0.8$ g/kg	$\leq \pm 1.0$ g/kg	$\leq \pm 1.0$ g/kg
Humidity Error	≤ 2.0 g/kg	≤ 2.0 g/kg	≤ 2.0 g/kg	≤ 2.0 g/kg
Humidity IOA	≥ 0.6	(not addressed)	(not addressed)	≥ 0.6
Wind Speed Bias	$\leq \pm 0.5$ m/s	$\leq \pm 1.5$ m/s	(not addressed)	$\leq \pm 1.5$ m/s
Wind Speed RMSE	≤ 2.0 m/s	≤ 2.5 m/s	(not addressed)	≤ 2.5 m/s
Wind Speed IOA	≥ 0.6	(not addressed)	(not addressed)	≥ 0.6
Wind Dir. Bias	$\leq \pm 10$ degrees	(not addressed)	(not addressed)	$\leq \pm 10$ degrees
Wind Dir. Error	≤ 30 degrees	≤ 55 degrees	(not addressed)	≤ 55 degrees

The output from the 2014 WRF 4-km domain was compared against meteorological data obtained from the National Climate Data Center's (NCDC) global-scale, quality-controlled DS3505 integrated surface hourly observational (ISHO) data (NOAA-NCDC, 2015) as verification data. Global hourly and synoptic observations are compiled from numerous sources into a single common ASCII format and common data model. The DS3505 database contains records of most official surface meteorological stations from airports, military bases, reservoirs/dams, agricultural sites, and other sources dating from 1901 to the present.

A standard set of statistical metrics from the METSTAT package was used. These metrics were calculated on hourly, daily and monthly time frames for wind speed, wind direction, temperature, and humidity at the surface, using all available observational weather data. The WRF surface meteorological model performance metrics were compared against the simple and complex model performance goals using "soccer plots." Soccer plots use two WRF performance metrics as X-axis and Y-axis values (e.g., temperature bias as X, and temperature error as Y) along with the performance benchmarks. The closer the symbols are to the zero origin, the better the model performance. It is also easy to see when the two WRF performance metrics fall within the benchmark lines.

2.4.1.4 Surface Wind Speed Performance

Figure 2-3 displays the WRF/NAM and WRF/ERA5 wind speed soccer plot that compares monthly measures of wind speed bias and error across surface monitoring sites in New Mexico with the simple and complex benchmarks. The monthly wind speed performance of the two WRF simulations are remarkably similar with both having near zero bias that achieves the simple benchmark ($\leq \pm 0.5$ m/s). The error (RMSE) for the two WRF simulations falls between the simple and complex benchmarks (i.e., between 2.0 and 2.5 m/s) for all four months (May through August).

2.4.1.5 Surface Wind Direction Performance

The monthly wind direction bias and error statistics for the two WRF simulations are also nearly identical with bias values of ~ 5 degrees that achieves the $\leq \pm 5$ degree simple benchmark and error statistics that falls between the 30 degree simple and 50 degree complex benchmarks (Figure 2-4).

2.4.1.6 Surface Temperature Performance

There are differences in the two WRF simulations temperature performance and more differences in the monthly values than seen for winds (Figure 2-5). The WRF/ERA5 simulations has a near zero temperature bias in May and June with the bias and error achieving the simple benchmark for both months. The WRF/NAM has a warm bias for May and June that straddle the simple benchmark upper bound ($+0.5$ K). The two WRF simulations have similar Jul and August performance that have a warm bias of ~ 1.0 K that fails to achieve the simple benchmark. For both WRF simulations, the temperature bias is right at but mostly within the 2.0 K simple benchmark.

2.4.1.7 Surface Humidity Performance

The WRF/ERA5 clearly has better surface humidity performance than WRF/NAM (Figure 2-6). For July and August, the WRF/NAM has a wet bias in July and August of ~ 1.5 g/kg so fails to achieve the simple ($\leq \pm 0.8$ g/kg) and complex ($\leq \pm 1.0$ g/kg) bias benchmarks. The WRF/ERA5 also has a wet bias for July and August that is not as large as WRF/NAM as it is right at the simple benchmark (~ 1.0 g/kg) but achieving the complex benchmark. The WRF/ERA5 also has better humidity error performance in July and August, although both simulations achieve the error performance benchmarks.

The two WRF simulations have better humidity performance in May and June that achieves the simple benchmark, albeit with a moist bias. May is the best performing month with nearly identical humidity model performance with a bias of ~ 0.6 g/kg and error of ~ 0.9 g/kg. In June, the WRF/ERA5 humidity performance is slightly better than WRF/NAM.

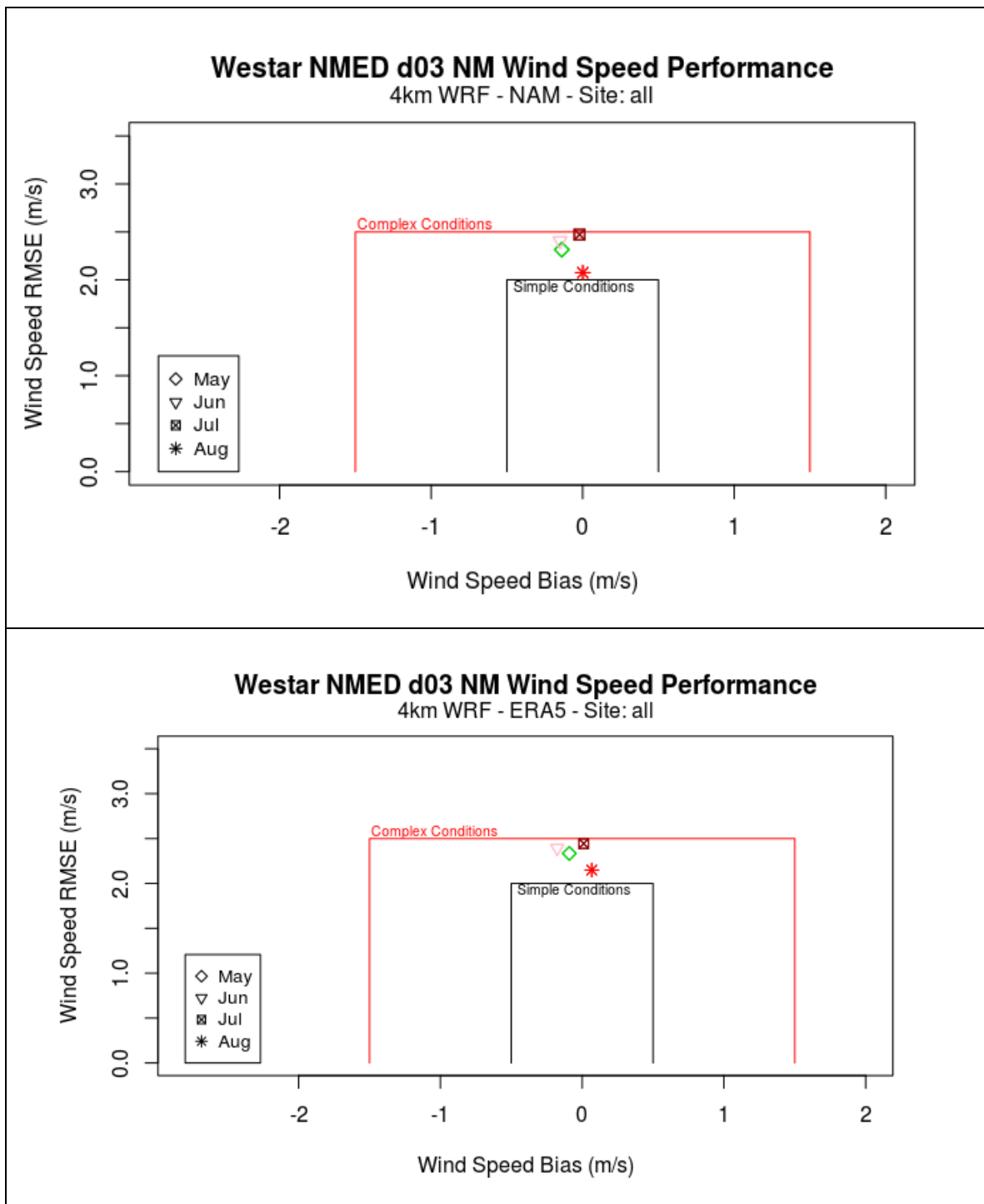


Figure 2-3. Soccer plot comparing WRF/NAM (top) and WRF/ERA5 (bottom) surface wind speed (m/s) model performance against the Simple and Complex Benchmarks for monthly RMSE (y-axis) and Mean Bias (x-axis).

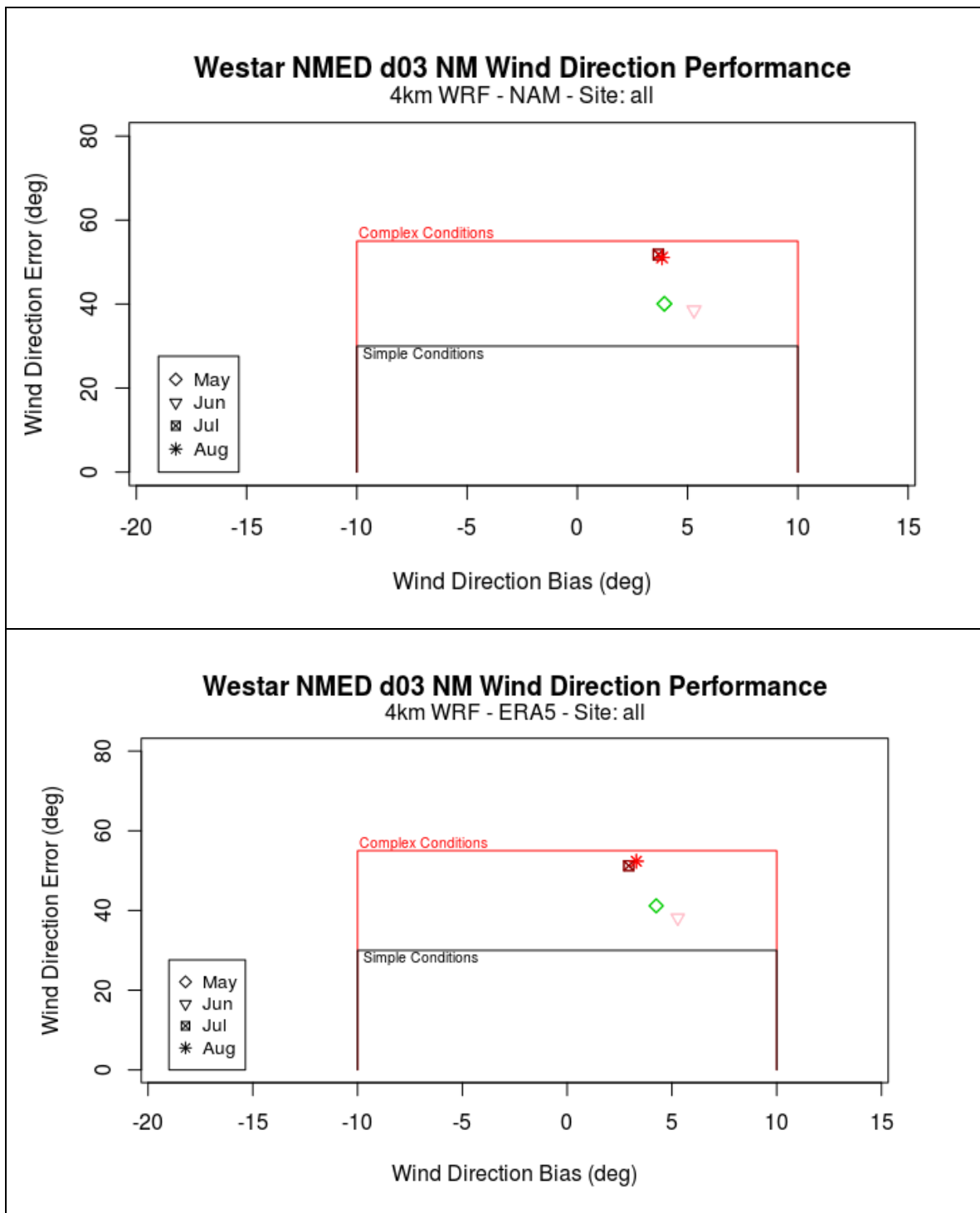


Figure 2-4. Soccer plot comparing WRF/NAM (top) and WRF/ERA5 (bottom) surface wind direction (degrees) model performance against the Simple and Complex Benchmarks for monthly RMSE (y-axis) and Mean Bias (x-axis).

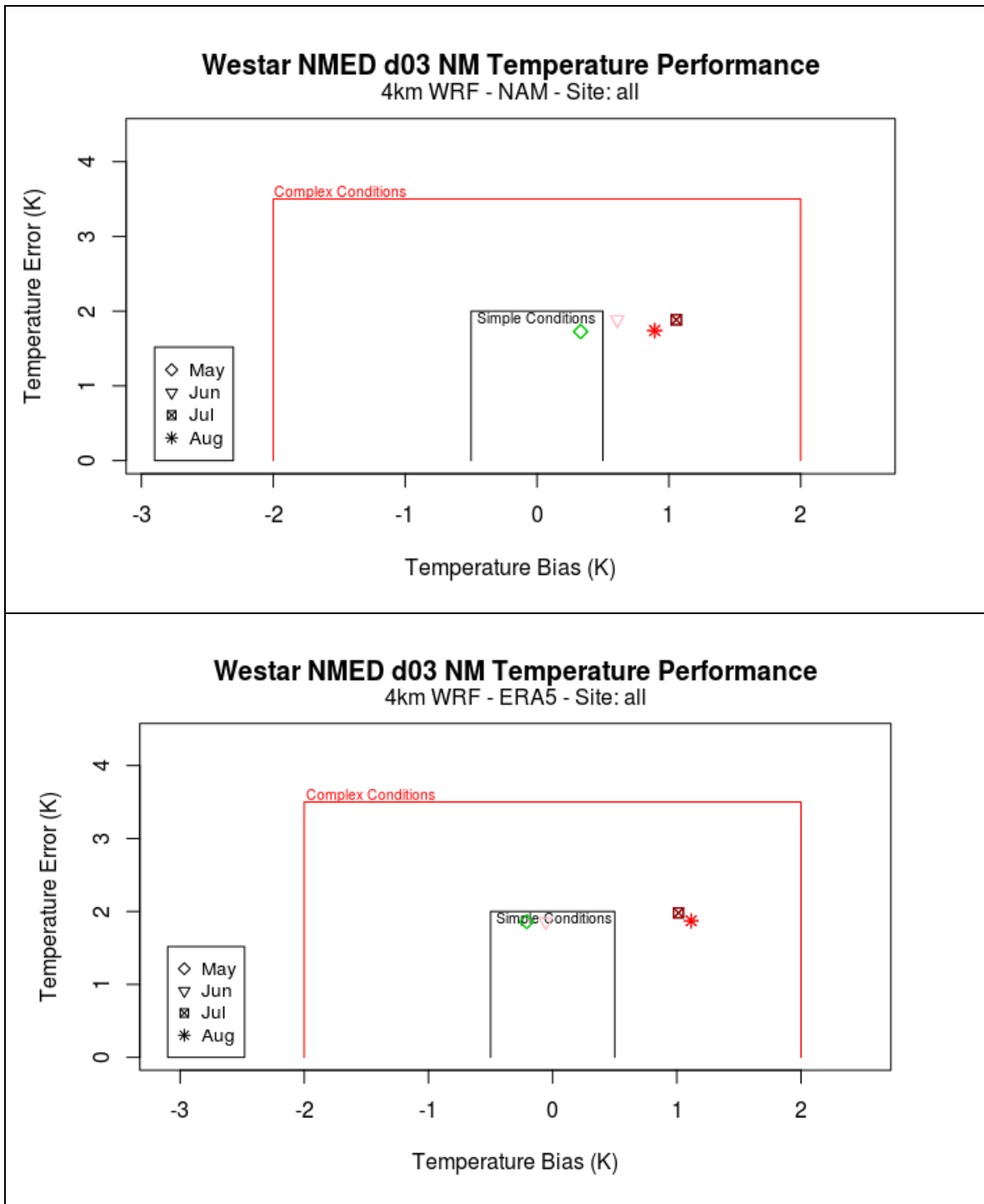


Figure 2-5. Soccer plot comparing WRF/NAM (top) and WRF/ERA5 (bottom) surface temperature (K) model performance against the Simple and Complex Benchmarks for monthly RMSE (y-axis) and Mean Bias (x-axis).

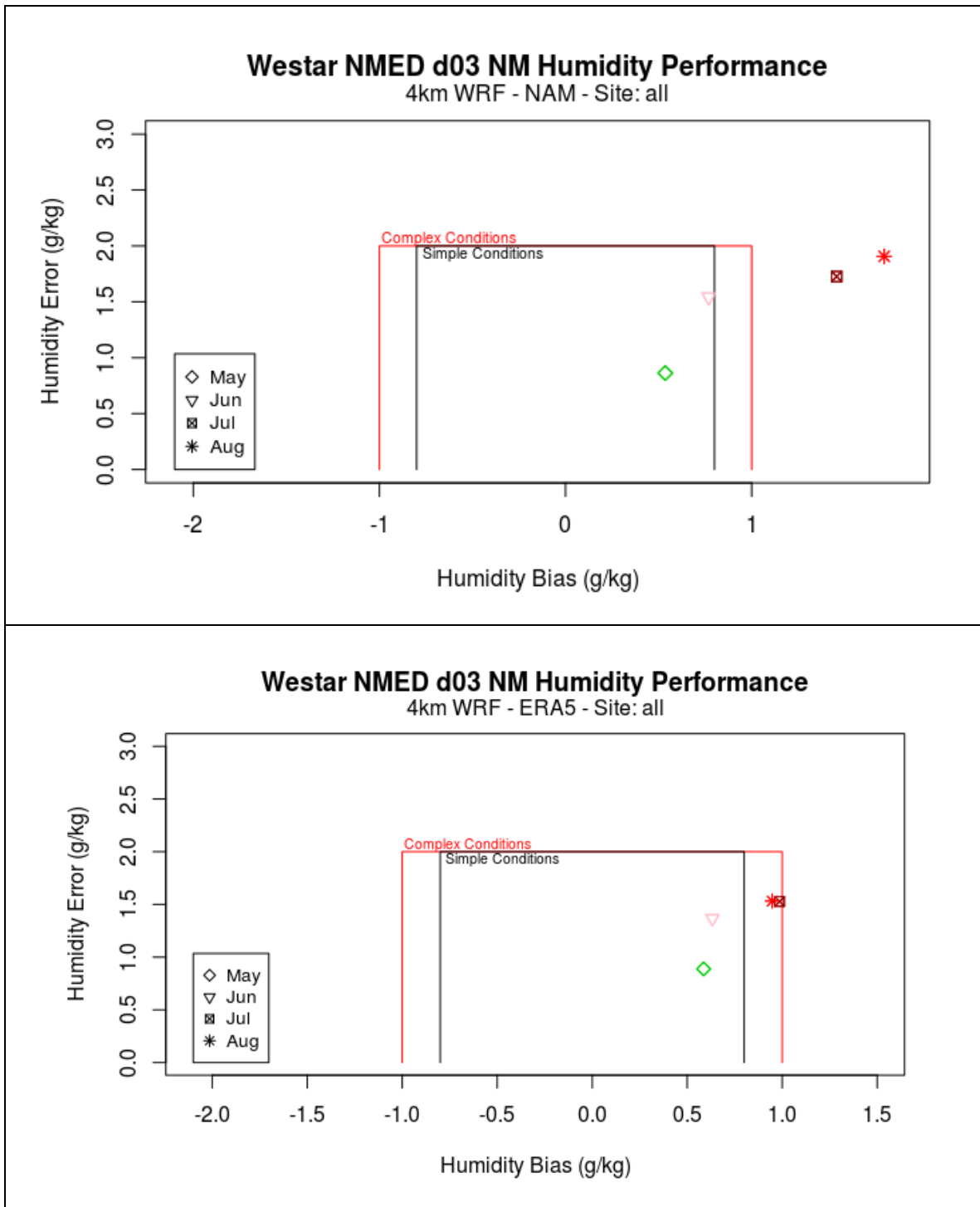


Figure 2-6. Soccer plot comparing WRF/NAM (top) and WRF/ERA5 (bottom) surface humidity (g/kg) model performance against the Simple and Complex Benchmarks for monthly RMSE (y-axis) and Mean Bias (x-axis).

2.4.1.8 Example Site-Specific Humidity Performance

METSTAT was used to evaluate the two WRF simulations for surface meteorological performance for each site in New Mexico. Figures 2-7 and 2-8 show example humidity model performance time series and soccer plots at the Las Cruces International Airport that is 8 miles west of the City of Las Cruces in Dona Ana County. In May, the two WRF simulations have nearly identical daily humidity performance at Las Cruces with a slight overestimation bias that is approximately 0.5 g/kg (Figure 2-7). In June, the humidity performance of the two WRF simulations at Las Cruces start to deviate from each other so by mid-June the WRF/NAM starts to have a large humidity overestimation bias that is as high as 4 g/kg; both simulations have large swings in variations in humidity bias. During the second half of June through July and August the WRF/NAM humidity bias tends to range from 0 to 3 g/kg, while the WRF/ERA5 bias ranges from -1 to +1.5 g/kg. These variations are likely due to the occurrence of monsoonal convective activity that can be very spotty and are also very difficult phenomena for a meteorological model to accurately reproduce.

The soccer plot of monthly humidity model performance at Las Cruces (Figure 2-8) shows that the WRF/ERA5 is clearly performing better with all months achieving the simple benchmark with a slight moist bias of from 0.2 to 0.6 g/kg. The WRF/NAM May humidity performance also achieves the simple benchmark and is nearly identical to WRF/ERA5, but for June, July and August the WRF/NAM monthly humidity performance at Las Cruces has a moist bias of from 1.5 to 2.1 g/kg that fails to achieve the benchmarks ($\leq \pm 1.0$ g/kg).

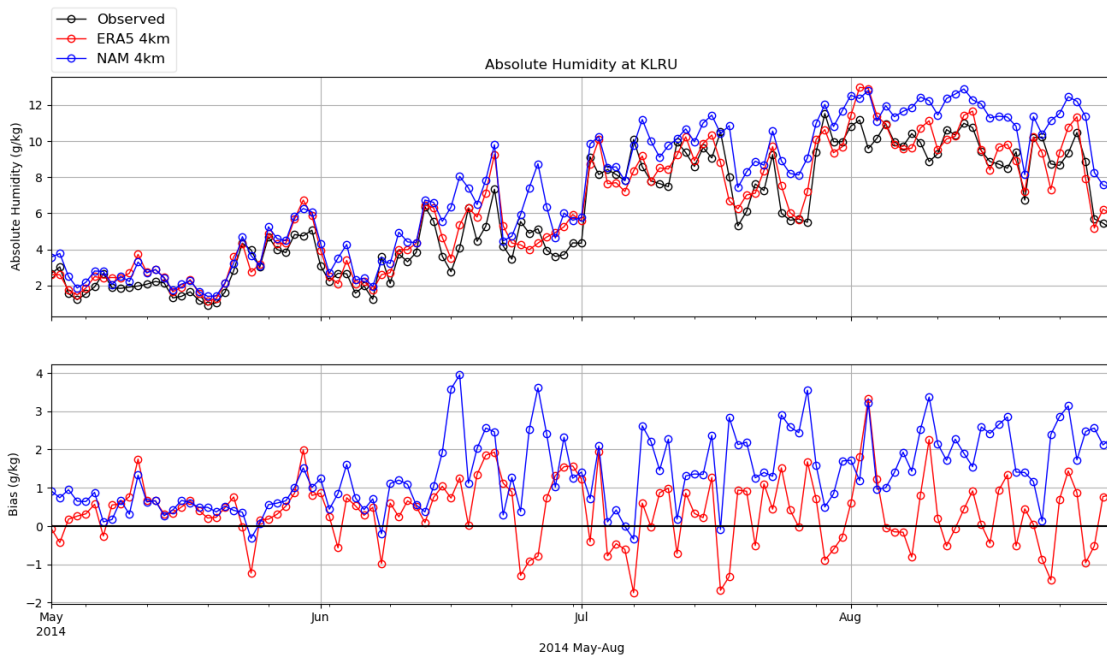


Figure 2-7. Time series plot of predicted and observed (black) daily humidity (g/kg) at Las Cruces International Airport for the WRF/ERA5 (red) and WRF/NAM (blue) simulations.

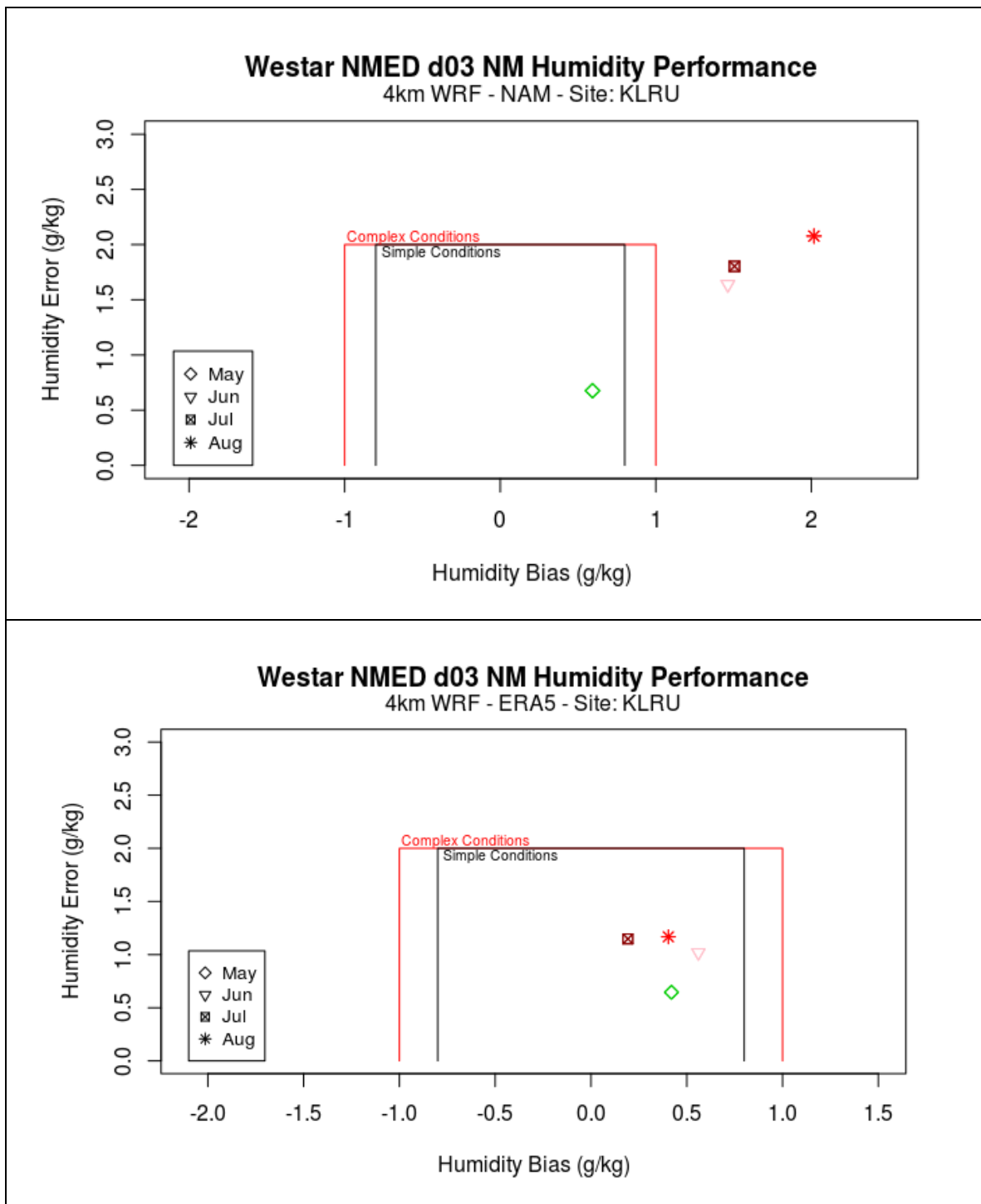


Figure 2-8. Soccer plot comparing WRF/NAM (top) and WRF/ERA5 (bottom) surface humidity (g/kg) model performance at Las Cruces International Airport against the Simple and Complex Benchmarks for monthly RMSE (y-axis) and Mean Bias (x-axis).

2.4.2 Qualitative Evaluations Using PRISM Data

Oregon State University (OSU) publishes precipitation analysis fields based on observations that can be used to qualitatively evaluate the WRF precipitation fields. The Parameter-elevation Relationships on Independent Slopes Model (PRISM²⁸) is used to generate the precipitation analysis fields (Daly et al., 2008). The PRISM interpolation method of observed precipitation reflect, as closely as possible, the current state of knowledge of spatial climate patterns in the United States. PRISM calculates a climate – elevation regression for each digital elevation model (DEM) grid cell, and stations entering the regression are assigned weights based primarily on the physiographic similarity of the station to the grid cell. Factors considered are location, elevation, coastal proximity, topographic facet orientation, vertical atmospheric layer, topographic position, and orographic effectiveness of the terrain.

Figure 2-9 compares the PRISM May monthly total precipitation across the 4-km New Mexico domain with the WRF/NAM and WRF/ERA5 model estimates. The PRISM and WRF estimate May precipitation amounts over New Mexico are similar with all three estimating little precipitation in the west and small amounts in the central eastern portion of New Mexico. However, neither WRF simulation reproduces the PRISM precipitation in the southeast corner of the 4-km domain in West Texas near Midland. And the WRF/NAM greatly overstates the PRISM precipitation over the Texas panhandle, with WRF/ERA5 just having a slight overstatement in this region.

The June monthly precipitation comparisons are provided in Figure 2-10. Both models have reasonable June monthly precipitation over New Mexico that is very light. And PRISM and the two WRF simulations agree with the much higher precipitation over the Texas panhandle, with WRF/ERA5 performing better than WRF/NAM that has an overestimation bias.

There is much more observed and estimated precipitation over New Mexico in July 2014 (Figure 2-11). WRF/NAM overestimates the July monthly precipitation over northeast New Mexico in July, with WRF/ERA5 having an overestimation bias in most northerly Texas. But both WRF simulations have a dry bias for monthly precipitation over the remainder of New Mexico.

WRF/ERA5 does a better job at reproducing the locations and magnitudes of the August monthly PRISM precipitation than WRF/NAM (Figure 2-12). WRF/NAM overstates the August precipitation in central-south New Mexico.

²⁸ <http://prism.oregonstate.edu/>

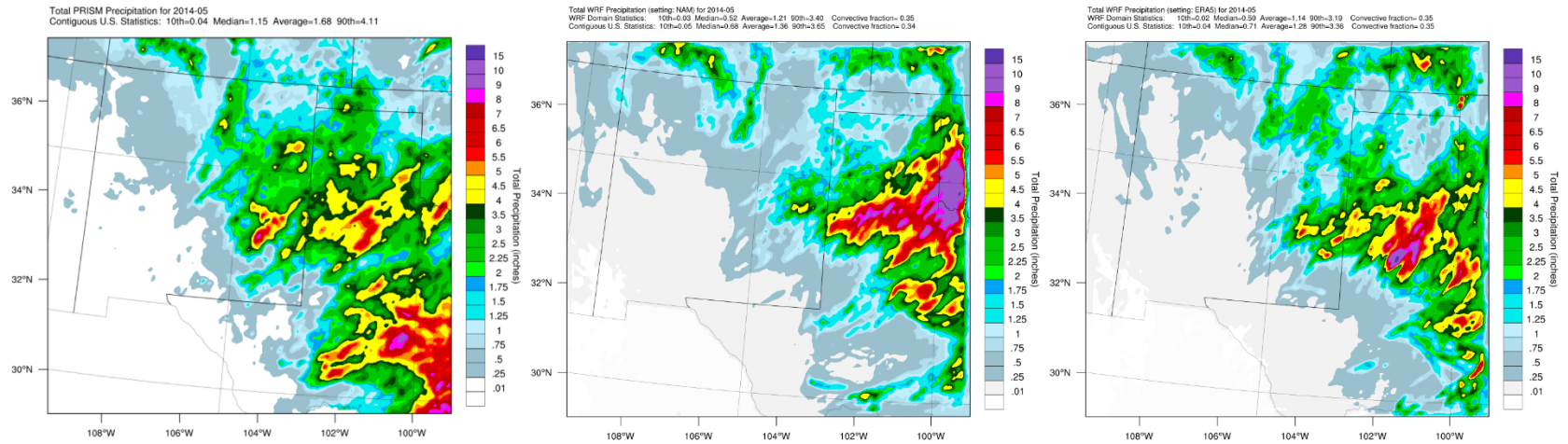


Figure 2-9. May monthly precipitation amounts from PRISM based on observations (left) and predicted by WRF/NAM (middle) and WRF/ERA5 (right).

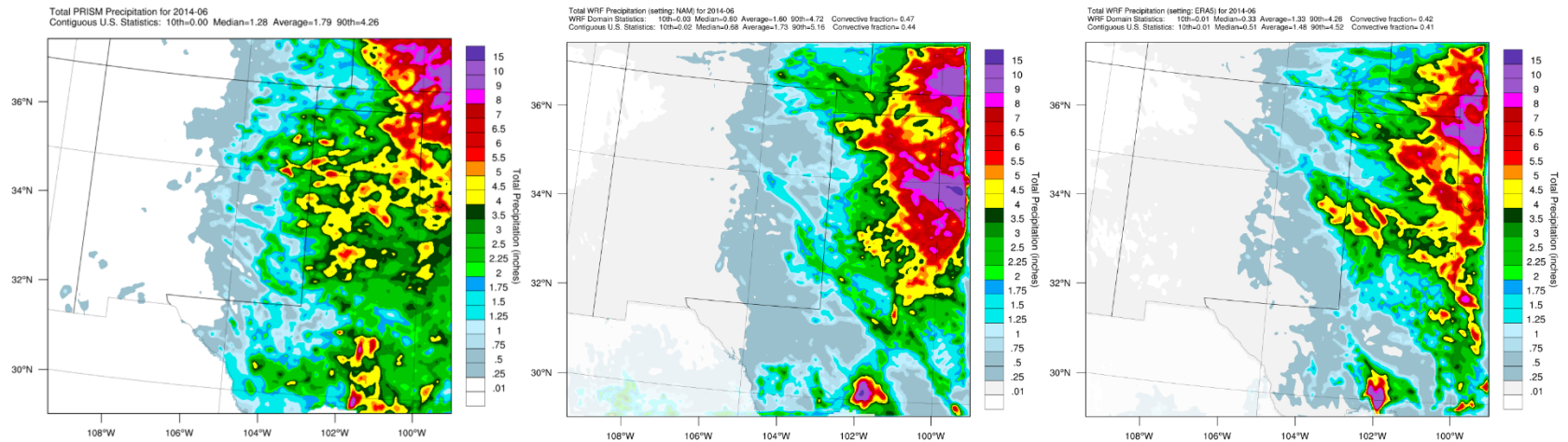


Figure 2-10. June monthly precipitation amounts from PRISM based on observations (left) and predicted by WRF/NAM (middle) and WRF/ERA5 (right).

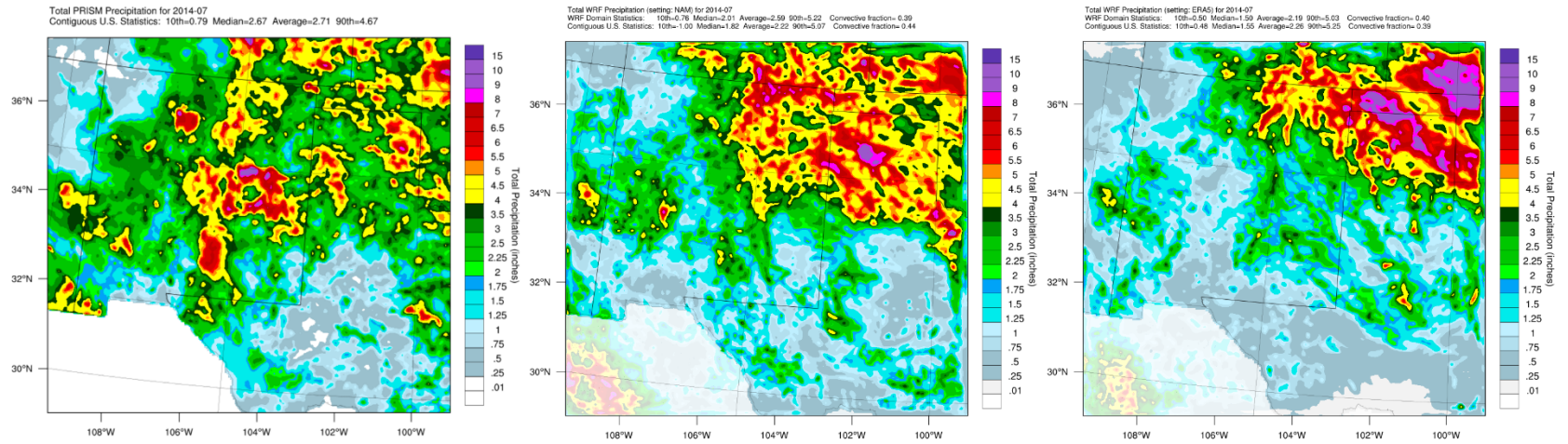


Figure 2-11. July monthly precipitation amounts from PRISM based on observations (left) and predicted by WRF/NAM (middle) and WRF/ERA5 (right).

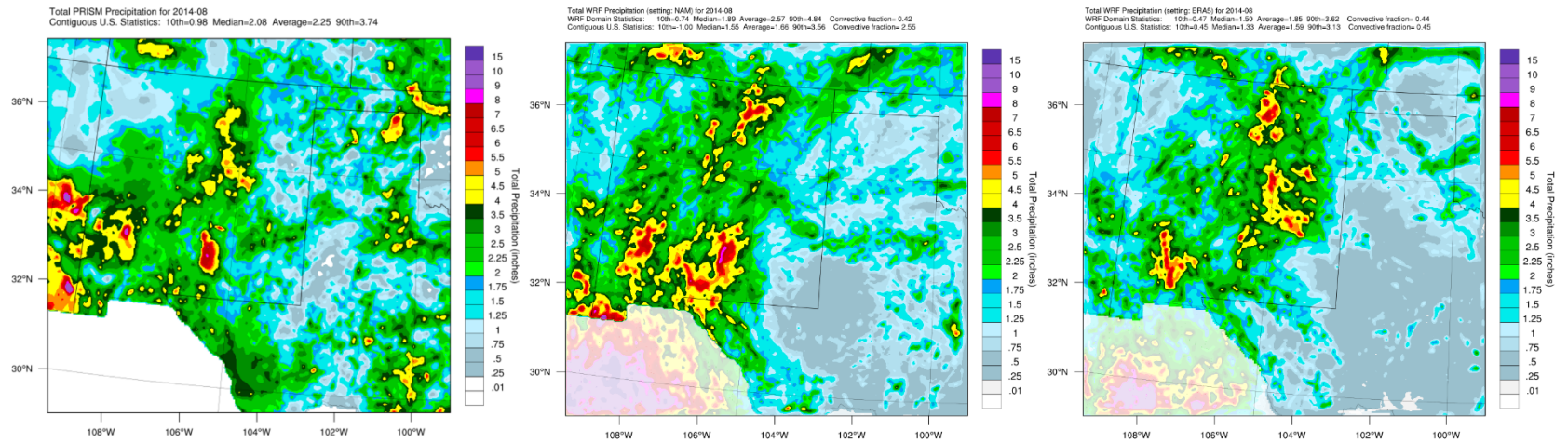


Figure 2-12. June monthly precipitation amounts from PRISM based on observations (left) and predicted by WRF/NAM (middle) and WRF/ERA5 (right).

2.4.3 Conclusions of 2014 WRF Model Performance

The model performance of both WRF simulations is reasonable and very similar for most meteorological variables (e.g., winds and temperature). This is in contrast to the WRAP-WAQS and EPA WRF 2014 simulations that had very different performance characteristics over New Mexico.²⁹ The biggest difference in the performance of the two WRF simulations was for humidity and precipitation. The WRF/NAM simulation had a moist bias for June-August that is likely partly associated with overactive convective precipitation that was greater in WRF/NAM than WRF/ERA5. It is unclear whether the WRF/NAM overstated precipitation is due to overactive convective events when they occur, or having events occur when they are not observed.

From the meteorological model performance evaluation, it is not possible to determine which set of WRF meteorological inputs will produce better ozone model performance when used as meteorological inputs for CAMx. There are variations in spatial and temporal model performance that are difficult to estimate what effects they will have on ozone concentrations. Furthermore, there may be meteorological inputs (e.g., level of mixing) that are more important for ozone modeling than the parameters we have data to evaluate the meteorological model for (i.e., winds, temperature, humidity and precipitation). Although it appears that WRF/NAM overstates the monthly precipitation, if that does not occur on high ozone days it may not matter to the ozone model performance.

CAMx was run for a portion of the summer of 2014 episode with meteorological inputs based on both the WRF/NAM and WRF/ERA5 simulations and the ozone estimates compared to determine which meteorological inputs performed best so were selected for use in the final CAMX 2014 36/12/4-km base case simulation. The meteorological diagnostic sensitivity tests using the CAMx photochemical model are described in Chapter 5.

²⁹ https://www.wrapair2.org/pdf/NM_OAI_Study_Webinar1_2020-05-28.pdf

3. BOUNDARY CONDITION INPUTS

The Boundary Conditions (BCs) for the CAMx most outer 36-km 36US modeling domain lateral boundaries were based on output from a 2014 simulation of the GEOS-Chem global chemistry conducted by WRAP for their 2014v2 modeling platform.

3.1 WRAP 2014 GEOS-Chem Modeling

The WRAP-WAQS 20914v1 36/12-km CAMx and CMAQ base case simulations used BCs based on EPA's 2014 GEOS-Chem simulation that was used in EPA's 2014 modeling platform used in the 2014 National Air Toxics Assessment (NATA³⁰). The CAMx and CMAQ 2014v1 base case simulation and sensitivity modeling found that the BCs based on EPA's 2014 GEOS-Chem caused year-long ozone overestimation bias throughout the western U.S.³¹ Thus, WRAP conducted their own 2014 GEOS-Chem simulation using newer version of the model with updated emissions that resulted in much better CAMx ozone model performance without the systematic ozone over-prediction bias.³² Table 3-1 presents the WRAP 2014 GEOS-Chem model configuration.

Table 3-1. 2014 GEOS-Chem simulation model configuration used by WRAP whose output is used to define the 2014 day-specific diurnally varying BC inputs for the NM OAI Study photochemical modeling.

Science Options	WRAP 2014 GEOS-Chem Base Case
Version	Version 12.2.0 (release date: 2019-02-19)
Vertical Grid Mesh	72 Layers
Chemistry mechanism	GEOS-Chem standard chemistry with complex SOA option ³³ .
Horizontal Grids	2x2.5 degree (Nx, Ny = 144, 91)
Initial Conditions	6-month spin-up; starting from provided initial conditions for standard chemistry
Meteorology	2014 GEOS-FP meteorology
Photolysis mechanism	Default (FAST-J)
Advection Scheme	Default (TPCORE)
Cloud convection scheme	On / Relaxed Arakawa-Schubert
Planetary Boundary Layer mixing	On / non-local scheme implemented by Lin and McElroy
Dry deposition scheme	Default (Wesely)
Chemistry Solver	Default (FLEXCHEM)
Parallelization	Open Multi-Processing (OMP)

³⁰ <https://www.epa.gov/national-air-toxics-assessment>

³¹ http://views.cira.colostate.edu/iwdw/docs/waqs_2014v1_shakeout_study.aspx

³² https://www.wrapair2.org/pdf/WRAP_Shake-Out_Phase-III_Update_RTOWG_2019-09-10v3a.pptx

³³ We recommend turning off semivolatile primary organic aerosol (POA) chemistry and isoprene SOA reactions via the volatility-based scheme (VBS) [Pye et al., 2010] to avoid risk of double-counting in the complex SOA chemistry scheme. For more information, see <http://maraisresearchgroup.co.uk/Publications/GC-v11-02-SOA-options.pdf>

3.2 2014 GEOS-Chem Model Evaluation

The results of the WRAP 2014 GEOS-Chem simulation and CAMx sensitivity modeling using the new BCs can be found on the WAQS-WRAP2014v2 model evaluation webpage³⁴. Relevant for the NM OAI Study is the fact that this updated 2014 GEOS-Chem BCs do lead to better CAMx model performance for ozone concentrations and corrects a persistent year-long ozone overestimation bias observed with the previous 2014 GEOS-Chem simulation conducted by EPA and used in the EPA 2014 modeling platform. The NM OAI Study evaluated the use of the WRAP 2014 GEOS-Chem BCs for CAMx modeling at several sites in New Mexico and found good ozone performance that achieved ozone model performance goals.³⁵ Thus, the WAQS-WRAP 2014v2 BC inputs based on the WRAP 2014 GEOS-Chem simulation were used as is for the NM OAI Study.

³⁴ http://views.cira.colostate.edu/iwdw/docs/WRAP_WAQS_2014v2_MPE.aspx

³⁵ https://www.wrapair2.org/pdf/NM_OAI_Study_Webinar1_2020-05-28.pdf

4. 2014 EMISSION INPUTS

4.1 Available Emissions Inventory Datasets

The emissions inventories for the CAMx 2014 36/2/4-km base case modeling were based on the WRAP-WAQS 2014v2 emissions inventory. Within the 36-km 36US North American and 12-km 12WUS2 western U.S. domains, the WRAP-WAQS CAMx 2014v2 base case emission inputs were used without any changes.

For the 4-km New Mexico domain, the WRAP-WAQS 2014v2 emissions have been reviewed and updated as needed by the NMED. For on-road mobile sources, the 4-km domain emissions were based on MOVES2014 model, 2014 activity data and day-specific hourly gridded 2014 WRF 4-km meteorology run through SMOKE-MOVES.

4.2 Development of CAMx Emission Inputs

CAMx emission inputs were generated mainly by the SMOKE and MEGAN emissions models. CAMx requires two emission input files for each day: (1) low level gridded emissions that are emitted directly into the first layer of the model from sources whose emissions are released at the surface with little or no plume rise; and (2) elevated point sources (stacks) with plume rise calculated from stack parameters and meteorological conditions. CAMx was operated using version 6 revision 4 of the Carbon Bond chemical mechanism (CB6r4) (Yarwood et al., 2010).

The 2014 base case (May to August) 4-km New Mexico domain CAMx emission inputs were based on the WRAP-WAQS 2014v2 emissions that rely on the 2014NEIv2 with updates provide by the western states. The New Mexico emissions from the 2014v2 database were reviewed and updated by the NMED. The 2014v2 emissions for New Mexico and portions of surrounding states within the 4-km New Mexico domain were processed by the Sparse Matrix Operator Kernel Emissions (SMOKE) modeling system (UNC, 2015). SMOKE version 4.7 was used, which is the current version of SMOKE that was released in October 2019.³⁶

4.2.1 Day-Specific On-Road Mobile Source Emissions

The 2014 on-road mobile source emission inputs for the 4-km New Mexico domain were generated using the SMOKE-MOVES emissions model. SMOKE-MOVES used a 2014 mobile source emission factor (EF) lookup table generated by the Motor Vehicle Emission Simulator (MOVES2014³⁷) model (EPA, 2014a,b,c). The SMOKE-MOVES default county-level 2014 vehicle activity data for New Mexico was reviewed by NMED and updated as needed. SMOKE-MOVES uses the 2014 MOVES EF lookup table, hourly gridded 4-km meteorological data from the 2014 WRF simulation conducted in this study and 2014 county-level activity data (e.g., vehicle miles travelled [VMT], speed, etc.) to generate 2014 day-specific hourly gridded on-road mobile source emission inputs for CAMx and the 4-km New Mexico domain.

³⁶ <https://www.cmascenter.org/smoke/>

³⁷ <http://www.epa.gov/oms/models/moves/#user>

4.2.2 Point Source Emissions

2014 point source emissions were based on the WRAP-WAQS 2014v2 emissions inventory. The 2014v2 New Mexico point source emissions were reviewed and updated by NMED. Point sources were processed in two streams: (1) major point sources with Continuous Emissions Monitoring (CEM) devices, which are primarily fossil-fueled Electrical Generating Units (EGU) with capacity of 25 MW or greater; and (2) point sources without CEMs. For point sources with CEM data, day-specific hourly NO_x and SO₂ emissions were used for the 2014 base case emissions scenario. The VOC, CO and PM emissions for point sources with CEM data were based on the annual emissions data in the 2014v2 inventory temporally allocated to each hour of the year using the CEM hourly heat input. The hourly CEM data available in the Acid Rain database on the EPA Clean Air Market Division (CAMD) website fills hours with missing CEM data with maximum potential to emit (PTE) emission rates and flags the data. This is because the purpose of the Acid Rain database is to assure that the source is not emitting higher emissions than its cap. Using PTE emissions rates for hours with missing CEM data is inappropriate for PGM modeling since the goal is to obtain an accurate estimate of emissions. Thus, a data filling program is used that uses the missing data flags to identify hours when the data filled PTE emissions occur, and they are replaced with typical emission rates.

For all point sources, the locations of the point sources were converted to the LCC coordinate system used in the modeling. Non-CEM point sources were processed by SMOKE to generate the temporally varying (i.e., seasonal, day-of-week and hour-of-day) speciated emissions needed by CAMx. The 2014 point source emissions without CEM data were processed using SMOKE using the default temporal (e.g., monthly, day-of-week and hourly) and speciation profiles.

4.2.3 Area and Non-Road Source Emissions

The 2014v2 area and non-road sources were spatially allocated to the 4-km New Mexico grid using an appropriate surrogate distribution (e.g., population for home heating, etc.). The area sources were temporally allocated by month and by hour of day using the SMOKE source-specific temporal allocation factors, while chemical speciation used the SMOKE source-specific CB6r4 speciation allocation profiles.

4.2.4 Episodic Biogenic Emissions

Biogenic emissions were generated using Version 3.1 of the MEGAN biogenic emissions model. MEGAN uses high resolution GIS data on plant types and biomass loadings and the 2014 WRF surface temperature fields, and solar radiation to develop hourly emissions for biogenic species on the 36/12/4-km grids. MEGAN generates gridded, speciated, temporally allocated emission files. The MEGAN biogenic emissions were used for the 36-km 36US, and 4-km New Mexico modeling domains. Note that the BEIS biogenic emissions were used in the 12-km WRAP-WAQS 2014v2 modeling platform. WRAP/WAQS conducted sensitivity tests using MEGAN v3.0 and BEIS biogenic emissions and found they produced comparable ozone estimates (because the isoprene emissions were similar) but CAMx with BEIS had better Organic Aerosol (OA)

performance³⁸ than CAMx with MEGAN v3.0 biogenic emissions so WAQS selected BEIS. Since then, MEGAN has been updated to version 3.1 and the CAMx OA performance is now similar using MEGAN v3.1 and BEIS.

Table 4-1 summarizes MEGAN v3.1 biogenic VOC (BVOC) and soil NO_x emissions by month for the 4-km New Mexico domain. Biogenic emissions are controlled by ambient environmental variables, most notably temperature and light. Increases in temperature normally lead to increased BVOC emissions because of higher biological activity as evident in the Table 4-1.

Table 4-1. 2014 base case biogenic emissions summary by month (in short tons per day) for the 4-km New Mexico domain.

Month	NO _x (in tons/day)	BVOC (in tons/day)
May	1,131	4,139
Jun	1,415	8,902
Jul	1,666	10,248
Aug	1,323	11,438

4.2.5 Wildfires, Prescribed Burns, Agricultural Burns

2014 emissions from open-land burning including wildfires, prescribed burns and agricultural burning were based on the WRAP-WAQS 2014v2 emissions inventory. The WRAP Fire and Smoke Work Group (FSWG³⁹) processed the 2014NEIv2 Bluesky/SMARTFIRE fire emissions for the U.S. and classified them as either wildfires (WF), prescribed burns (Rx) or agricultural burning (Ag) and made other updates for the 2014v2 inventory. The 2014NEIv2 fire emissions for Mexico and Canada was used without any changes.

4.2.6 Other Natural Emissions

Lightning NO_x (LNO_x), and windblown dust (WBD) emissions were generated for the 4-km domain using special CAMx processors and WRF 2014 meteorological data. Oceanic emissions such as sea salt spray aerosol (SSA) and dimethyl sulphide (DMS) were not generated for the 4-km New Mexico domain since this domain does not include any ocean within it. However, the LNO_x, WBD and oceanic emissions for the 36-km and 12km were based on the WRAP-WAQS 2014v2 emissions and were included in the modeling.

4.2.7 QA/QC of Emissions Processing and Emissions Merging

The emissions for the 4-km New Mexico domain were processed by major source category in several different processing “streams”, including area sources, on-road mobile sources, non-road mobile sources, biogenic sources, non-CEM point sources, CEM point sources using day-specific hourly emissions, and emissions from fires. Separate Quality Assurance (QA) and Quality Control (QC) were performed for each stream of emissions processing and in each step following the procedures developed by

³⁸ http://views.cira.colostate.edu/iwdw/docs/waqs_2014v1_shakeout_study.aspx

³⁹ <https://www.wrapair2.org/FSWG.aspx>

WRAP (Adelman, 2004). SMOKE includes advanced quality assurance features that include error logs when emissions are dropped or added. In addition, the following visual displays were generated:

- Spatial plots of the hourly emissions for each major species (e.g., NO_x, VOC, and CO).
- Summary tables of emissions for major species for each grid and by major source category.
- QA information examined against the original point and area source data and summarized in an overall QA/QC assessment.

Scripts to perform the emissions merging of the appropriate biogenic, on-road, non-road, area and low-level point sources (i.e., point sources with little or no plume rise so they are released into the first layer of the PGM) emission files were written to generate the CAMx-ready two-dimensional day and domain-specific hourly speciated gridded emission inputs. The point source and fire, emissions were then processed into the day-specific hourly speciated emissions in the CAMx-ready point source format.

For the 36/12-km domains the model-ready emissions from the WRAP/WAQS 2014v2 modeling platform were used in this study.

The resultant CAMx model-ready emissions were subjected to a final QA using spatial maps to: (1) assure that the emissions were merged properly and CAMx inputs contain the same total emissions; and (2) provide additional QA/QC information.

4.2.8 Use of the Plume-in-Grid (PiG) Subgrid-Scale Plume Treatment

CAMx includes a Plume-in-Grid (PiG) sub-model that treats the early plume chemistry and dynamics of emissions from point sources and then releases the emissions into the grid model farther downwind at such time that the plume is adequately resolved by the grid. Large NO_x emissions point sources within the 4-km New Mexico domain were selected for treatment by the subgrid-scale PiG module when their emissions rate were 5 tons per day or larger.

4.2.9 QA/QC of Model-Ready Emissions

In addition to the CAMx-ready emission input files generated for each hour of all days modeled in the May-August 2014 modeling period, a number of quality assurance (QA) files were prepared and used to check for gross errors in the emissions inputs. Importing the model-ready emissions into PAVE or VERDI and examine both the spatial and temporal distribution of the emission to investigate the quality and accuracy of the emissions inputs.

- Visualizing the model-ready emissions with the scale of the plots set to a very low value, we can determine whether there are areas omitted from the raw inventory or if emissions sources are erroneously located in water cells;
- Spot-checking the holiday emissions files to confirm that they are temporally allocated like Sundays;

- Producing pie charts emission summaries that highlight the contribution of each emissions source component (e.g. non-road mobile);
- Normalizing the emissions by population for each state illustrates where the inventories may be deficient and provide a reality check of the inventories.

State inventory summaries prepared prior to the emissions processing were used to compare against SMOKE output report totals generated after each major step of the emissions generation process. To check the chemical speciation of the emissions to CB6 species, we compared reports generated with SMOKE to target these specific areas of the processing. For speciation, the inventory state import totals were compared against the same state totals with the speciation matrix applied.

4.2.10 Summary of Emissions for 4-km New Mexico Domain

This section presents 2014 base case anthropogenic emissions summary for the 4-km New Mexico domain. The emissions were processed by major source category in several different “streams” of emissions modeling. Each stream of emissions modeling generates a pre-merged CAMx-ready emissions model input with all pre-merged emissions inputs merged together to generate the final CAMx-ready two-dimensional gridded low-level (layer 1) and point source emission inputs. Table 4-2 lists an example of separate streams of emissions modeling by source category that are used.

Table 4-2. New Mexico 4-km domain emissions processing categories.

Country/Region	Sector	Description
US Anthro	afdust_adj	Area fugitive dust
	ag	Agricultural ammonia sources
	nonpt	Other nonpoint sources
	np_oilgas_wrap	Non-point Oil and Gas for 7 WRAP States (CO, MT, NM, ND, SD, UT, WY)
	np_oilgas	Non-point Oil and Gas
	nonroad	Non-road mobile
	rail	Locomotive
	onroad	On-road mobile
	ptegu	EGU point sources
	ptnonipm	Non-EGU point sources
	pt_oilgas_wrap	Point Oil and Gas for 7 WRAP States (CO, MT, NM, ND, SD, UT, WY)
	pt_oilgas_wrap	Point Oil and Gas
	rwc	Residential Wood Combustion
Mexico Anthro	onroad_mex	Mexico onroad mobile
	othar	Mexico area
	othpt	Mexico point sources
Natural	MEGAN	Biogenic
	LtNOx	Lightning Nox
	AG fire	Ag Fire
	RX fire	Prescribed Fire
	WF fire	Wild Fire
	Ptfire_othna	Mexico fire
	WBD	Windblown Dust

Table 4-3 summarizes criteria air pollutant emissions in episode average short tons per day by source category for the 4-km New Mexico domain. These data represent the model-ready emissions input to the CAMx air quality model for the 2014 base case. Generally, emissions are summarized from the SMOKE reports generated by the SMKMRG program. There are a couple of exceptions to this general approach, fugitive dust and EGU sources. The fugitive dust emissions were adjusted after SMOKE processing to account for fugitive dust correction factors that are derived from the Biogenic Emission Landuse Database version 4 (BELD4). The correction factors are necessary to account for dust removal due to local vegetation scavenging so are not

transported downwind. Model-ready emissions for EGU and Mexico point sources were obtained from WRAP/WAQS 2014 platform so were summarized for the 4-km domain outside of SMOKE.

Table 4-3. 2014 base case anthropogenic emissions summary (episode average short tons per day) by source category for the 4-km New Mexico domain.

Country/Category	Source Category	CO	NH ₃	NO _x	PM _{2.5}	PM ₁₀	SO ₂	VOC
US Anthro	Area fugitive dust	0.0	0.0	0.0	253.3	1,788.2	0.0	0.0
	Agricultural ammonia sources	0.0	764.7	0.0	0.0	0.0	0.0	43.4
	Non-point Oil and Gas for 7 WRAP States (CO, MT, NM, ND, SD, UT, WY)	237.7	0.0	157.8	4.4	4.4	11.3	567.3
	Remaining Non-point Oil and Gas	286.8	0.0	311.7	6.9	6.9	30.0	1,642.5
	Residential Wood Combustion	7.0	0.1	0.1	0.5	0.5	0.0	1.2
	Other nonpoint sources	141.3	1.5	28.5	9.3	13.4	4.5	213.2
	On-road mobile	1,476.2	6.0	444.5	13.2	20.1	1.7	150.6
	Locomotive	22.9	0.1	122.7	2.9	3.1	0.1	6.2
	Non-road mobile	570.3	0.2	133.4	9.0	9.4	0.3	73.2
	EGU point sources	89.2	3.4	210.6	12.9	17.8	160.0	5.0
	Point Oil and Gas for 7 WRAP States (CO, MT, NM, ND, SD, UT, WY)	89.9	0.0	114.7	1.4	1.4	23.8	56.1
	Remaining Point Oil and Gas	113.8	0.1	205.2	3.2	3.3	27.1	48.4
	Non-EGU point sources	74.4	4.9	47.5	11.4	32.5	49.3	24.4
Mexico Anthro	Mexico area	19.9	33.2	42.2	5.8	15.7	1.7	103.3
	Mexico onroad mobile	356.3	0.6	98.4	1.5	2.6	1.4	34.4
	Mexico point sources	28.4	0.7	20.2	4.8	5.7	16.4	8.3

Figure 4-1 presents pie charts showing the two main ozone precursor (VOCs and NO_x) emissions from anthropogenic sources by source category for New Mexico and portion of surrounding states within the 4-km domain. Point and nonpoint oil and gas sectors account for majority of NO_x emissions followed by on-road mobile and EGU sources. In New Mexico, oil and gas sources are the largest anthropogenic VOC emitters and accounts for nearly 80% of 4-km domain VOC emissions.

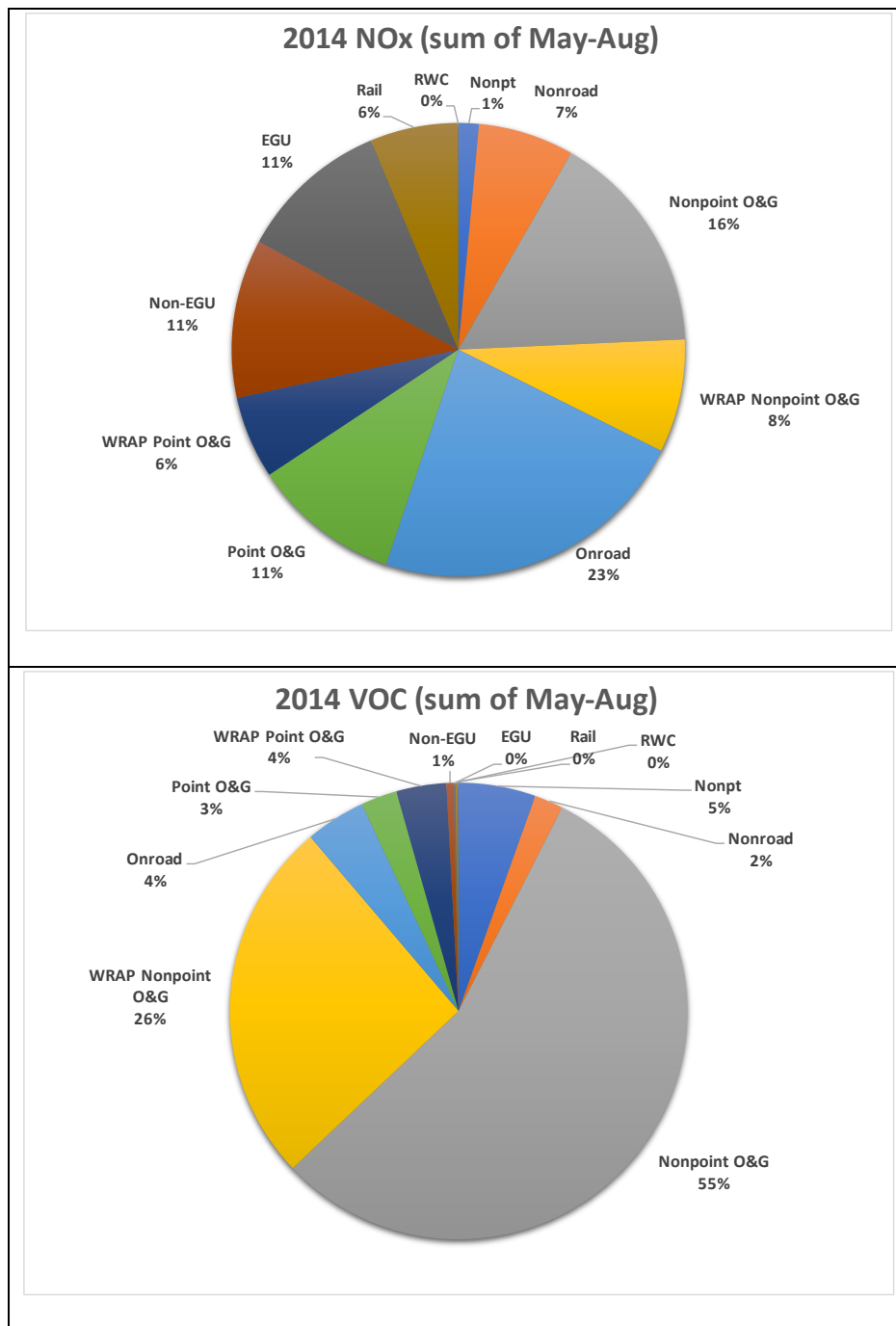


Figure 4-1. New Mexico 2014 base case anthropogenic NOx and VOC emissions by source category.

Figure 4-2 displays spatial maps of NO_x and VOC anthropogenic emissions from the oil and gas sector across the 4-km New Mexico domain. Top panel shows emission maps for non-point O&G sources while bottom panel shows point O&G sources. The San Juan and Permian basins are clearly visible on the emissions map and confirm correct spatial allocation of oil and gas emissions. Figure 4-3 shows emission maps for on-road mobile (top panel), rail (middle panel) and non-point sources including non-road equipment (bottom panel).

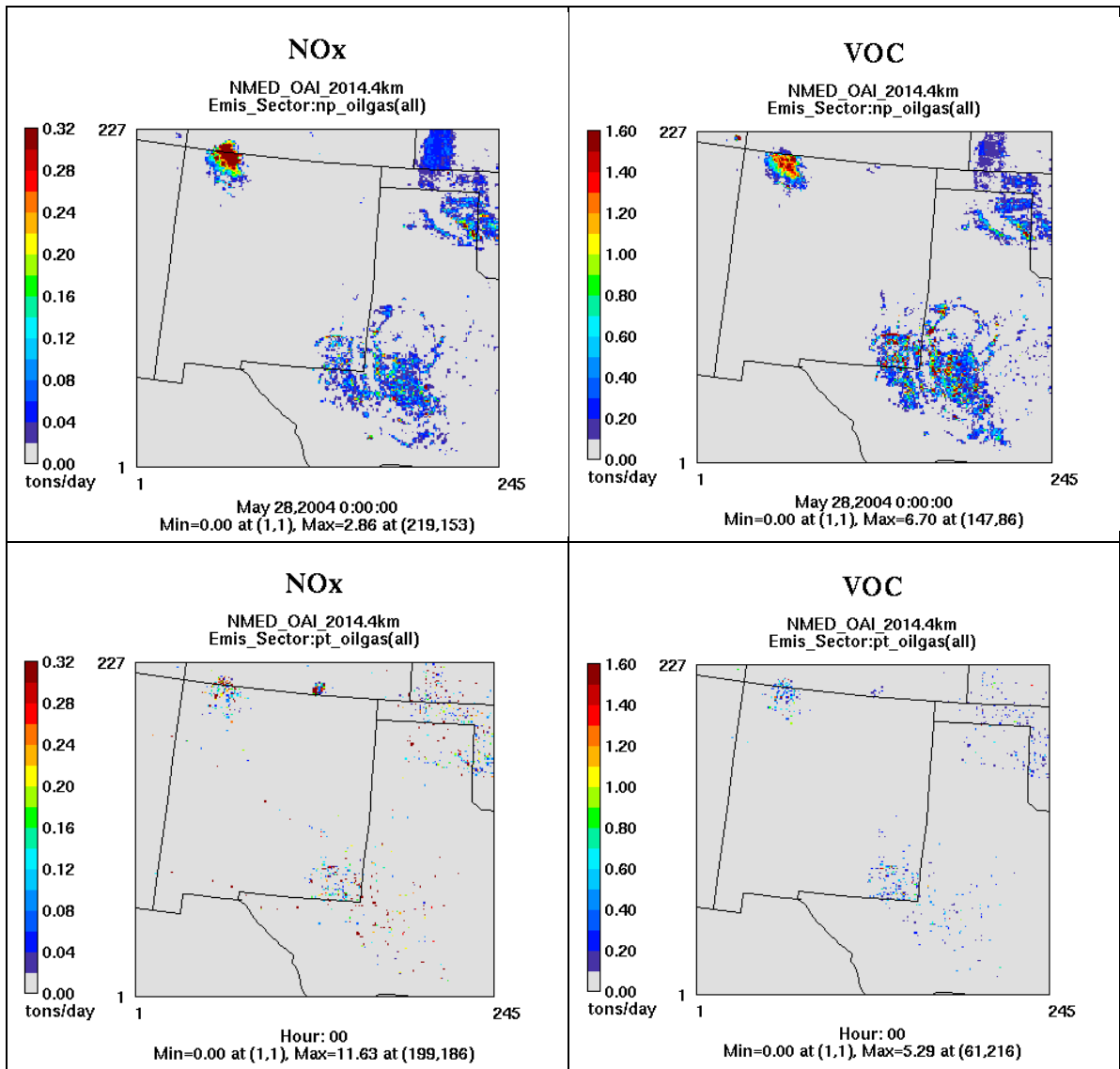


Figure 4-2. Spatial distribution of the non-point (top) and point (bottom) source oil and gas NO_x (left) and VOC (right) emissions (episode avg tons per day) for New Mexico 4-km domain.

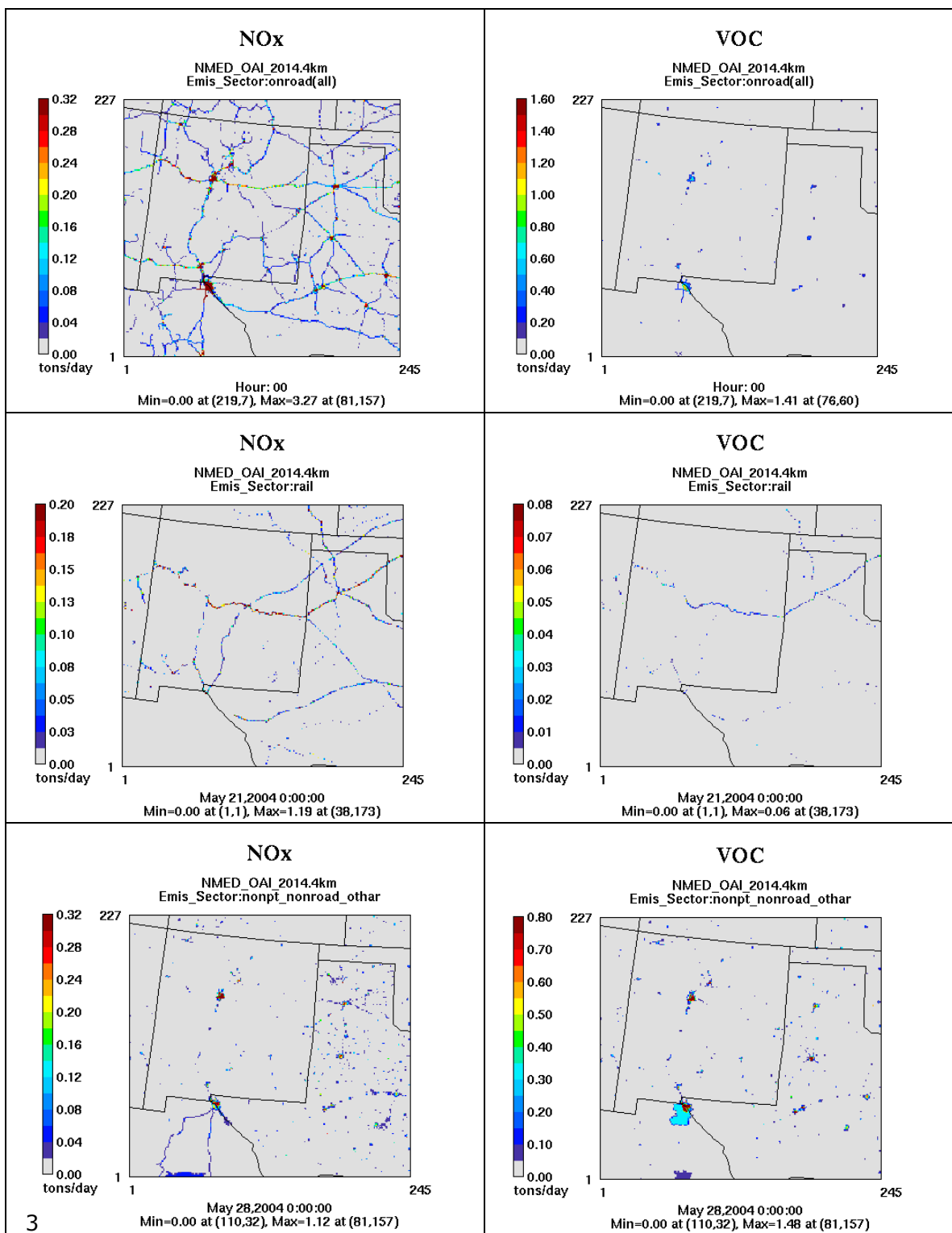


Figure 4-3. Spatial distribution of on-road (top), rail (middle) and non-point/non-road equipment (bottom) NOx (left) and VOC (right) emissions (episode avg tons per day) for New Mexico 4-km domain.

5. DIAGNOSTIC SENSITIVITY TESTS

Several CAMx diagnostic sensitivity tests were conducted to evaluate alternative meteorological inputs based on the 2014 36/12/4-km WRF meteorological model simulations discussed in Chapter 2. To develop the CAMx meteorological inputs, the WRF model output data must first be processed by the WRFCAMx processor.

5.1 WRFCAMx Processing of 2014 WRF Output

The WRFCAMx processor maps WRF meteorological fields to the format required by CAMx. It also calculates turbulent vertical exchange coefficients (Kv) that define the rate and depth of vertical mixing in CAMx. Steps in the WRFCAMx processing are as follows:

- Reading in WRF meteorological model output data;
- Extracting meteorological data for CAMx domain(s);
- Collapsing meteorological data if coarser vertical resolution data is requested in CAMx than used in WRF;
- Computing vertical diffusivities (Kv); and
- Output the meteorological fields in the formats used by CAMx.

Several options are available in WRFCAMx to derive vertical turbulent exchange coefficient (also known as: Kv, Kz or vertical diffusivity) fields from WRF output. When TKE (turbulent kinetic energy) is not available from the WRF output (as is the case with the YSU PBL selected WRF physics options), Kv fields are diagnosed from wind, temperature, and Planetary Boundary Layer (PBL) parameters in WRFCAMx. For this application, the WRFCAMx processing was performed to generate two sets of Kv profiles using two different Kv options in WRFCAMx, the CMAQ-like and YSU Kv profile options.

5.1.1 Treatment of Minimum Kv

The CAMx Kv_patch pre-processor program sets the minimum Kv value to 0.1 to 1.0 m²/s in the lowest 100 m of the atmosphere depending on the amount urban land use category in a grid cell. This is done to account for the urban heat island effect that enhances vertical mixing through-out the day and night.

5.1.2 Layer Collapsing Strategy

WRF was run with 36 vertical levels (35 vertical layers) as shown in Table 2-1. For the NM OAI Study, a layer collapsing strategy was employed that reduced the 35 WRF vertical layers to 25 layers in CAMx, which reduces the CAMx run time by about a third. Table 5-1 displays the WRF to CAMx layer collapsing strategy. This is the same layer collapsing study employed by WRAP-WAQS.

Table 5-1. WRF to CAMx vertical layer collapsing strategy used in the NM OAI Study.

CAMx Layers	WRF Layers	WRF hybrid eta	WRF Pressure (mb)	Height (m)
	0	1.0000	1000.0	0
	1	0.9985	998.6	12
1	2	0.9970	997.2	24
	3	0.9950	995.3	40
2	4	0.9930	993.4	56
	5	0.9910	991.5	72
3	6	0.9880	988.6	97
	7	0.9850	985.8	121
4	8	0.9800	981.0	162
5	9	0.9700	971.5	243
6	10	0.9600	962.0	326
7	11	0.9500	952.5	409
	12	0.9400	943.0	492
8	13	0.9300	933.5	577
9	14	0.9100	914.5	747
10	15	0.8900	895.5	921
11	16	0.8700	876.5	1098
12	17	0.8400	848.0	1369
13	18	0.8000	810.0	1742
14	19	0.7600	772.0	2130
15	20	0.7200	734.0	2533
16	21	0.6800	696.0	2954
17	22	0.6400	658.0	3393
18	23	0.6000	620.0	3854
19	24	0.5500	572.5	4463
	25	0.5000	525.0	5115
20	26	0.4500	477.5	5816
	27	0.4000	430.0	6576
21	28	0.3500	382.5	7408
	29	0.3000	335.0	8328
22	30	0.2500	287.5	9360
	31	0.2000	240.0	10541
23	32	0.1500	192.5	11930
	33	0.1000	145.0	13630
24	34	0.0600	107.0	15355
	35	0.0270	75.7	17205
25	36	0.0000	50.0	19260

5.2 CAMx Meteorological Diagnostic Sensitivity Tests

Four separate CAMx 2014 36/12/4-km diagnostic sensitivity tests were conducted for the first portion of the summer 2014 modeling episode that spanned May 15 to June 4, 2014. The purpose of the four meteorological inputs CAMx sensitivity tests was to identify the optimal meteorological inputs for the final CAMx 2014 base case simulation. The four sets of CAMx simulations were based on the WRF/NAM and WRF/ERA5 2014 36/12/4-km simulations described in Chapter 2 processed by WRFCAMx to generate two sets of vertical mixing coefficient (Kv) as described above:

1. WRF/NAM with CMAQ Kv
2. WRF/NAM with YSU Kv
3. WRF/ERA5 with CMAQ Kv
4. WRF/ERA5 with YSU Kv

Ozone model predictions from each sensitivity test were compared with observed ozone concentrations in New Mexico. Figures 5-1 and 5-2 summarize the normalized mean bias (NMB) and error (NME) for each site in New Mexico during the modeling period. The statistics presented in these figures were calculated using a 60 ppb cutoff value relative to observed MDA8 ozone concentrations to understand the performance of each sensitivity test when ozone concentrations are most relevant to the NAAQS. Figure 5-1 shows that the NMB is generally within $\pm 10\%$ (colored grey) at almost all sites (note that the NMB performance goal is $\pm 5\%$ and criteria is $\pm 15\%$). All of the sensitivity simulations have an under-prediction bias for observed ozone greater than 60 ppb at sites in the southern portion of the domain such that for one or two sites have a bias even lower than -10% (i.e., colored bright green). The WRF/NAM with CMAQ Kv sensitivity test has slightly better performance than the others with less underestimation bias (e.g., all sites but one are within $\pm 10\%$ compared to two sites for the other tests). Figure 5-2 shows that the NME is also generally within the performance goal (less than 15%) in all cases, with the southern portions of NM showing the largest errors but still within the performance criteria (less than 25%). The figure shows that CAMx using the WRF/NAM inputs tends to have slightly lower error and better ozone performance than when the WRF/ERA5 meteorological inputs are used.

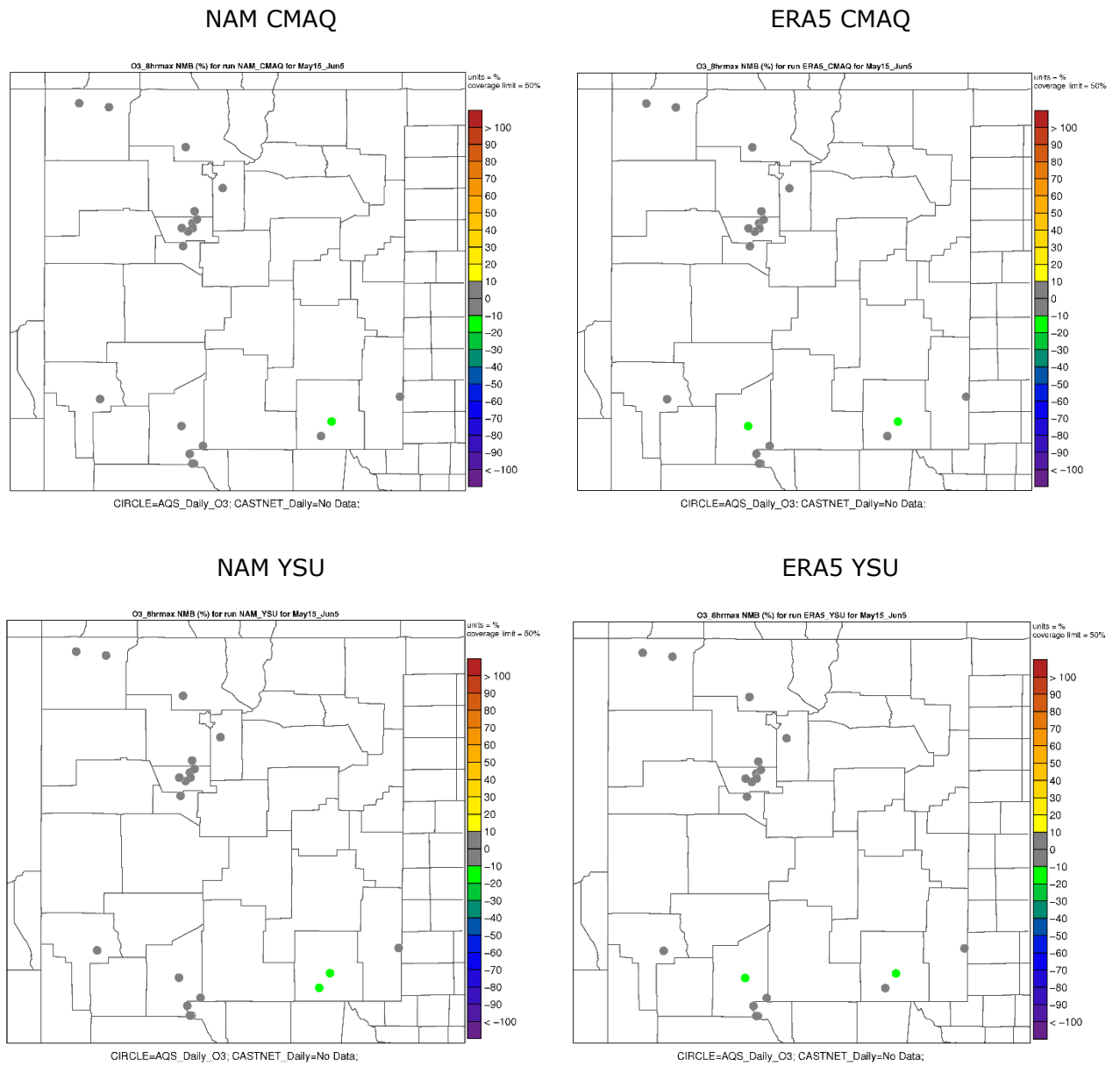


Figure 5-1. Comparison of sensitivity tests NMB with 60 ppb cutoff spatial plots over NM.

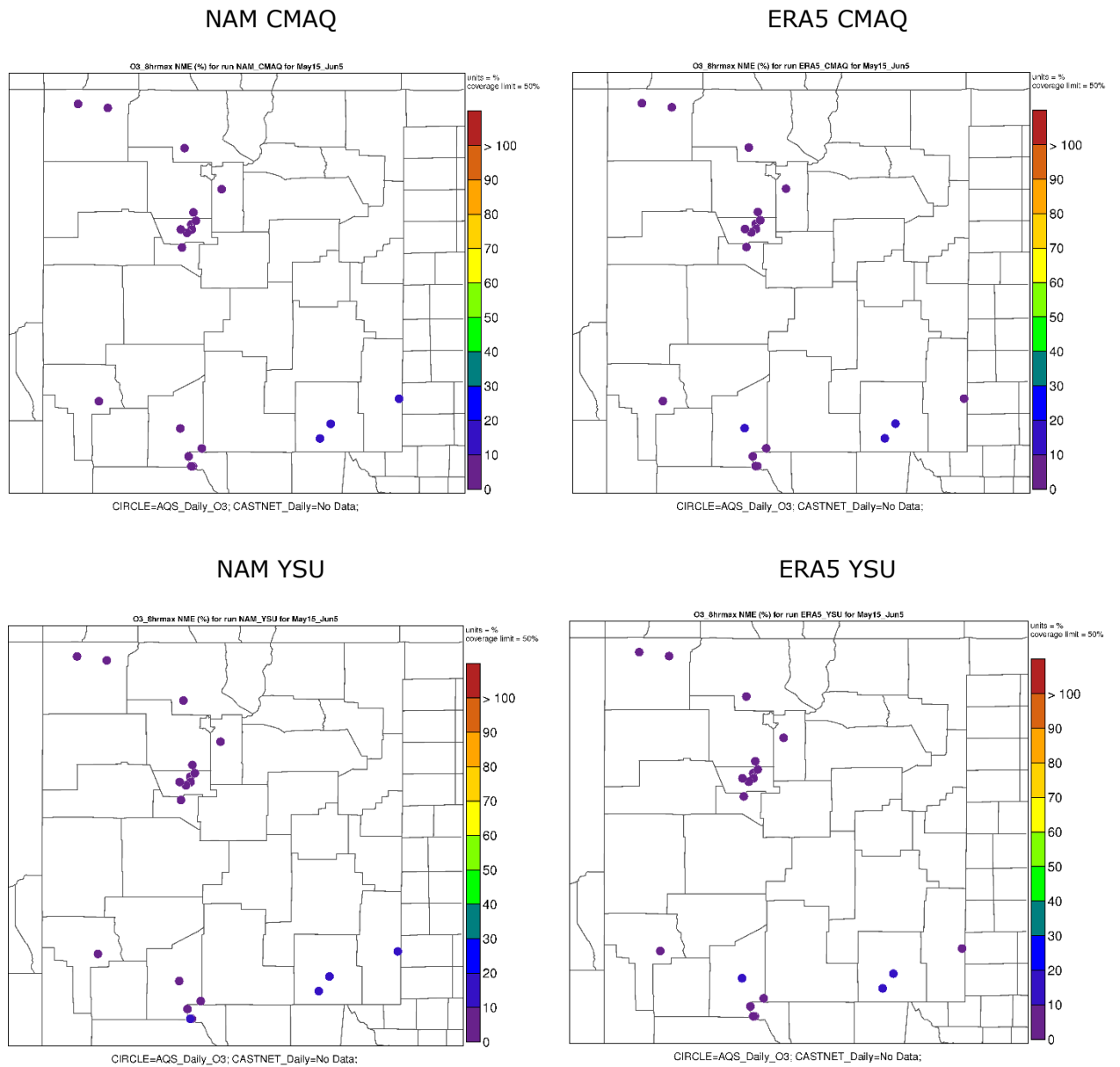


Figure 5-2. Comparison of sensitivity tests NME with 60 ppb cutoff spatial plots over NM.

Figure 5-3 presents soccer plots of bias and error for observed ozone above 60 ppb and all four CAMx sensitivity tests. This figure plots site-specific bias versus error with performance lines in the shape of a soccer goal, when the site-specific bias and error symbol falls within the soccer goal area (i.e., the red box) it is easy to see when the ozone performance goals are achieved. The figure shows that all sites have NMB and NME that fall within the performance criteria for bias ($\leq \pm 15\%$) and error ($\leq 25\%$), with most sites having an underestimation bias of the high (> 60 ppb) observed ozone concentrations. The CAMx simulations with the WRF/NAM meteorological inputs has slightly better performance than when the WRF/ERA5 inputs are used as more sites fall within the performance soccer goal area. Comparison between the NAM cases indicate that the test with CMAQ Kv has slightly smaller errors relative to the test with YSU Kv.

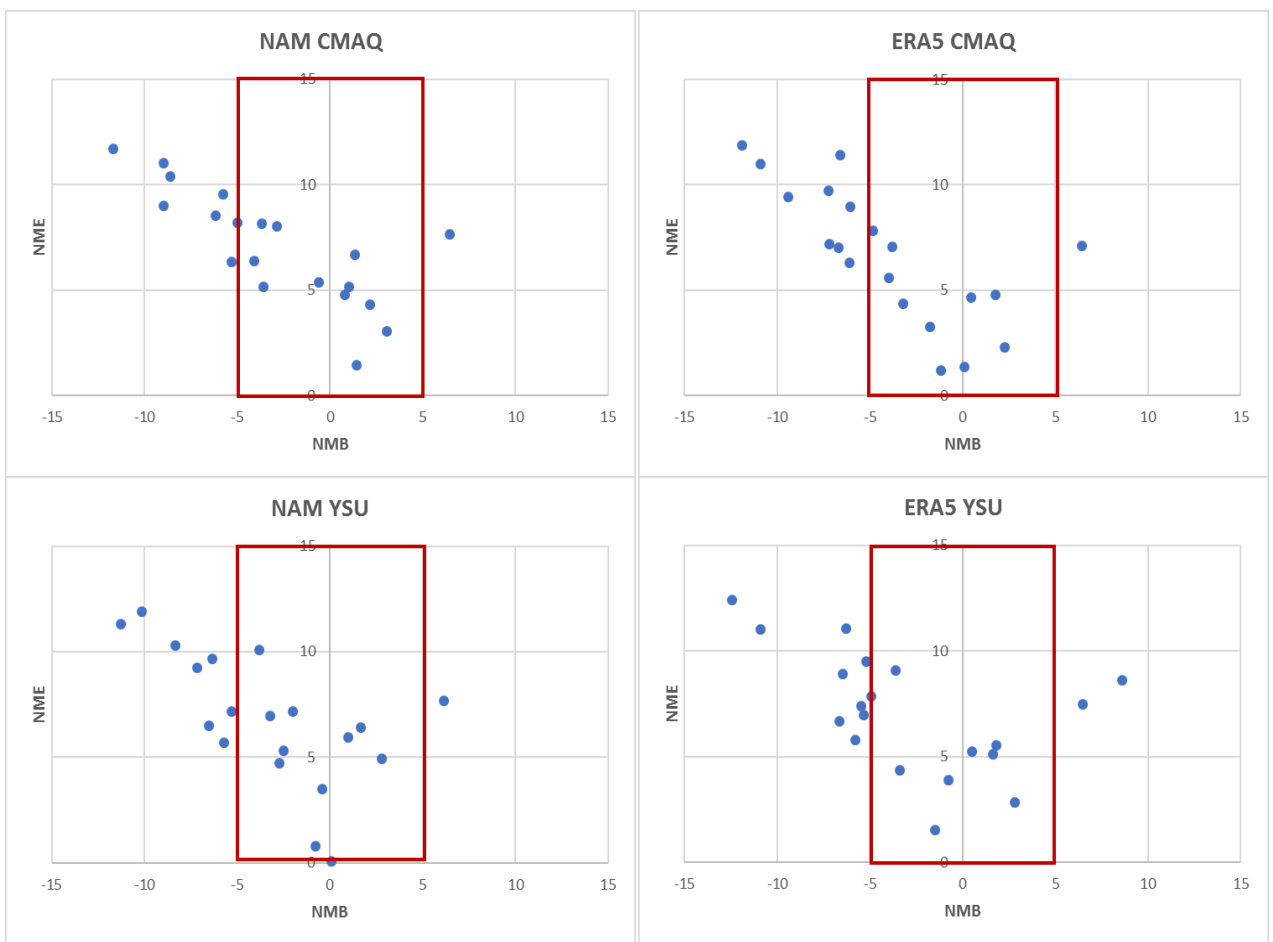


Figure 5-3. Comparison of sensitivity tests soccer plots with 60 ppb cutoff. Red rectangle indicates the performance goal soccer area.

Figures 5-4 to 5-7 present time series of predicted and observed MDA8 ozone concentrations for selected sites in Dona Ana, Eddy and Sandoval counties. At the Solano Road site in Dona Ana County the time series shows that the observed peak ozone concentration on May 29 is matched very well by the CAMx WRF/NAM sensitivity tests, while the CAMx WRF/ERA5 sensitivity test under-predicts by approximately 10 ppb (Figure 5-4). At the Desert View site, which is also in Dona Ana County, all four CAMx sensitivity tests underestimate the high observed ozone on May 28-29, but the CAMx WRF/NAM tests perform slightly better than the CAMx WRF/ERA5 test (Figure 5-5). At the Carlsbad site in Eddy County all test cases under-predict the high ozone concentration from May 27 to May 31 (Figure 5-6). For the site in Sandoval county (Figure 5-7) all four CAMx sensitivity tests track the daily variations of the observed MDA8 ozone including getting the timing and values of the observed ozone peak on May 29, but the CAMx WRF/NAM with CMAQ Kv test exhibits the lowest biases.

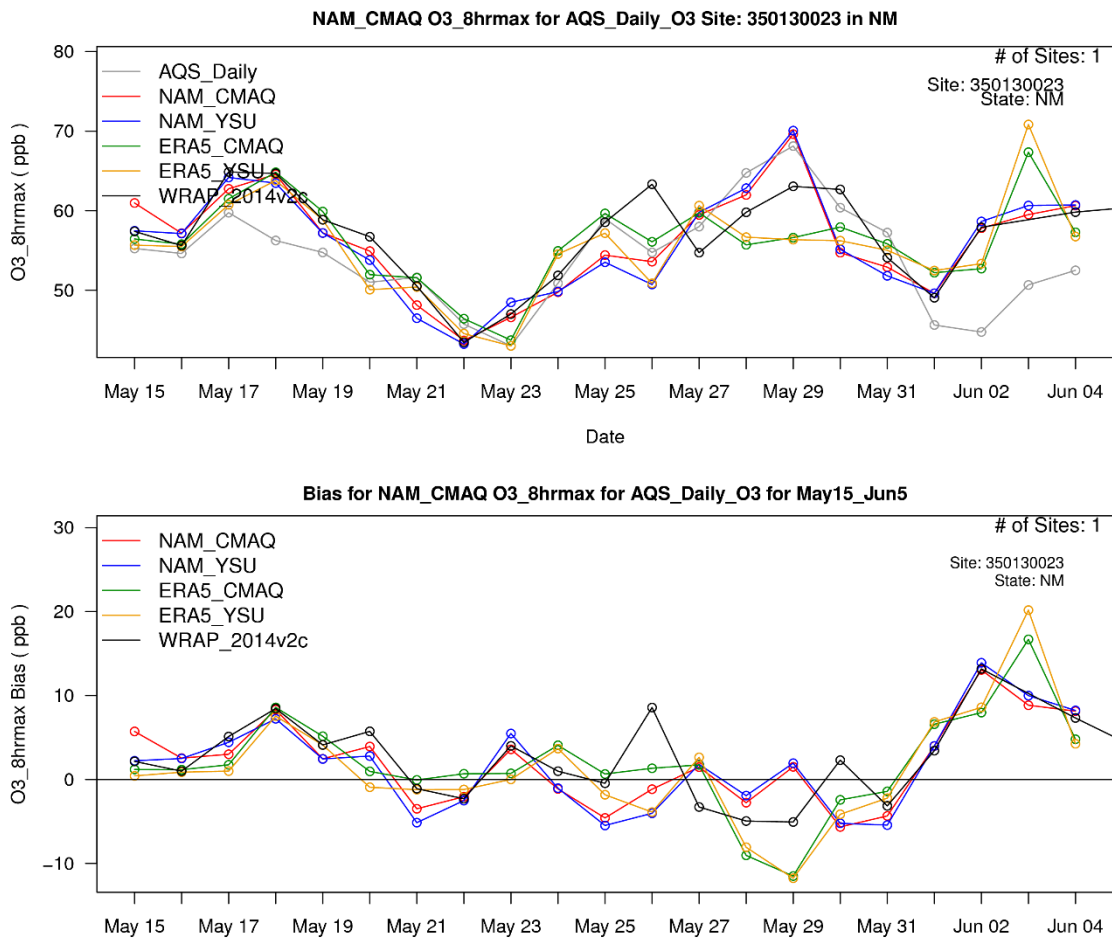


Figure 5-4. Timeseries comparison of sensitivity tests with observations (top) and bias (bottom) at Solano Road site, Dona Ana County

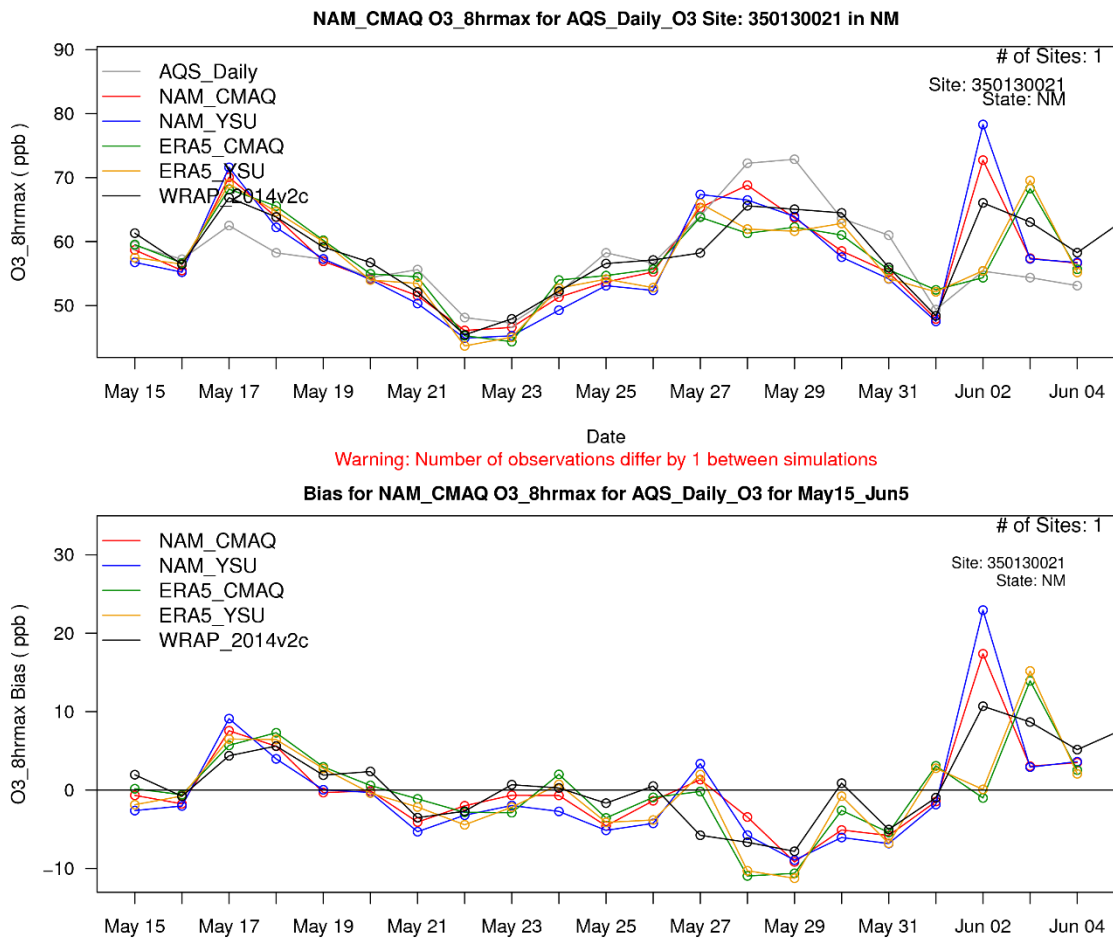


Figure 5-5. Timeseries comparison of sensitivity tests with observations (top) and bias (bottom) at Desert View site, Dona Ana County

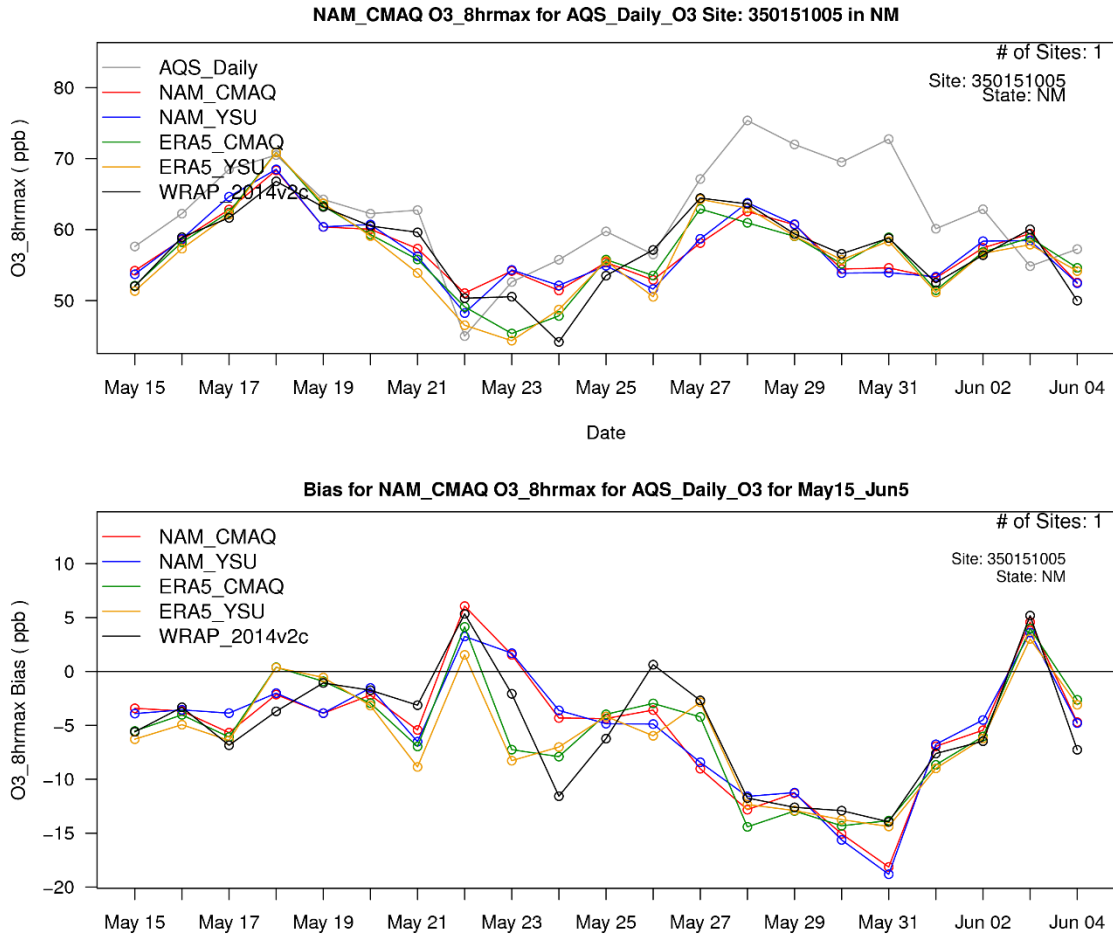


Figure 5-6. Timeseries comparison of sensitivity tests with observations (top) and bias (bottom) at Carlsbad site, Eddy County

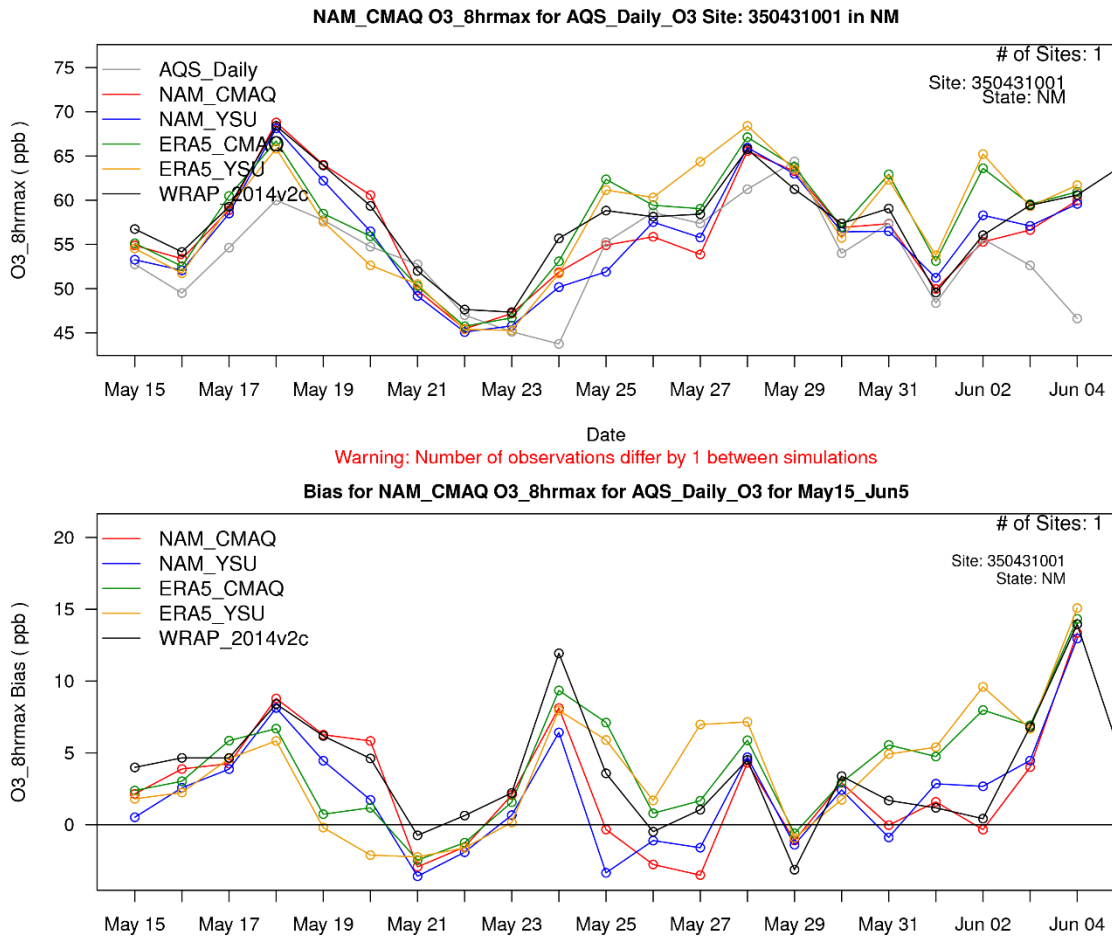


Figure 5-7. Timeseries comparison of sensitivity tests with observations (top) and bias (bottom) at Albuquerque site, Sandoval County

5.3 Summary CAMx Diagnostic Sensitivity Tests

All four of the CAMx meteorological sensitivity cases have biases and errors well within the performance criteria and in most cases even within the more stringent performance goals. For the modeled episode, the differences in performance among all the cases considered are relatively minor. On some sites and days, CAMx using the WRF/NAM meteorology tends to capture peak ozone concentrations better than when the WRF/ERA5 meteorology is used. Note that the sensitivity tests were performed on a period in late spring (May to June) when ozone concentrations exceeded the NAAQS, however they may not reflect the observed precipitation biased observed in the WRF MPE for the period of June to August. Also, the WRF performance showed that precipitation biases could occur over northeast NM where there are no ozone monitors so CAMx model performance is unknown in that region. Based on the results presented here, the final CAMx 2014 base case model configuration will use the WRF/NAM with CMAQ Kv treatment meteorological inputs.

6. FINAL MODEL BASE CASE CONFIGURATION

This section summarizes the final CAMx base case model configuration for the summer of 2014 modeling of New Mexico that includes the meteorological, emissions, and air quality inputs as well as CAMx option and configuration. The modeling procedures used in the NM OAI Study modeling are consistent with EPA’s latest ozone modeling guidance documents (EPA, 2018d) and past modeling studies of the western U.S. and followed the procedures laid out in the NM OAI Study modeling protocol (WESTAR and Ramboll, 2020a).

6.1 Meteorological Inputs

Procedures for WRF meteorological modeling for the NM OAI Study 2014 36/12/4-km applications are described in Chapter 2. Chapter 5 describes the CAMx diagnostic sensitivity tests using four different meteorological inputs that were based on two 2014 WRF simulations (WRF/NAM and WRF/ERA5) that were processed to generate CAMx inputs using two different two vertical mixing (Kv) options in the WRFCAMx processor (CMAQ-like and YSU). Although the ozone model performance for the four CAMx meteorological sensitivity tests were similar, the CAMx simulation using the WRF/NAM with CMAQ-like vertical mixing coefficients inputs was selected based on the best ozone model performance.

6.2 Emission Inputs

The 36-km and 12-km emissions used in the NM OAI Study CAMx 2014 base case simulation were based on the WRAP-WAQS 2014v2 emissions. Chapter 4 describes the updates to the WRAP-WAQS 2014v2 emissions for New Mexico and the development of the emission inputs for the New Mexico 4-km domain.

6.3 Photochemical Model Inputs

6.3.1 PGM Science Configuration and Input Configuration

This section describes the final CAMx 2014 base case configuration and science options used in the NM OAI Study ozone modeling. Table 6-1 summarizes the CAMx configuration and option used, with more details provided below.

6.3.1.1 PGM Model Versions

The latest version 7.0 (v7.0) of CAMx was used in the NM OAI Study. This is the same version used in the WRAP-WAQS 2014v2 modeling and as well as EPA in their national Regional Haze modeling (EPA, 2019). The model was configured to predict both ozone and PM species.

6.3.1.2 PGM Grid Nesting Strategy

CAMx was operated using the 36/12/4-km nested grid structure shown in Figure 1-10 using two-way grid nesting for all simulations.

6.3.1.3 Initial and Boundary Conditions

Boundary Conditions (BCs) for the CAMx most outer 36-km 36US modeling domain lateral boundaries were based on output from a 2014 simulation of the GEOS-Chem global chemistry conducted by WRAP for their 2014v2 modeling platform. A zero-gradient top BC was specified where the concentrations above the top of CAMx are assumed to be the same as in the top layer of CAMx.

CAMx was started on May 1, 2016 using the 36/12/4-km domains that allowed the model over two-weeks to initialize the model and wash out the initial concentrations before the first high ozone day on May 17, 2014.

6.3.1.4 Other PGM Model Options

The CAMx model options and setup are defined in Table 6-1. The PPM advection solver (Colella and Woodward, 1984) was used for horizontal transport along with the spatially varying (Smagorinsky) horizontal diffusion approach. K-theory was used for vertical diffusion using the CMAQ-like Kv profiles from the WRF/CAMx processing of the WRF/NAM output. The CB6r4 gas-phase chemical mechanism was selected because it includes the very latest chemical kinetic rates with halogen chemistry that affects ozone levels over the ocean. The latest aerosol mechanism was used in CAMx along with the standard wet and dry deposition schemes. The Plume-in-Grid module was used to treat the near-source chemistry and dispersion of major NO_x emissions sources in the New Mexico 4-km domain for sources with greater than 5 tons per day NO_x emissions.

Table 6-1. Final CAMx model configuration for the NM OAI Study.

Science Options	CAMx	Comment
Model Codes	CAMx v7.0	Latest version of CAMx made publicly available May 2020 (www.camx.com)
Horizontal Grid Mesh	36/12/4-km	
36-km grid	148 x 112 cells	36US domain
12-km grid	227 x 215 cells	12WUS2 domain. Includes buffer cells
4-km grid	245 x 227 cells	New Mexico 4-km domain. Includes buffer cells
Vertical Grid Mesh	25 vertical layers, defined by WRF	Layer 1 thickness ~20 m. Model top at 50 mb (~19 km). Layer collapsing from 35 vertical layers in WRF
Grid Interaction	36/12/4 km two-way nesting	
Initial Conditions	Start on May 1, 2014	First high ozone day is May 17, 2014
Boundary Conditions	WRAP 2014 GEOS-Chem	For 36US domain lateral boundaries
Emissions		
Baseline Emissions Processing	SMOKE, SMOKE-MOVES2014, MEGAN	WRAP/WAQS 2014v2 emissions and EPA 2023fh for future year
Sub-grid-scale Plumes	Plume-in-Grid for major NO _x sources in New Mexico	Point sources with NO _x emission s greater than 5 tons per day
Chemistry		
Gas Phase Chemistry	CB6r4	Latest chemical reactions and kinetic rates with halogen chemistry (Yarwood et al., 2010)
Meteorological Processor	WRFCAMx	Compatible with CAMx v7.0
Horizontal Diffusion	Spatially varying	K-theory with Kh grid size dependence
Vertical Diffusion	CMAQ-like Kv	Evaluated YSU Kv scheme
Diffusivity Lower Limit	Kv-min = 0.1 to 1.0 m ² /s in lowest 100 m	Depends on urban land use fraction
Deposition Schemes		
Dry Deposition	Zhang dry deposition scheme	(Zhang et. al, 2001; 2003)
Wet Deposition	CAMx -specific formulation	rain/snow/graupel
Numerics		
Gas Phase Chemistry Solver	Euler Backward Iterative(EBI)	EBI fast and accurate solver
Vertical Advection Scheme	Implicit scheme w/ vertical velocity update	Emery et al., (2009a,b; 2011)
Horizontal Advection Scheme	Piecewise Parabolic Method (PPM) scheme	Colella and Woodward (1984)
Integration Time Step	Wind speed dependent	~0.5-1 min (4-km), 1-5 min (12-km), 5-15 min (36-km)

7. 2014 BASE CASE MODELING AND MODEL PERFORMANCE EVALUATION

This Chapter describes the CAMx 2014 base case simulations and model performance evaluation (MPE). The primary purposes of the MPE is to establish the reliability of the CAMx 2014 base case modeling for predicting maximum daily average 8-hour (MDA8) ozone and related concentrations in New Mexico to have confidence that the modeled ozone responses to changes in emissions are accurate enough for air quality planning in New Mexico. The CAMx 2014 base case model estimates are compared against the observed ambient ozone and other concentrations to establish that the model is able to reproduce the current year observed concentrations, so it is likely a reliable tool for estimating future year ozone levels. The model performance evaluation includes many types of graphical and statistical comparisons of the predicted and observed ozone concentrations, including spatial plots, scatter plots and time series analysis.

7.1 2014 Base Case Modeling

A CAMx 2014 May-August 36/12/4-km base case simulation was performed following the procedures outlined in the previous Chapters.

7.2 EPA Model Performance Evaluation Recommendations

7.2.1 Overview of EPA Model Performance Evaluation Recommendations

EPA's ozone modeling guidance (EPA, 2018d) describes a MPE framework that has four components:

- Operation Evaluation: The Operation Evaluation compares the modeled concentration estimates against concurrent observations using statistical and graphical analysis aimed at determining how well the model simulates the base year observed concentrations (i.e., does the model get the right answer).
- Diagnostic Evaluation: The Diagnostic Evaluation evaluates various components of the modeling system. It focuses on process-oriented evaluation and whether the model simulates the important processes for the air quality problem being studied (i.e., does the model get the right answer for the right reason).
- Dynamic Evaluation: The ability of the model's air quality predictions to correctly respond to changes in emissions and meteorology is part of the Dynamic Evaluation. This can include running the model for historical years to see whether the model's predictions match the changes in observations; comparison of model performance on weekdays versus weekend days can also help elucidate whether the model response to changes in emissions correctly.
- Probabilistic Evaluation: The Probabilistic Evaluation assess the level of confidence in the model predictions and estimates model uncertainty through techniques such as ensemble model simulations.

EPA's guidance recommends that "At a minimum, a model used for air quality planning should include a complete operational MPE using all available ambient monitoring data for the base case model simulations period" (EPA, 2018d, pg. 68). And goes on to say,

“Where practical, the MPE should also include some level of diagnostic evaluation.” EPA notes that there is no single definite test for evaluating model performance, but instead there are a series of statistical and graphical MPE elements to examine model performance in as many ways as possible while building a “weight of evidence” (WOE) that the model is performing sufficiently well for the air quality problem being studied.

For the NM OAI Study we conducted an operational MPE for MDA8 ozone focusing on ozone model performance within the state of New Mexico. We also conducted some elements of a diagnostic evaluation as described in Chapter 5.

7.3 Overview of Evaluation of CAMx 2014 Base Case Procedures

This section provides an overview of the approach, procedures and tools used the procedures for evaluating the performance of the CAMx model focusing on ozone in New Mexico.

7.3.1 Photochemical Model Evaluation Methodology

The CAMx model performance evaluations will follow the procedures recommended in the EPA’s latest photochemical modeling guidance (EPA, 2018d), some elements of EPA MPE Checklist (EPA, 2015a,b), and procedures discussed by Boylan and Russell (2006), Simon, Baker and Phillips (2012) and Emery and co-workers (2016).

7.3.2 Model Performance Goals and Benchmarks

EPA first proposed the use of ozone model performance goals in their 1991 ozone modeling guidance (EPA, 1991) with goals for bias ($\leq \pm 15\%$) and error ($\leq 35\%$). Since then, EPA has de-emphasized the use model performance goals as some users were focusing on achieving the model performance goals not on whether the model was accurately simulating atmospheric processes that led to the high ozone concentrations. However, model performance goals are still useful for helping interpret model performance and putting the model performance into context. Since the EPA 1991 ozone guidance performance goals, Boylan and Russell (2006) extended the performance goals to PM species and visibility. Simon, Baker and Phillips (2012) summarized the model performance statistics from 69 PGM applications from 2006 to 2012 and found lots of variability but were able to isolate model performance statistical levels for the best performing models.

Emery et al., (2016) built off the work of Simon, Baker and Phillips (2012) adding additional PGM model applications and coming up with a set of PGM model performance goals and criteria based on the variability in the past PGM model performance. “Goals” indicate statistical values that about a third of the top performance past PGM applications have met and should be viewed as the best a model can be expected to achieve. “Criteria” indicates statistics values that about two thirds of past PGM applications have met and should be viewed as what a majority of the models have achieved. In this Chapter we compare the CAMx 2014 base case simulations model performance statistics for normalized mean bias (NMB), normalized mean error (NME) and correlation coefficient (r) against the model performance goals and criteria summarized by Emery et al., (2016) that are given in Table 7-1.

Table 7-1. Recommended benchmarks for photochemical model statistics (Source: Emery et al., 2016).

Species	NMB		NME		r	
	Goal	Criteria	Goal	Criteria	Goal	Criteria
1-hr & MDA8 Ozone	<±5%	<±15%	<15%	<25%	>0.75	>0.50
24-hr PM _{2.5} , SO ₄ , NH ₄	<±10%	<±30%	<35%	<50%	>0.70	>0.40
24-hr NO ₃	<±15%	<±65%	<65%	<115%	NA	NA
24-hr OC	<±15%	<±50%	<45%	<65%	NA	NA
24-hr EC	<±20%	<±40%	<55%	<75%	NA	NA

7.3.3 Available Aerometric Data for the Evaluations

There are two main ozone monitoring networks operating in New Mexico in 2014:

EPA AQS Surface Air Quality Data: Data files containing hourly-averaged concentration measurements at a wide variety of state and EPA monitoring networks are available in the Air Quality System (AQS⁴⁰) database throughout the U.S. Typical surface measurements at the ground level routine AIRS monitoring stations include ozone, NO₂, NO_x and CO.

CASTNet Monitoring Network: The Clean Air Status and Trends Network (CASTNet⁴¹) operates approximately 80 monitoring sites in mainly rural areas across the U.S. CASTNet sites typically collect hourly ozone and weekly speciated PM_{2.5}, including HNO₃. There is one CASTNet site located in the northwest corner of New Mexico (Chaco Culture NHP), although there are three more CASTNet sites in the 4-km New Mexico modeling domain: Mesa Verde in Colorado, Petrified Forest in Arizona and Palo Duro in Texas.

7.3.4 Atmospheric Model Evaluation Tool (AMET)

The Atmospheric Model Evaluation Tool (AMET⁴²) (Appel et al., 2011) is a suite of software designed to facilitate the analysis and evaluation of predictions from meteorological and air quality models. AMET matches the model output for grid cells with observations from monitoring site locations from one or more networks of monitors. AMET also does species mappings to map the modeled species to the corresponding observations. These pairings of values (model and observation) are then used to statistically and graphically analyze the model's performance using a variety of techniques, many of which were used in the CAMx 2014 base case MPE. The latest version of AMET is version 1.4, but AMET website doesn't have any information on its release date or documentation so we assume the documentation for AMET v1.3⁴³ is pertinent for AMET v1.4.

⁴⁰ <https://www.epa.gov/aqs>

⁴¹ <https://www.epa.gov/castnet>

⁴² <https://www.cmascenter.org/amet/>

⁴³ <https://www.cmascenter.org/help/documentation.cfm>

7.4 Ozone Evaluation Across the 4-km New Mexico Domain

Figure 7-1 shows the scatter plots of predicted and observed MDA8 ozone concentrations across AQS and CASTNet sites. The AQS sites (Figure 7-1, left) represent mainly the urban locations and whereas CASTNET (Figure 7-1, right) represent monitoring sites that are more rural. Most of the observation-model pair dots in the scatter plots appear to lie along the 1:1 line with very few outliers. The center of the AQS MDA8 ozone scatter plot lies slightly above the 1:1 line of perfect agreement indicating a slight overestimation bias. These scatter plots also displays the Normalized Mean Bias (NMB) and Error (NME) metrics. The average NMB for all MDA8 ozone concentrations and across all AQS sites shows an average overestimation bias of 6.2%, which is slightly higher than the bias performance goal ($\leq \pm 5\%$) but within the bias performance criteria ($\leq \pm 15\%$). The NME for MDA8 ozone across all AQS sites in the 4-km domain is 10.9%, which is well within the error performance goal ($\leq 15\%$).

The average MDA8 ozone NMB at all CASTNet sites is 0.1% which is very low and quite good ozone performance well within the bias performance goal. The MDA8 ozone NME across the CASTNet sites is also very good at 7.9%.

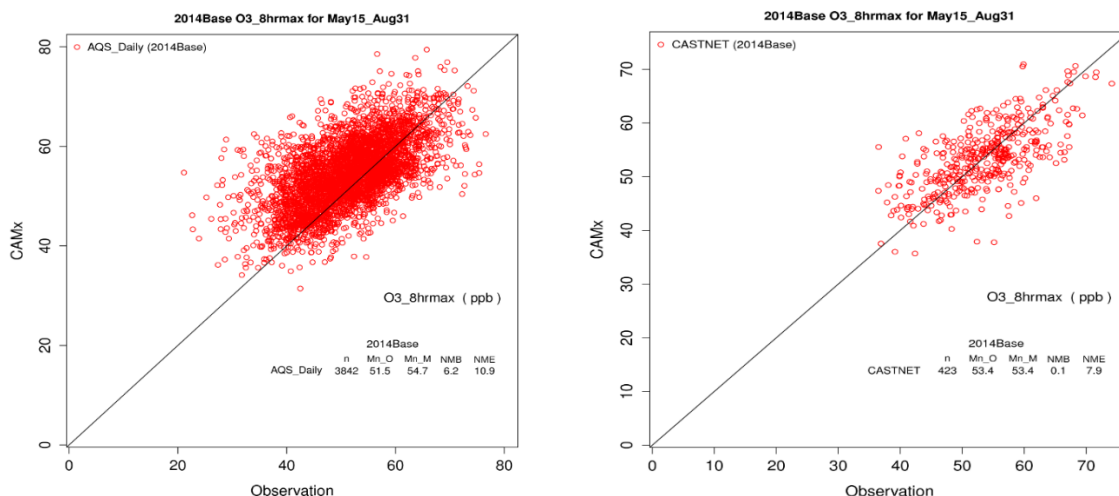


Figure 7-1. Scatter plot of predicted and observed MDA8 ozone across the AQS and CASTNET monitoring sites within the 4-km New Mexico domain during the modeling period (May 15-Aug 31, 2014) for the CAMx 2014 base case simulations.

Figure 7-2 displays the spatial distribution of the AQS and CASTNet site-specific NMB for the modeling period and for all MDA8 ozone (left) and MDA8 ozone when the observed ozone is above a 60 ppb cut-off (here after referred as MDA8_above60). Throughout the domain, the model NMB for all MDA8 ozone achieved the ozone bias performance goal ($\leq \pm 5\%$) at majority of the sites (i.e., symbols colored grey). At few sites, the model showed an overprediction (yellow color) in predicting all MDA8 ozone concentrations. With one exception for a site colored orange in El Paso, the sites with the overestimation bias are colored bright yellow that indicates bias in the +5% to +15% range so achieve the ozone bias performance criteria.

For MDA8_above60 (Figure 7-2, right panel) for most sites in the 4-km domain the NMB symbols are colored grey indicating that they achieve the ozone bias performance goal. Several sites are colored bright green that indicates an underestimation bias that are unable to achieve bias performance goal ($\leq \pm 5\%$) but is within the ozone bias performance criteria ($\leq \pm 15\%$) so the bias is between -5% and -15%.

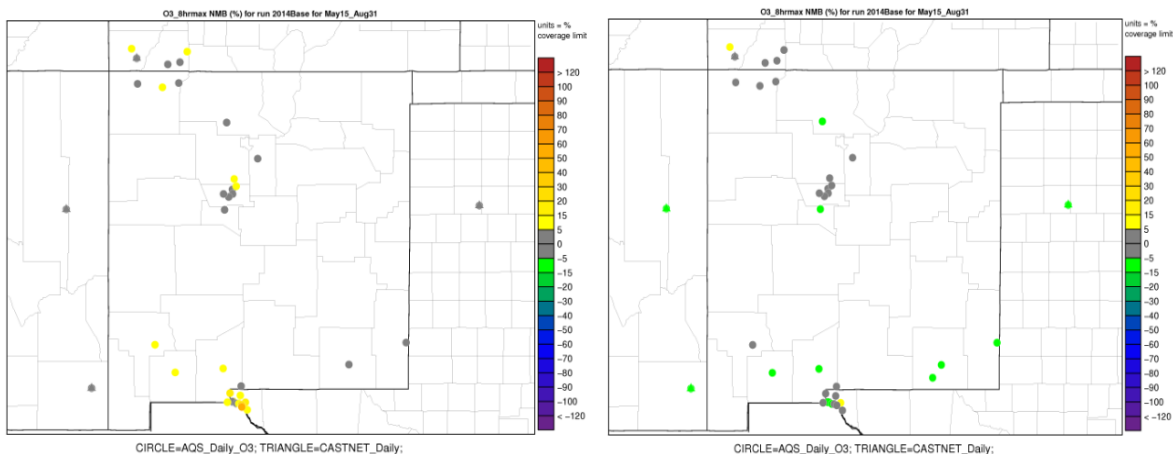


Figure 7-2. Spatial distribution of CAMx 2014 base case simulation period (May15-Aug 31) site-specific Normalized Mean Bias within the 4-km domain for MDA8 O3 (left) and MDA8 O3 above 60ppb cut-off (right).

7.5 Ozone Evaluation Across New Mexico

In this section we evaluated the modeled MDA8 ozone and MDA8_above60 ozone in the state of New Mexico at all AQS monitoring sites using scatter, soccer and spatial overlay plots. Figure 7-3 presents scatter plots of MDA8 and MDA8_above60 ozone modeled and observation paired concentrations, it indicate that the modeled values are close to the observations as majority of them lie along and in the vicinity of 1:1 line. The domain wide all AQS sites MPE statistics of MDA8 and MDA8_above60 ozone NMB (5.0%, -4.3%) and NME (9.8%, 8.0%) metrics are within the ozone performance goals (i.e., $NMB < \pm 5\%$ and $NME < 15\%$).

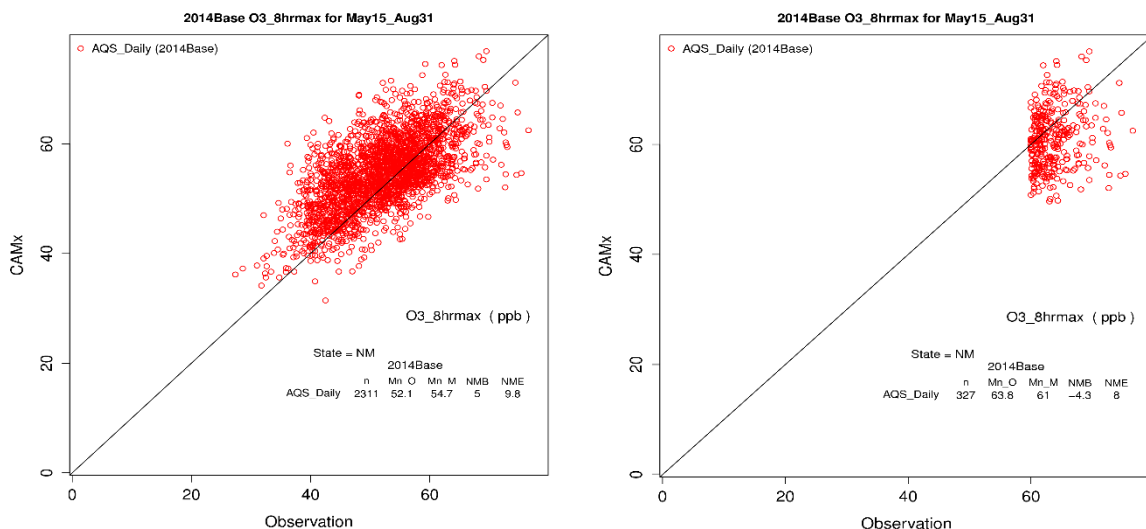


Figure 7-3. Scatter plots of predicted and observed MDA8 ozone (left) and MDA8 ozone when observed value is above 60 ppb cut-off (right) across the AQS monitoring sites in New Mexico during modeling period (May15-Aug 31) for the CAMx 2014 base case simulations.

Figure 7-4 displays the monthly soccer plot for sites in New Mexico and for MDA8 (left) and MDA8_above60 (right) ozone concentrations with the inner rectangle being the performance goal (NMB<±5% and NME<15%) and the outer rectangle being the performance criteria (NMB<±15% and NME<25%). Considering all MDA8 ozone data with no cut-off (i.e., Figure 7-4 left panel), the model is overestimating in the months of July and August achieving the performance criteria but not the performance goals. The months of May and June achieve the performance goals.

Considering the ozone data with 60 ppb cut-off (i.e., Figure 7-4 right panel), the model achieves the ozone performance goals in June, July and August months with an underestimation bias. In May, the underestimation bias for MDA8_above60 is lower than -5% so fails to achieve the bias performance goal, but does achieve the performance criteria. Overall, the soccer plots indicate that the model captures the observed MDA8 and MDA8-above60ppb ozone concentrations well during each month of the summer of 2014

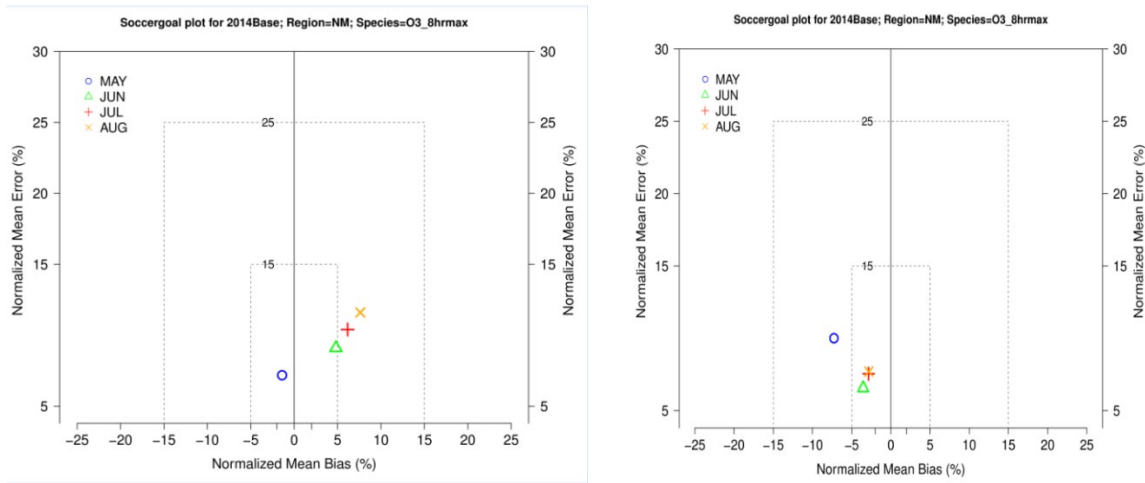


Figure 7-4. Soccer plots of MDA8 ozone (left) and MDA8 ozone when observed value is above a 60 ppb cut-off (right) with monthly average NMB and NME values across sites in New Mexico. The dashed lines represents the performance goals and criteria.

As shown in site-specific spatial NMB plot for New Mexico sites in Figure 7-5, the overestimation of MDA8 ozone (considering all values) that fails to achieve the bias performance goal occurs mainly at southern sites along with three other northerly sites (Bloomfield, North Valley and Foothills). The underestimation of MDA8_>60 that fails to achieve the bias performance goal occurs primarily at southern sites along with two more northerly sites (Coyote Ranger and Los Lunas).

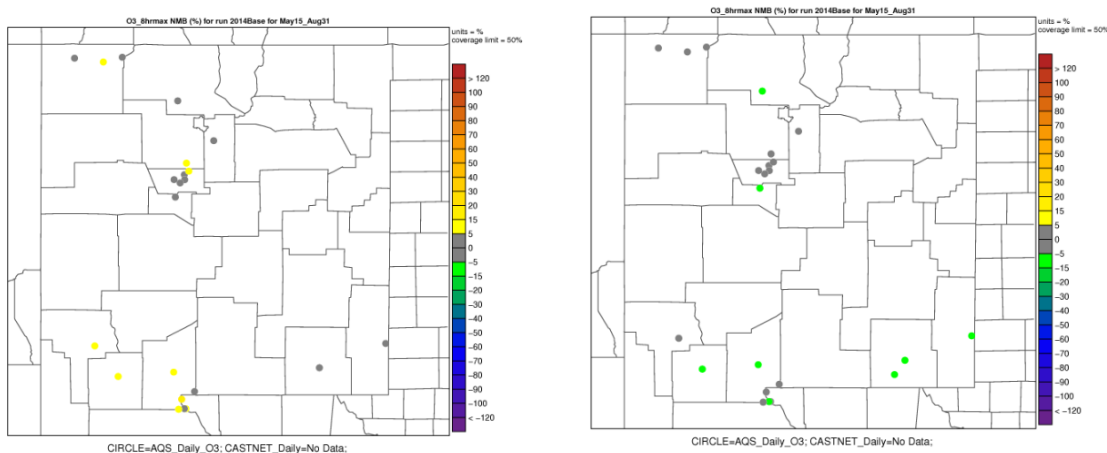


Figure 7-5. Spatial distribution of site-specific Normalized Mean Bias for sites in New Mexico and the CAMx 2014 May-August base case simulation for all MDA8 ozone data (left) and MDA8 ozone with observed value above a 60 ppb cut-off (right).

7.6 Ozone Evaluation in New Mexico Subregions

As shown in the New Mexico ozone performance above, and discussed in the conceptual model in Chapter 1, there are three distinct large regions of ozone formation conditions in New Mexico, each with their own subregional variations: northern New Mexico that shares ozone attributes of other sites in other states in the Four Corners region, Bernalillo County that has many of the attributes of the northern New Mexico sites only also including the presence of a major city; and sites in southern New Mexico. The ozone MPE is conducted separately for each of these major subregions in New Mexico. Table 7-2 shows the AQS sites available in the New Mexico with ozone data during 2014 that are categorized into northern New Mexico (blue), Bernalillo County (yellow) and south New Mexico (orange) subregions. The NMB and NME values shown in Table 7-3 are averaged across all sites in these regions and color coded based on the performance benchmarks for both MDA8 ozone and MDA8above60: green if achieve the performance goal; yellow if falling between the performance goal and criteria; and red if fails to achieve the performance criteria. Both northern and Bernalillo County regions achieve the ozone bias and error performance goal for both MDA8 ozone concentrations without and with an observed MDA8 ozone 60 ppb cut-off threshold. The southern region has NMB that fall between the ozone bias performance goal and criteria due to either a too high overestimation bias (all MDA8 data) or too low underestimation bias (MDA8_above60ppb). Although the bias just barely falls outside of the performance goal.

Table 7-2. AQS monitoring sites categorized into subregions of southern New Mexico (orange), Bernalillo County (yellow) and southern New Mexico (blue).

Site ID	Site Name	County	Latitude	Longitude
350130022	Santa Teresa	Dona Ana	31.79	-106.68
350130017	Sunland Park Yard	Dona Ana	31.80	-106.56
350130021	Desert View	Dona Ana	31.80	-106.58
350130008	La Union	Dona Ana	31.93	-106.63
350130020	Chaparral	Dona Ana	32.04	-106.41
350290003	Deming Airport	Luna	32.26	-107.72
350130023	Solano	Dona Ana	32.32	-106.77
350151005	Carlsbad	Eddy	32.38	-104.26
350171003	Chino Copper Smelter	Grant	32.69	-108.13
350250008	Hobbs Jefferson	Lea	32.73	-103.12
350610008	Los Lunas	Valencia	34.81	-106.74
350010029	South Valley	Bernalillo	35.02	-106.66
350010024	South East Heights	Bernalillo	35.06	-106.58
350010032	Westside	Bernalillo	35.06	-106.76
350010023	Del Norte	Bernalillo	35.13	-106.59
350011012	Foot Hills	Bernalillo	35.19	-106.51
350431001	Bernalillo	Sandoval	35.30	-106.55
350490021	Santa Fe Airport	Santa Fe	35.62	-106.08
350390026	Coyote Ranger District	Rio Arriba	36.19	-106.70
350450009	Bloomfield	San Juan	36.74	-107.98
350451005	Sub Station	San Juan	36.80	-108.47
350450018	Navajo Lake	San Juan	36.81	-107.65

Table 7-3. Region specific NMB and NME values for MDA8 Ozone and MDA8 Ozone when Observed Value is above 60 ppb.

Region	MDA8 O3		MDA8 _above60	
	NMB (%)	NME (%)	NMB (%)	NME (%)
North NM	4.3	9.1	0	6.4
Bernalillo	4.3	9.4	-2.8	7.1
South NM	5.8	10.5	-6.1	8.5

7.7 Ozone Evaluation at Individual New Mexico Monitoring Sites

Table 7-4 contain individual AQS site MDA8 ozone model performance statistics for the CAMx 2014 base case simulation from May 15 to Aug 31, 2014. Among the 22 sites in the state, 13 sites (59%) achieve the bias performance goal (green color, $NMB \leq \pm 5\%$) and 8 sites (36%) exceeded the bias performance goal but achieve the bias performance criteria (orange color, $NMB \leq \pm 15\%$) leaving only one site (La Union in Dona Ana County) whose NMB fails to achieve the bias performance goal. With the exception of the Carlsbad monitor whose MDA8 ozone has a slight underestimation bias (NMB of -1.1%), all sites have a positive NMB when compared to all ozone observations indicating an overestimation bias, with just La Union having an NMB so large (17.4%) that it fails to achieve the ozone bias performance criteria. Also shown in Table 7-4 is the Fractional Bias (FB) whose results are similar to the NMB with just the La Union having a FB (16.4%) that fails to achieve the bias performance criteria.

In terms of NME, all sites achieve the error performance criteria and all sites except for two sites (La Union and Foot Hills) achieve the error performance goal ($NME \leq 15\%$). The results for the Fractional Error (FE) are similar to NME. Overall based on the average NMB and NME values at each site the model appeared to perform well during the modeling period.

Although not color-coded, the correlation (r) performance criteria (> 0.50) for MDA8 ozone is achieved at all monitoring sites. However, the correlation performance goal (> 0.75) is only achieved at one site.

Table 7-4. CAMx 2014 base case model performance statistics for MDA8 Ozone concentrations by monitoring site for summer (May15-Aug) modeling period.

Site ID	Site Name	N	Avg Obs	Avg Mod	MB	ME	NMB	NME	FB	FE	r
350010023	Del Norte	107	54.0	54.9	0.9	4.4	1.7	8.2	1.8	8.3	0.657
350010024	SE Heights	107	53.8	55.4	1.6	4.5	3.1	8.3	3.1	8.3	0.662
350010029	S Valley	108	53.8	55.4	1.6	4.2	3.1	7.7	3.1	7.7	0.69
350010032	Westside	109	54.2	54.8	0.6	4.3	1.1	7.9	1.1	7.9	0.632
350011012	Foot Hills	107	50.4	57.2	6.9	7.6	13.6	15.1	13.0	14.3	0.571
350130008	La Union	108	47.4	55.6	8.2	8.8	17.4	18.6	16.4	17.4	0.72
350130017	Sunland Park	109	50.3	54.8	4.5	6.1	9.0	12.1	9.1	11.8	0.702
350130020	Chaparral	100	52.3	54.8	2.5	4.9	4.8	9.4	5.0	9.2	0.73
350130021	Desert View	108	54.0	55.7	1.7	4.8	3.2	8.9	3.5	8.7	0.717
350130022	Santa Teresa	83	50.5	54.6	4.2	5.3	8.2	10.5	8.1	10.2	0.769
350130023	Solano	108	51.0	54.0	3.1	4.8	6.1	9.4	6.0	9.1	0.727
350151005	Carlsbad	97	53.7	53.1	-0.6	4.9	-1.1	9.0	-0.2	9.0	0.702
350171003	Chino Smelter	105	47.2	51.5	4.3	5.6	9.1	12.0	9.0	11.7	0.693
350250008	Hobbs Jefferson	105	52.9	54.1	1.1	5.1	2.1	9.6	3.0	9.7	0.586
350290003	Deming Airport	108	49.2	52.2	3.0	4.4	6.2	9.0	6.2	8.9	0.745
350390026	Coyote Ranger	105	52.4	54.2	1.7	5.1	3.3	9.8	3.5	9.8	0.55
350431001	Bernalillo	93	52.6	56.9	4.3	5.5	8.1	10.5	7.9	10.2	0.63
350450009	Bloomfield	109	51.6	55.4	3.7	5.3	7.2	10.3	6.9	10.0	0.62
350450018	Navajo Lake	80	54.1	55.3	1.2	3.8	2.2	7.0	2.0	6.9	0.681
350451005	Sub Station	104	54.1	54.8	0.7	4.2	1.4	7.9	1.0	7.9	0.705
350490021	Santa Fe Airport	107	52.8	54.8	2.0	4.6	3.8	8.7	3.8	8.6	0.591
350610008	Los Lunas	107	53.8	54.3	0.4	4.0	0.8	7.5	0.9	7.5	0.633

Similar to Table 7-4, Table 7-5 contain the individual AQS site performance statistics for MDA8 ozone with predicted and observed pairs when the observed value is above a 60 ppb cut-off threshold. Out of the 22 sites, 16 sites (73%) achieve the bias performance goal and the remainder 6 sites (27%) fall between the bias performance goal and criteria. Overall, all the sites showed a consistent slight under-prediction indicating that the model was unable to predict all of the observed ozone peak concentrations. The NME for all sites achieved the ozone error performance goal. The results for FB and FE are consistent with NMB and NME. Almost all of the correlation coefficients fail to achieve the performance criteria for MDA8_above60ppb, although the

sample size for the site-specific MDA8_above60ppb statistics is very small for some sites so the statistics are less meaningful.

Table 7-5. 2014 Base Case model performance statistics of MDA8 Ozone with an observed ozone 60 ppb cut-off by monitoring site for summer (May 15-Aug) modeling period.

Site ID	Site names	N	Avg Obs	Avg Mod	MB	ME	NMB	NME	FB	FE	r
350010023	Del Norte	26	62.2	59.8	-2.4	4.8	-3.9	7.7	-4.2	7.9	-0.167
350010024	SE Heights	20	62.8	61.3	-1.5	4.4	-2.4	7.0	-2.7	7.1	0.31
350010029	South Valley	18	63.0	61.3	-1.8	4.1	-2.8	6.6	-3.1	6.7	0.333
350010032	Westside	21	62.5	60.4	-2.1	4.5	-3.4	7.2	-3.8	7.4	0.045
350011012	Foot Hills	6	62.0	63.2	1.2	4.0	2.0	6.5	1.8	6.4	-0.23
350130008	La Union	7	65.2	64.2	-1.0	4.4	-1.6	6.8	-1.7	6.9	0.128
350130017	Sunland Park	15	64.9	62.6	-2.3	4.9	-3.6	7.6	-3.8	7.8	-0.041
350130020	Chaparral	18	65.4	62.3	-3.0	5.1	-4.7	7.8	-5.1	8	0.565
350130021	Desert View	25	66.2	62.8	-3.4	5.7	-5.1	8.7	-5.4	8.9	0.221
350130022	Santa Teresa	9	64.9	65.0	0.1	4.1	0.1	6.3	0	6.1	0.39
350130023	Solano	11	63.9	59.8	-4.1	4.1	-6.5	6.5	-6.7	6.7	0.807
350151005	Carlsbad	22	65.8	57.7	-8.1	8.1	-12.3	12.3	-13.0	13	0.283
350171003	Chino Smelter	9	63.3	62.7	-0.6	2.2	-1.0	3.4	-1.0	3.4	0.595
350250008	Hobbs Jefferson	20	64.2	57.8	-6.3	7.1	-9.9	11.0	-10.4	11.5	-0.251
350290003	Deming Airport	4	62.2	59.1	-3.1	5.2	-5.0	8.3	-5.4	8.6	0.118
350390026	Coyote Ranger	13	64.3	60.8	-3.5	3.9	-5.4	6.1	-5.7	6.4	0.432
350431001	Bernalillo	11	61.4	63.8	2.4	4.3	3.8	7.0	3.5	6.8	0.117
350450009	Bloomfield	10	62.7	64.3	1.6	3.1	2.5	5.0	2.3	5	0.624
350450018	Navajo Lake	10	62.9	62.5	-0.4	3.8	-0.6	6.1	-0.9	6.1	0.177
350451005	Sub Station	11	62.6	64.6	2.1	4.8	3.3	7.6	2.8	7.4	0.457
350490021	Santa Fe Airport	12	62.9	61.8	-1.1	4.2	-1.7	6.7	-2.1	7	0.373
350610008	Los Lunas	17	62.9	58.8	-4.1	4.7	-6.5	7.5	-6.9	7.9	0.167

Time series of predicted and observed MDA8 ozone concentrations at five representative sites (Bloomfield, Coyote Ranger, South Valley, Desert View and Carlsbad) are shown in Figure 7-6 to Figure 7-10. Time series sites for all sites are contained in Appendix A. Each time series plot consists of two panels: an upper panel that shows the predicted (blue) and observed (red) daily MDA8 ozone concentrations

from May 15 to August 31, 2014; and a bottom panel that shows the difference (i.e., daily bias) in the daily predicted and observed MDA8 ozone concentrations. At the Bloomfield monitor in San Juan County in northern New Mexico, the predicted and observed MDA8 ozone concentrations match each other remarkably well in May and June and into the first part of July. However, by mid-July the model estimates a series of three mini ozone episodes at the end of July, beginning of August and mid-August that are not reflected in the observations.

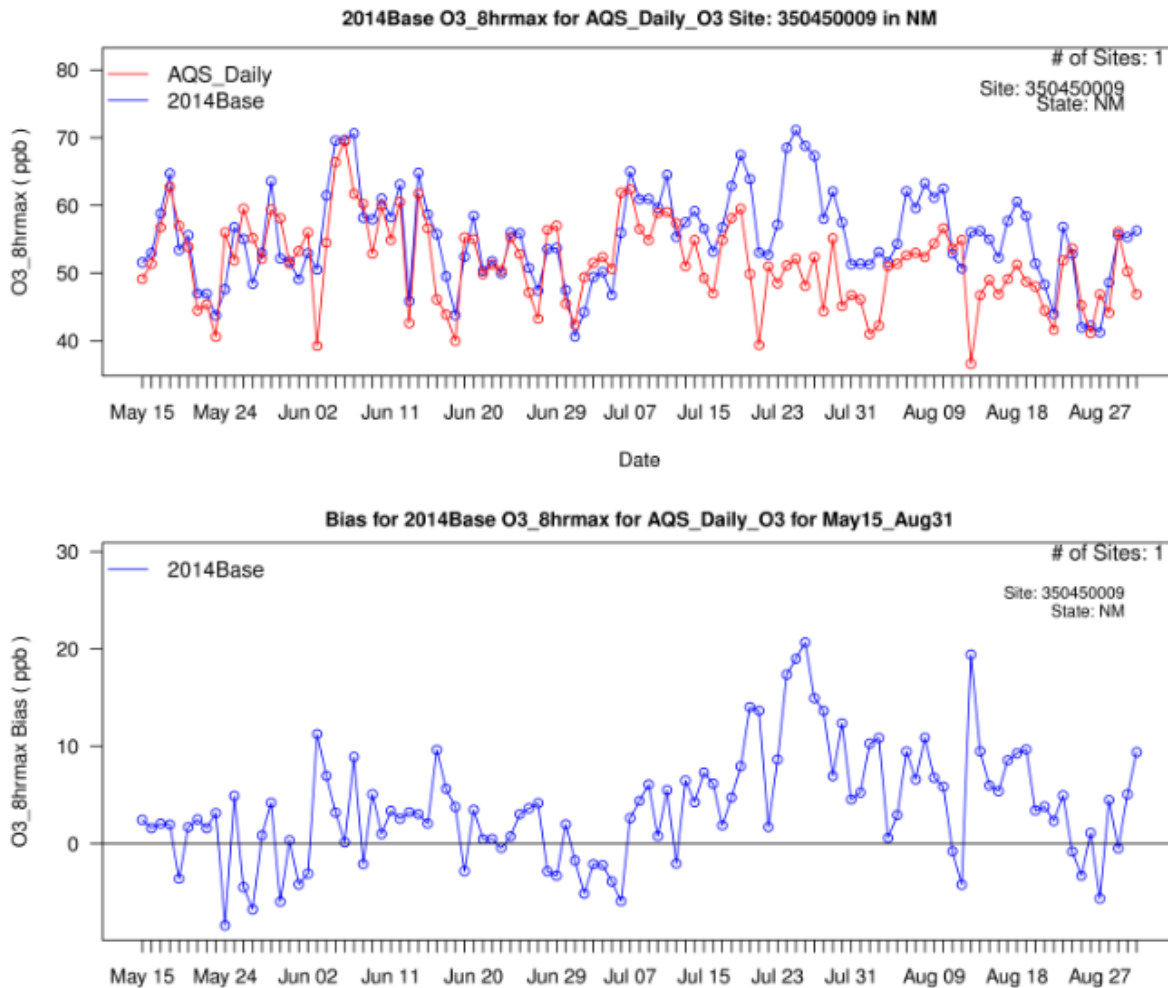


Figure 7-6. Time series of predicted and observed MDA8 ozone concentrations (ppb; top) and daily bias (ppb; bottom) at Bloomfield monitoring site (Site ID: 350450009).

The MDA8 ozone times series Coyote Ranger District site in Rio Arriba County shown in Figure 7-7 shares many of the same characteristics seen at Bloomfield. Extremely good daily MDA8 ozone performance is seen in May and June and the beginning of July. A third of the way into July, however, the model starts to exhibit an ozone overestimation bias with ozone peaks that are 10-20 ppb greater than observed, although better daily ozone performance is seen at Coyote Ranger District the end of August.

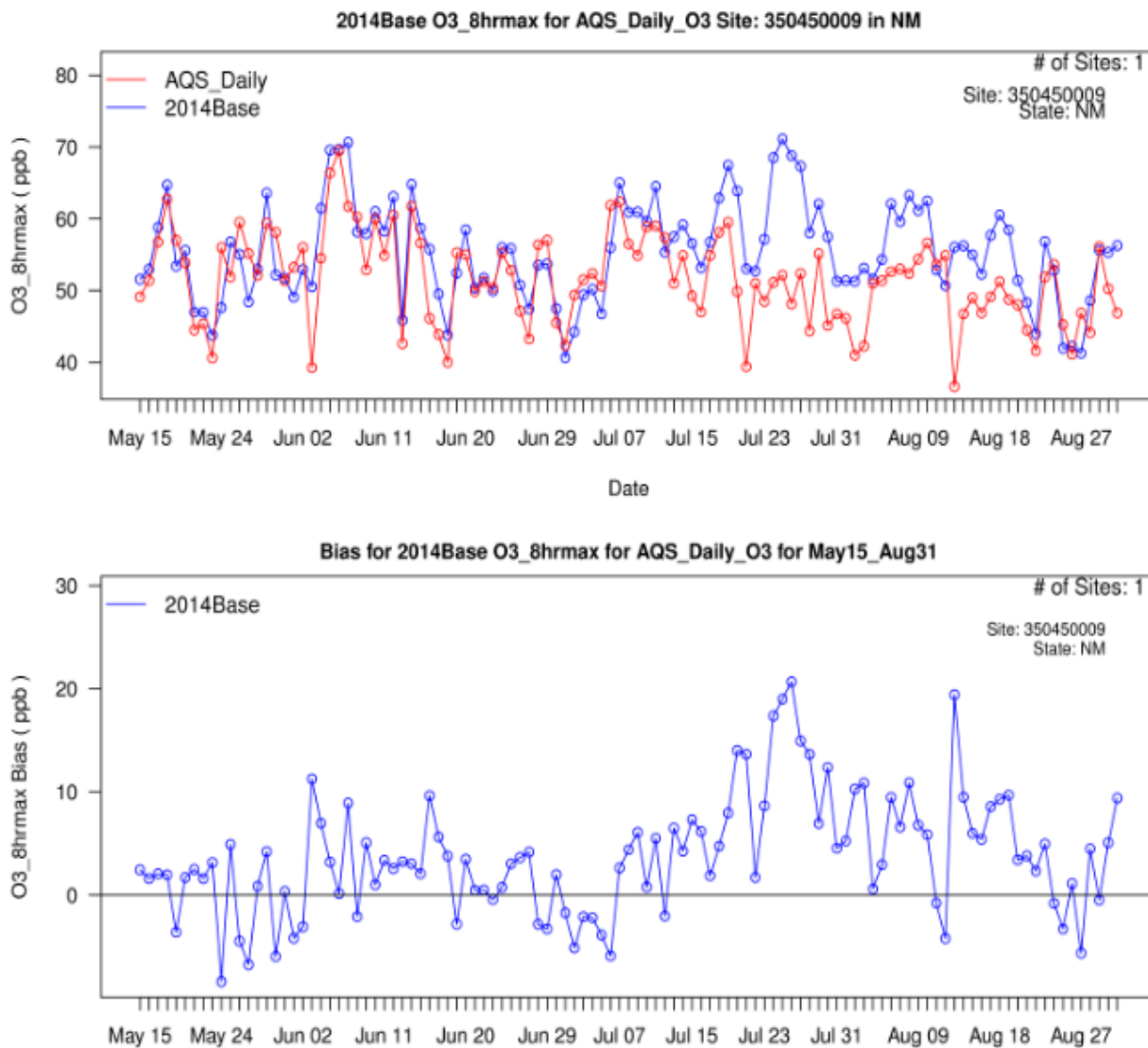


Figure 7-7. Time series of predicted and observed MDA8 ozone concentrations (ppb; top) and daily bias (ppb; bottom) at Coyote Ranger monitoring site (Site ID: 350390026).

The ozone time series at the South Valley site in Bernalillo County is fairly good throughout the May to August episode (Figure 7-8). The daily bias is almost always within $\pm 10\%$ and usually lower than that. The July-August systematic ozone estimation seen at the two northern New Mexico sites is not present, although there is a hint of that phenomena in mid-August.

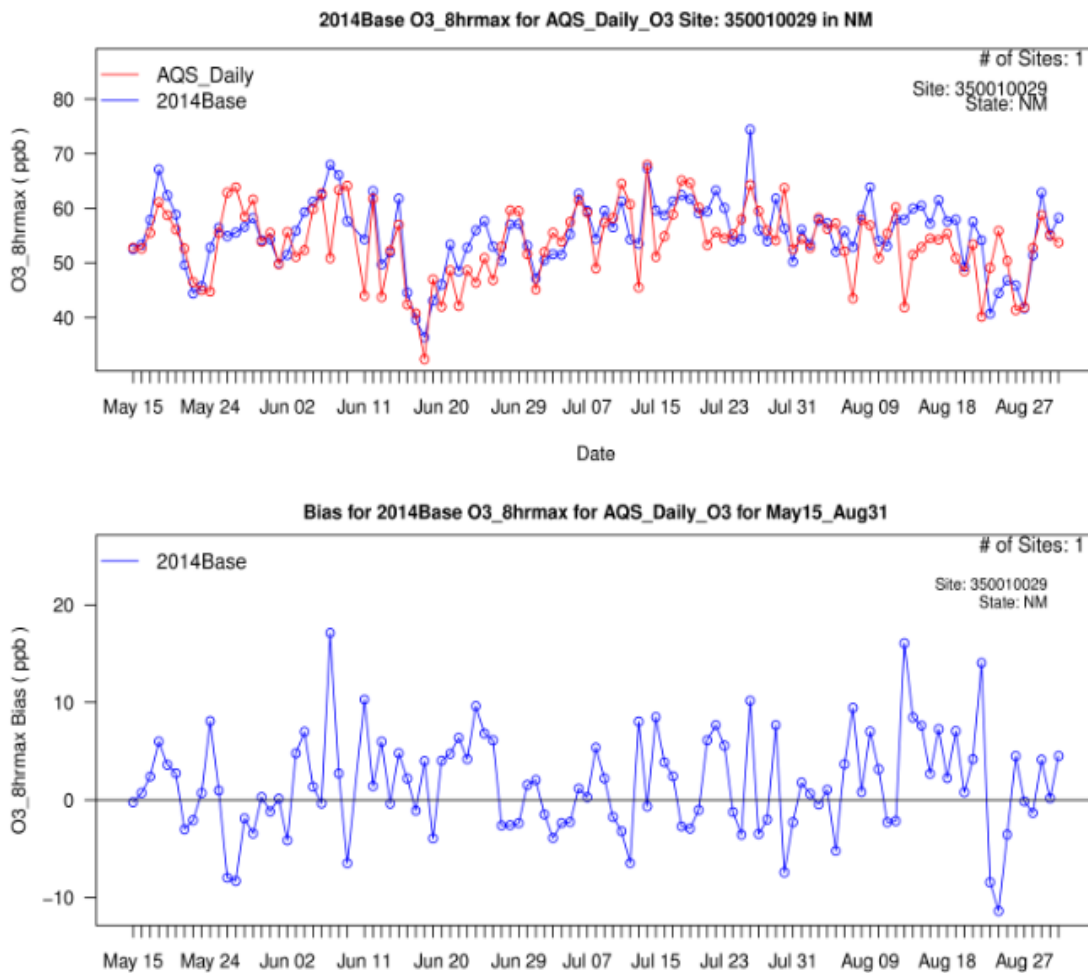


Figure 7-8. Time series of predicted and observed MDA8 ozone concentrations (ppb; top) and daily bias (ppb; bottom) at South Valley monitoring site (Site ID: 350010029).

The observed high MDA8 ozone concentrations at the Desert View monitoring site in Dona Ana County occur as ozone spikes that are a day or two in duration (Figure 7-9). In general, the model follows the observed daily variation on the observed MDA8 ozone concentrations well except for not capturing the observed ozone spikes during May, June and the first part of July. However, for the second half of July and in August the model does a good job in reproducing the observed ozone spikes at Desert View.

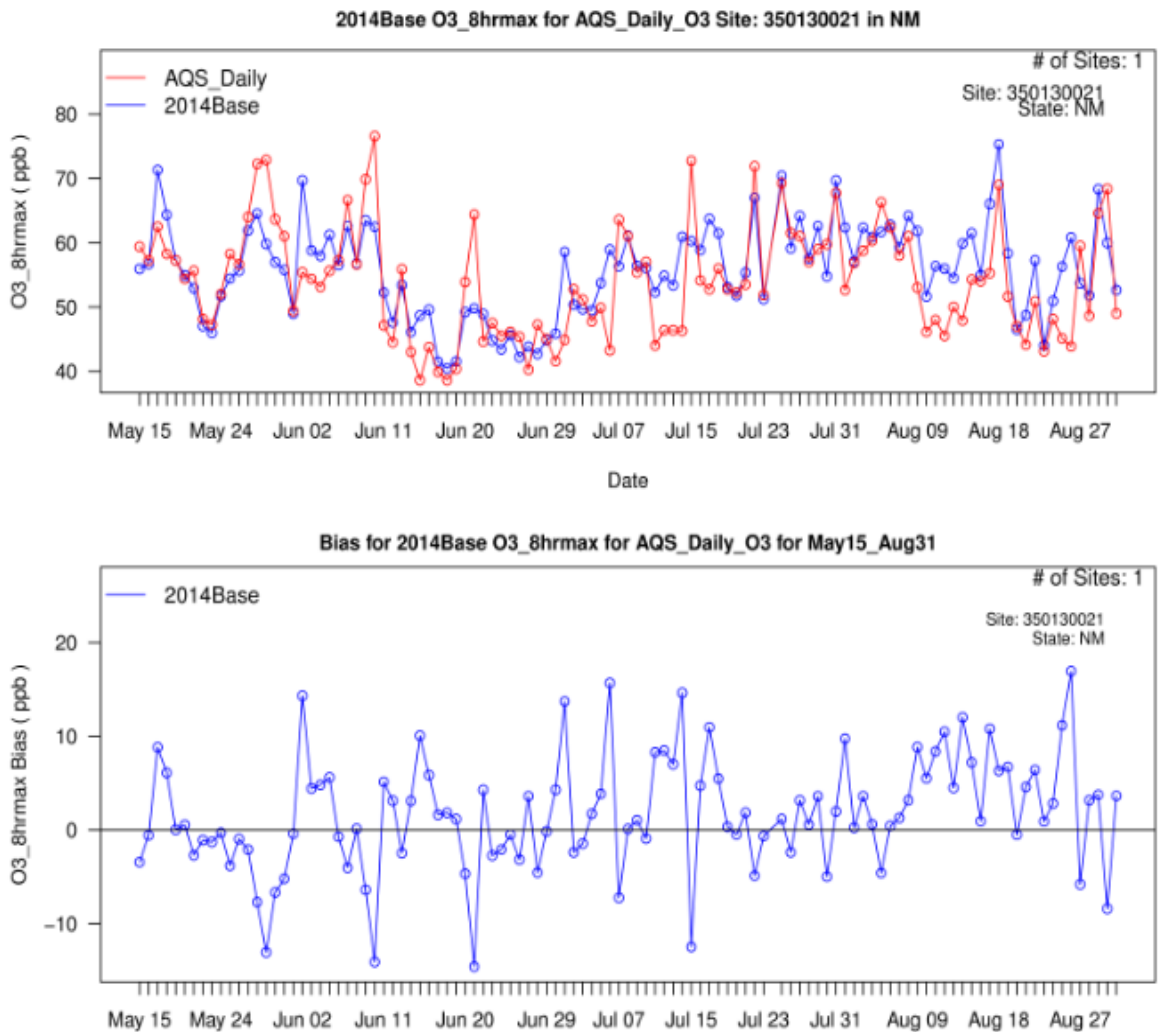


Figure 7-9. Time series of predicted and observed MDA8 ozone concentrations (ppb; top) and daily bias (ppb; bottom) at Desert View monitoring site (Site ID: 350130021).

The observed MDA8 ozone episode during May 29 to June 1 at the Carlsbad site in Eddy County in southeast New Mexico is completely missed by the model (Figure 7-10). Better performance is seen the remainder of the modeling period, although the model misses high ozone periods the end of July and early August. There is also a lot of missing observed data in August, which is unfortunate given the potential presence of high observed ozone during this period based on the data at Desert View.

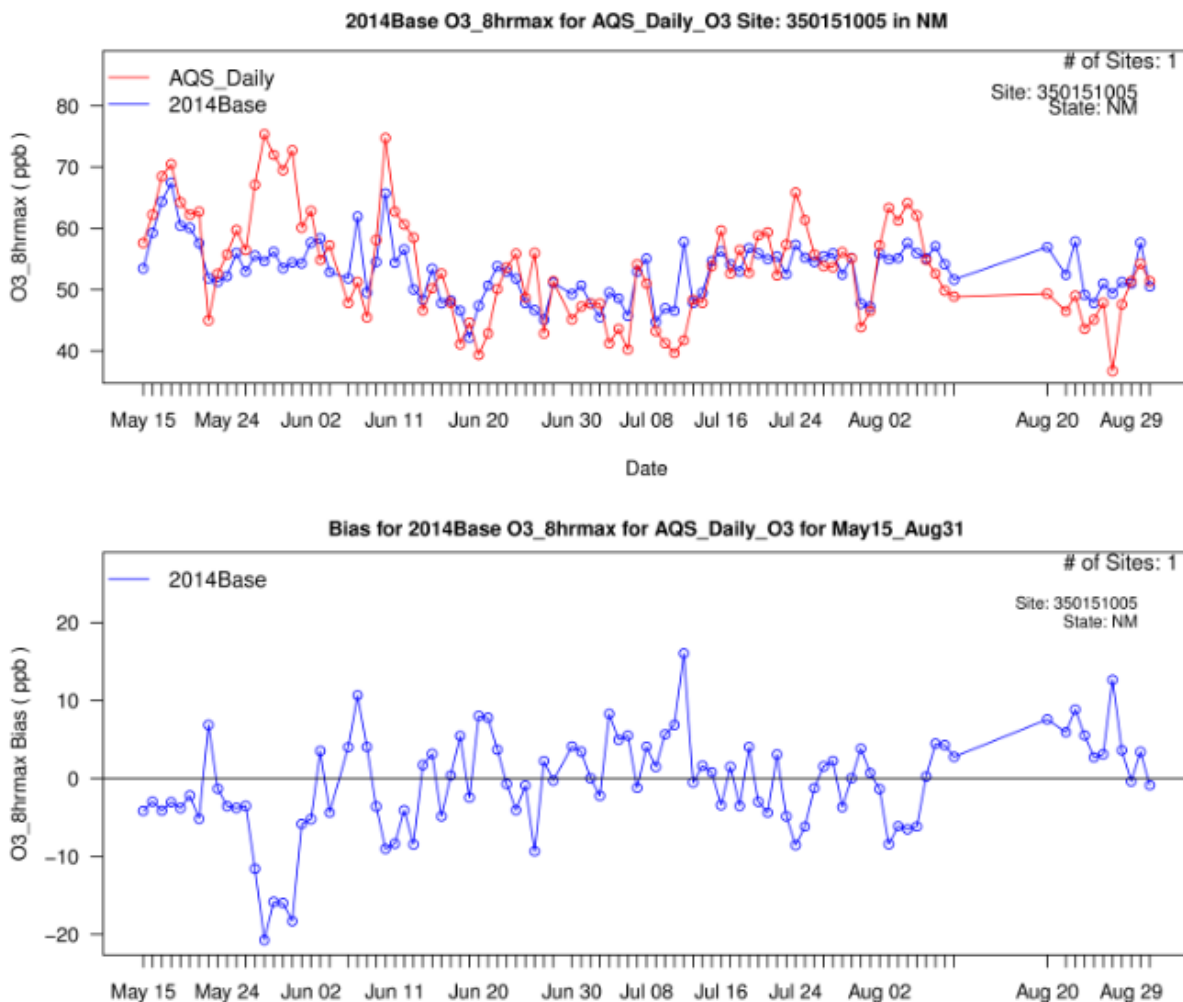


Figure 7-10. Time series of predicted and observed MDA8 ozone concentrations (ppb; top) and daily bias (ppb; bottom) at Carlsbad monitoring site (Site ID: 350151005).

7.8 Ozone Performance Related to Future Year Ozone Projections

EPA’s ozone modeling guidance (EPA, 2018d) recommends making future year ozone design value projections using the relative changes in the future year to base year modeled MDA8 ozone concentrations for the 10 highest base year modeled MDA8 ozone concentrations. Thus, the model performance of the CAMx 2014 base case simulation for the 10 highest modeled ozone concentrations is of particular importance. In this

section we examine this issue for three sites: Bloomfield in San Juan County; Desert View in Dona Ana County; and Carlsbad in Eddy County.

7.8.1 Bloomfield Top 10 Ozone Performance

Table 7-2 displays the CAMx 2014 base case 36 highest modeled MDA8 ozone days at Bloomfield with concurrent observed MDA8 ozone, and the bias presented as concentration and percent. The observed top 20 highest MDA8 ozone concentrations are colored yellow, with the darker yellow indicating an observed top 10 MDA8 ozone concentration day. The 10 highest modeled MDA8 ozone concentrations at Bloomfield are also top 20 observed MDA8 ozone days for 6 of the 10 days; the top 10 observed MDA8 ozone concentration days occurring on 5 of the top 10 modeled ozone days. So, there is a good overlap of the top 10 modeled and top 20 observed highest MDA8 ozone days at Bloomfield.

The red shading on the bias percent in Table 7-2 indicates days in the top 10 modeled ozone days whose daily bias exceeds $\pm 10\%$. An alternative future year ozone design value projection approach to the EPA-recommended modeled top 10 MDA8 ozone days is to use the top 10 modeled ozone days that meet a model performance requirement, such as within $\pm 10\%$ of the observed value. With a 10% MPE criteria projection approach, the additional days used to replace those whose bias exceeds $\pm 10\%$ (i.e., shaded red) are colored blue in Table 7-2. Under the 10% MPE criteria projection approach, the 10 modeled days used in the projection all overlap with the top 20 observed ozone days and 7 of the days are a top 10 observed MDA8 ozone day.

This analysis indicates that the model performance on the modeled top 10 days used for making ozone projections at Bloomfield is quite reasonable and has good overlap with the observed highest ozone days.

Table 7-6. Predicted and observed MDA8 ozone concentrations (ppb) at Bloomfield for CAMx 2014 base case for modeled ranked 36 highest MDA8 ozone concentrations.

Bloomfield	Obs	Prd	Bias	%
7/25/2014	52.1	71.1	19.0	36.4%
6/7/2014	61.7	70.6	8.9	14.4%
6/6/2014	69.5	69.7	0.2	0.2%
6/5/2014	66.4	69.6	3.2	4.8%
7/26/2014	48.1	68.8	20.7	42.9%
7/24/2014	51.1	68.5	17.4	34.0%
7/19/2014	59.5	67.5	8.0	13.4%
7/27/2014	52.4	67.3	14.9	28.5%
7/7/2014	62.4	65.0	2.6	4.2%
6/14/2014	61.8	64.8	3.0	4.9%
5/18/2014	62.8	64.7	2.0	3.1%
7/11/2014	59.0	64.5	5.5	9.3%
7/20/2014	49.9	63.9	14.0	28.1%
5/29/2014	59.4	63.6	4.2	7.1%
8/8/2014	52.4	63.3	10.9	20.8%
6/12/2014	60.5	63.1	2.6	4.3%
7/18/2014	58.1	62.9	4.7	8.2%
8/10/2014	56.6	62.5	5.9	10.4%
8/6/2014	52.6	62.1	9.5	18.0%
7/29/2014	55.1	62.1	6.9	12.6%
6/4/2014	54.5	61.5	7.0	12.8%
8/9/2014	54.4	61.2	6.8	12.5%
6/10/2014	60.0	61.0	1.0	1.7%
7/9/2014	54.9	60.9	6.1	11.1%
7/8/2014	56.5	60.9	4.4	7.8%
8/18/2014	51.3	60.5	9.3	18.1%

7.8.2 Desert View Top 10 Ozone Performance

The evaluation of the CAMx 2014 base case for the top 10 modeled MDA8 ozone concentrations at Desert View is shown in Table 7-3. 7 of the top 10 modeled MDA8 ozone concentrations are also top 20 observed ozone days, with 5 of those days also being in the top 10 observed ozone days. Thus, there is good overlap between the highest modeled and observed ozone days at Desert View. 5 of the top 10 modeled ozone days have daily bias that does not meet a within $\pm 10\%$ performance criteria. Imposing a within $\pm 10\%$ performance criteria for selecting the top 10 modeled ozone days results in all 10 days overlapping with observed days in the top 20 of the observed distribution with 7 of those days being top 10 observed ozone days.

Table 7-7. Predicted and observed MDA8 ozone concentrations (ppb) at Desert View for CAMx 2014 base case for modeled ranked 36 highest MDA8 ozone concentrations.

Desert View	Obs	Prd	Bias	%
8/18/2014	69.0	75.3	6.3	9.1%
5/17/2014	62.5	71.3	8.8	14.1%
7/25/2014	69.3	70.4	1.2	1.7%
6/2/2014	55.4	69.7	14.3	25.8%
7/31/2014	67.7	69.7	2.0	2.9%
8/29/2014	64.6	68.3	3.7	5.8%
7/22/2014	71.9	67.0	-4.9	-6.8%
8/17/2014	55.3	66.0	10.8	19.5%
5/28/2014	72.3	64.5	-7.7	-10.7%
5/18/2014	58.3	64.3	6.1	10.4%
8/8/2014	61.0	64.2	3.2	5.2%
7/27/2014	61.0	64.1	3.1	5.2%
7/17/2014	52.8	63.7	10.9	20.7%
6/9/2014	69.9	63.5	-6.4	-9.2%
8/6/2014	62.4	62.8	0.4	0.7%
7/29/2014	59.0	62.6	3.6	6.1%
6/7/2014	66.6	62.6	-4.0	-6.1%
6/10/2014	76.6	62.5	-14.1	-18.4%
8/1/2014	52.6	62.4	9.7	18.5%
8/3/2014	58.8	62.3	3.6	6.1%
5/27/2014	64.0	61.9	-2.1	-3.3%
8/9/2014	53.0	61.8	8.8	16.7%
8/5/2014	66.3	61.7	-4.6	-6.9%
8/15/2014	54.3	61.5	7.2	13.2%
7/18/2014	56.0	61.5	5.5	9.8%
6/5/2014	55.6	61.2	5.6	10.0%

7.8.3 Carlsbad Top 10 Ozone Performance

6 of the top 10 modeled ozone days at Carlsbad occur during observed top 20 ozone days, 4 of those days within the top 10 of the observed ozone distribution (Table 7-4). Five of the modeled top 10 ozone days have bias that does not achieve the within $\pm 10\%$ criteria. When imposing the within $\pm 10\%$ performance criteria for the top 10 modeled ozone days, 7 of those days overlap with observed top 20 days.

Table 7-8. Predicted and observed MDA8 ozone concentrations (ppb) at Carlsbad for CAMx 2014 base case for modeled ranked 36 highest MDA8 ozone concentrations.

Carlsbad	Obs	Prd	Bias	%
5/18/2014	70.5	67.5	-3.0	-4.3%
6/10/2014	74.8	65.7	-9.0	-12.1%
5/17/2014	68.5	64.4	-4.1	-6.0%
6/7/2014	51.3	61.9	10.7	20.8%
5/19/2014	64.3	60.5	-3.8	-5.9%
5/20/2014	62.3	60.1	-2.2	-3.5%
5/16/2014	62.3	59.3	-3.0	-4.8%
6/3/2014	54.9	58.4	3.5	6.5%
8/23/2014	49.0	57.9	8.9	18.1%
7/12/2014	41.8	57.8	16.1	38.5%
6/2/2014	62.9	57.7	-5.2	-8.3%
8/30/2014	54.3	57.7	3.4	6.3%
8/5/2014	64.1	57.6	-6.5	-10.1%
5/21/2014	62.8	57.6	-5.2	-8.2%
7/24/2014	65.9	57.3	-8.5	-13.0%
8/8/2014	52.6	57.1	4.5	8.5%
8/20/2014	49.4	57.0	7.6	15.4%
7/19/2014	52.8	56.8	4.1	7.7%
6/12/2014	60.7	56.6	-4.1	-6.7%
7/16/2014	59.7	56.3	-3.4	-5.7%
5/29/2014	72.0	56.2	-15.8	-22.0%
5/25/2014	59.8	56.0	-3.8	-6.3%
8/6/2014	62.1	56.0	-6.2	-9.9%
7/28/2014	53.7	55.9	2.3	4.2%
8/2/2014	57.3	55.9	-1.3	-2.4%
7/20/2014	58.9	55.9	-3.0	-5.1%

8. SUMMARY AND CONCLUSIONS

The evaluation of the NM OAI Study CAMx 2014 base case simulation focused on Maximum Daily 8-hour Average (MDA8) ozone model performance across all sites in the 4-km New Mexico domain, across all sites within New Mexico, within three subregions in New Mexico (northern, Bernalillo County, and southern) and at individual sites in New Mexico. When examining MDA8 ozone performance across groups of sites, the CAMx 2014 base case always achieves the ozone performance criteria and usually achieves the ozone performance goals. When examining MDA8 ozone performance across all observations, the model tended to have an ozone overestimation tendency but still always achieved the bias performance criteria ($\leq \pm 15\%$) and usually achieved the bias performance goal ($\leq \pm 5\%$). When comparing the model's ability to reproduce the highest observed ozone concentrations greater than 60 ppb, the model still always achieved the bias performance criteria and usually achieved the bias performance goal, albeit with an underestimation tendency. The MDA8 ozone error essentially always achieves the performance goal whether examining all ozone observations or just those observations greater than 60 ppb. More specifically:

- Across the 4-km New Mexico domain for all ozone observations, the Normalized Mean Bias (NMB) for the AQS network was 6.2% that achieves the bias performance criteria but not the bias performance goal. However, across the more rural CASTNet network the NMB (0.1%) is near zero achieving the performance goal.
- With New Mexico, the NMB achieves the performance goal whether using all ozone data (5.0%) or just ozone data when the observed ozone is greater than 60 ppb (-4.3%).
- Similar performance attributes are seen in the New Mexico subregional evaluation whether using all data or the 60 ppb ozone cut-off with the NMB in the northern New Mexico (4.3% and 0.0%) and Bernalillo County (4.3% and -2.8%) subregions achieving the bias performance goal. However, the NMB in the southern New Mexico region (5.8% and -6.1%) just barely falls outside of the performance goal region, but achieves the performance criteria.
- At individual monitoring sites using all ozone data the NMB achieves the bias performance criteria at all sites but one (La Union) with a majority of the sites (13 of 22 or 59%) also achieving the bias performance goal.
- The time series of predicted and observed MDA8 ozone concentrations shows that the model has very good agreement and tracks the day-to-day variations of the observed ozone in the northern New Mexico and Bernalillo County sites for the first half of the May-August 2014 modeling period. The second half of the modeling period the model generally has an ozone overestimation tendency at the northern New Mexico sites.
- Time series at the southern New Mexico show that the model has difficulty in reproducing the observed daily ozone spikes in the first half of the modeling period, but does a better job in reproducing the daily observed high ozone concentrations in the second half of the episode.

An evaluation of the model performance for the top 10 modeled ozone days that are used for making future year ozone projections reveals that they are also high observed ozone days over half of the time.

In conclusion, the NM OAI Study CAMx 2014 base case ozone model performance within New Mexico is as good or better than most recent PGM applications (e.g., WRAP-WAQS, EPA 2016v1 and Denver ozone SIP) and appears to be a reliable PGM modeling platform for evaluating emission reduction strategies for reducing ozone concentrations in New Mexico.

9. REFERENCES

- Abt. 2014. Modeled Attainment Test Software – User’s Manual. Abt Associates Inc., Bethesda, MD. April. (http://www.epa.gov/ttn/scram/guidance/guide/MATS_2-6-1_manual.pdf).
- Adelman, Z. 2004. Quality Assurance Protocol – WRAP RMC Emissions Modeling with SMOKE, Prepared for the WRAP Modeling Forum by the WRAP Regional Modeling Center, Riverside, CA.
- Appel, W., R. Gilliam, N. Davis, A. Zubrow, and S. Howard. 2011. Overview of the atmospheric model evaluation tool (AMET) v1.1 for evaluating meteorological and air quality models. *Environmental Modeling & Software*. 26. 434-443. 10.1016/j.envsoft.2010.09.007.
- Boylan, J. W. 2004. Calculating Statistics: Concentration Related Performance Goals, paper presented at the EPA PM Model Performance Workshop, Chapel Hill, NC. 11 February.
- Boylan, J. W. and A. G. Russell. 2006. PM and light extinction model performance metrics, goals, and criteria for three-dimensional air quality models. *Atmos. Env.* Vol. 40, Issue 26, pp. 4946-4959. August. (<https://www.sciencedirect.com/science/article/pii/S1352231006000690>).
- Coats, C.J. 1995. Sparse Matrix Operator Kernel Emissions (SMOKE) Modeling System, MCNC Environmental Programs, Research Triangle Park, NC.
- Colella, P., and P.R. Woodward. 1984. The Piecewise Parabolic Method (PPM) for Gas-dynamical Simulations. *J. Comp. Phys.*, **54**, 174201.
- Daley, C., M. Halbleib, J. Smith, W. Gibson, M. Doggett, G. Taylor, J. Curtis and P. Pasteris. 2008. Physiographically sensitive mapping of climatological temperature and precipitation across the conterminous United States. *Intl. J. Climate*. (http://prism.oregonstate.edu/documents/Daly2008_PhysiographicMapping_IntlClim.pdf).
- Emery, C., E. Tai, and G. Yarwood. 2001. Enhanced Meteorological Modeling and Performance Evaluation for Two Texas Episodes, report to the Texas Natural Resources Conservation Commission, prepared by ENVIRON, International Corp, Novato, CA.
- Emery, C.A., E. Tai, E., R. E. Morris, G. Yarwood. 2009a. Reducing Vertical Transport Over Complex Terrain in CMAQ and CAMx. AWMA Guideline on Air Quality Models Conference, Raleigh, NC, October 26-30, 2009.
- Emery, C.A., E. Tai, R.E. Morris, G. Yarwood. 2009b. Reducing Vertical Transport Over Complex Terrain in Photochemical Grid Models. 8th Annual CMAS Conference, Chapel Hill, NC, October 19-21, 2009.
- Emery, C., E. Tai, G. Yarwood and R. Morris. 2011. Investigation into approaches to reduce excessive vertical transport over complex terrain in a regional photochemical grid model. *Atmos. Env.*, Vol. 45, Issue 39, December 2011, pp. 7341-7351. (<http://www.sciencedirect.com/science/article/pii/S1352231011007965>).

- Emery, C.E., Z. Liu, A.G. Russell, M.T. Odman, G. Yarwood and N. Kumar. 2016. Recommendations on statistics and benchmarks to assess photochemical model performance. *J. of the Air and Waste Management Assoc.*, Vol. 67, Issue 5. DOI: 10.1080/10962247.2016.1265027. (<https://www.tandfonline.com/doi/full/10.1080/10962247.2016.1265027>).
- EPA. 1991. Guidance for Regulatory Application of the Urban Airshed Model (UAM). Office of Air Quality Planning and Standards, U.S. Environmental Protection Agency, Research Triangle Park, N.C.
- EPA. 1999. Draft Guidance on the Use of Models and Other Analyses in Attainment Demonstrations for the 8-hr Ozone NAAQS". U.S. Environmental Protection Agency, Office of Air Quality Planning and Standards, Research Triangle Park, N.C. May.
- EPA. 2001. Guidance Demonstrating Attainment Air Quality Goals for PM_{2.5} and Regional Haze. Draft Final. U.S. Environmental Protection Agency, Atmospheric Sciences Modeling Division, Research Triangle Park, N.C.
- EPA. 2015a. Recommendations for Evaluating the Performance of the 3SAQS Photochemical Grid Model Platform. U.S. Environmental Protection Agency, Region 8. April 2. (http://vibe.cira.colostate.edu/wiki/Attachments/Modeling/DRAFT_EPAR8_Recommended_PGM_MPE_Analyses_3SAQS_04022015.pdf).
- EPA. 2016c. Air Quality Modeling Technical Support Document for the Final Cross State Air Pollution Rule Update. U.S. Environmental Protection Agency, Office of Air Quality Planning and Standards. Research Triangle Park, NC. August. (https://www.epa.gov/sites/production/files/2017-05/documents/aq_modeling_tsd_final_csapr_update.pdf).
- EPA. 2017a. Revisions to the Guideline on Air Quality Models: Enhancements to the AERMOD Dispersion Modeling System and Incorporation of Approaches To Address Ozone and Fine Particulate Matter. 40 CFR Part 51 [EPA-HQ-OAR-2015-0310; FRL-9956-23- OAR]. Federal Register / Vol. 82, No. 10 / Tuesday, January 17, 2017 / Rules and Regulations. (https://www3.epa.gov/ttn/scram/appendix_w/2016/AppendixW_2017.pdf).
- EPA. 2017b. Emissions Inventory Guidance for Implementation of Ozone and Particulate Matter National Ambient Air Quality Standards (NAAQS) and Regional Haze Regulations. U.S. Environmental Protection Agency, Office of Air Quality Planning and Standards, Air Assessment Division. Research Triangle Park, NC. EPA-454/B-17-003. July. (https://www.epa.gov/sites/production/files/2017-07/documents/ei_guidance_may_2017_final_rev.pdf).
- EPA. 2017c. Use of Photochemical Grid Models for Single-Source Ozone and secondary PM_{2.5} impacts for Permit Program Related Assessments and for NAAQS Attainment Demonstrations for Ozone, PM_{2.5} and Regional Haze. Memorandum from Tyler Fox, Group Leader, Air Quality Modeling Group. U.S. Environmental Protection Agency, Office of Air Quality Planning and Standards. August 4. (https://www3.epa.gov/ttn/scram/guidance/clarification/20170804-Photochemical_Grid_Model_Clarification_Memo.pdf).
- EPA. 2017d. Implementation of the 2015 National Ambient Air Quality Standards for Ozone: Nonattainment Area State Implementation Plan Requirements. Federal

- Register / Vol. 83, No. 234 / Thursday, December 6, 2018 / Rules and Regulations. 40 CFR Part 51, [EPA-HQ-OAR-2016-0202; FRL-9986-53-OAR]. (<https://www.gpo.gov/fdsys/pkg/FR-2018-12-06/pdf/2018-25424.pdf>).
- EPA. 2017e. Emissions Inventory Guidance for Implementation of Ozone and Particulate Matter National Ambient Air Quality Standards (NAAQS) and Regional Haze Regulations. U.S. Environmental Protection Agency, Office of Air Quality Planning and Standards, Air Assessment Division. Research Triangle Park, NC. EPA-454/B-17-003. July. (https://www.epa.gov/sites/production/files/2017-07/documents/ei_guidance_may_2017_final_rev.pdf).
- EPA. 2018a. Implementation of the 2015 National Ambient Air Quality Standards for Ozone: Nonattainment Area State Implementation Plan Requirements, Final Rule. 40 CFR Part 51, [EPA-HQ-OAR-2016-0202; FRL- -OAR] RIN 2060-AS82. U.S. Environmental Protection Agency. Signed November 7, 2018. (https://www.epa.gov/sites/production/files/2018-11/documents/2015_ozone_srr_final_preamble_20181101.pdf).
- EPA. 2018b. Additional Air Quality Designations for the 2015 Ozone National Ambient Air Quality Standards, Final Rule. U.S. Environmental Protection Agency. Federal Register / Vol. 83, No. 107 / Monday, June 4, 2018 / Rules and Regulations. 40 CFR Part 81; [EPA-HQ-OAR-2017-0548; FRL-9977-72-OAR]; RIN 2060-AT94. (<https://www.govinfo.gov/content/pkg/FR-2018-06-04/pdf/2018-11838.pdf>).
- EPA. 2018c. Determinations of Attainment by the Attainment Date, Extensions of the Attainment Date, and Reclassification of Several Areas Classified as Moderate for the 2008 Ozone National Ambient Air Quality, Proposed Rule. U.S. Environmental Protection Agency. Federal Register /Vol. 83, No. 220 /Wednesday, November 14, 2018 / Proposed Rules. 40 CFR Parts 52 and 81; [EPA-HQ-OAR-2018-0226; FRL-9986-44-OAR]; RIN 2060-AT97. (<https://www.govinfo.gov/content/pkg/FR-2018-11-14/pdf/2018-24816.pdf>).
- EPA. 2018d. Modeling Guidance for Demonstrating Air Quality Goals for Ozone, PM_{2.5}, and Regional Haze. U.S. Environmental Protection Agency, Office of Air Quality Planning and Standards, Air Assessment Division. Research Triangle Park, NC. EPA 454/R-18-009. November 29. (https://www3.epa.gov/ttn/scram/guidance/guide/O3-PM-RH-Modeling_Guidance-2018.pdf).
- EPA. 2019. Technical Support Document for EPA's Updated 2028 Regional Haze Modeling. U.S. Environmental Protection Agency, Office of Air Quality Planning and Standards. September. (https://www3.epa.gov/ttn/scram/reports/Updated_2028_Regional_Haze_Modeling-TSD-2019.pdf).
- Guenther, A. and C. Wiedinmyer. 2004. User's Guide to the Model of Emissions of Gases and Aerosols from Nature (MEGAN). National Center for Atmospheric Research (NCAR), Boulder, Colorado (http://acd.ucar.edu/~christin/megan1.0_userguide.pdf).
- Guenther, A., X. Jiang, T. Duhl, T. Sakulyanontvittaya, J. Johnson and X. Wang. 2014. MEGAN version 2.10 User's Guide. Washington State University, Pullman, WA. May 12. (http://lar.wsu.edu/megan/docs/MEGAN2.1_User_GuideWSU.pdf).

- Heath, N., J. Pleim, R. Gillian, D. Kang, M. Woody, K. Foley and W. Appel. 2016. Impacts of WRF Lightning Assimilation on Offline CMAQ Simulations. Presented at 2016 CMAS Conference, Chapel Hill, NC. October 24-26. (https://cfpub.epa.gov/si/si_public_record_report.cfm?dirEntryId=335757&Lab=NERL).
- Kalnay, E. et al. 1996. The NCEP/NCAR 40-Year Reanalysis Project. *Bull. Am. Meteorol. Soc.*, 77(3), 437-471. (<https://rda.ucar.edu/datasets/ds090.0/docs/bams/bams1996mar/bams1996mar.pdf>).
- Michalakes, J., J. Dudhia, D. Gill, J. Klemp and W. Skamarock. 1998. Design of a Next-Generation Regional Weather Research and Forecast Model. Mesoscale and Microscale Meteorological Division, National Center for Atmospheric Research, Boulder, CO. (<http://www.mcs.anl.gov/~michalak/ecmwf98/final.html>).
- Michalakes, J., S. Chen, J. Dudhia, L. Hart, J. Klemp, J. Middlecoff and W. Skamarock. 2001. Development of a Next-Generation Regional Weather Research and Forecast Model. Developments in Teracomputing: Proceedings of the 9th ECMWF Workshop on the Use of High Performance Computing in Meteorology. Eds. Walter Zwiefelhofer and Norbet Kreitz. World Scientific, Singapore. Pp. 269-276. (<http://www.mmm.ucar.edu/mm5/mpp/ecmwf01.htm>).
- Michalakes, J., J. Dudhia, D. Gill, T. Henderson, J. Klemp, W. Skamarock and W. Wang. 2004. The Weather Research and Forecast Model: Software Architecture and Performance. Proceedings of the 11th ECMWF Workshop on the Use of High Performance Computing in Meteorology. October 25-29, 2005, Reading UK. Ed. George Mozdzyński. (http://wrf-model.org/wrfadmin/docs/ecmwf_2004.pdf).
- Moore, C.T. et al. 2011. "Deterministic and Empirical Assessment of Smoke's Contribution to Ozone – Final Report. Western Governors' Association, Denver, CO. (https://wraptools.org/pdf/11-1-6-6_final_report_DEASCO3_project.pdf)
- Park, S., J.B. Klemp, and J. Kim, 2019: Hybrid Mass Coordinate in WRF-ARW and Its Impact on Upper-Level Turbulence Forecasting. *Mon. Wea. Rev.*, 147, 971–985, <https://doi.org/10.1175/MWR-D-18-0334.1>.
- Ramboll. 2013. METSTAT Meteorological Model Statistical Evaluation Package. Ramboll, Novato, California. December 9. (<http://www.camx.com/download/support-software.aspx>).
- Ramboll. 2018a. User's Guide Comprehensive Air-quality Model with extensions Version 6.5. Ramboll, Novato, California. April. (http://www.camx.com/files/camxusersguide_v6-10.pdf).
- Ramboll. 2020a. User's Guide Comprehensive Air-quality Model with extensions Version 7.0. Ramboll, Novato, California. May.
- Ramboll and WESTAR. 2020a. New Mexico Ozone Attainment Initiative Photochemical Modeling Study – Draft Modeling Protocol. Ramboll US Corporation, Novato, CA. Western States Air Resources Council, Santa Fe, NM. May. (https://www.wrapair2.org/pdf/NM_OAI_Modeling_Protocol_v5.pdf).
- Ramboll and WESTAR. 2020a. New Mexico Ozone Attainment Initiative Photochemical Modeling Study – Draft Work Plan. Ramboll US Corporation, Novato, CA.

- Western States Air Resources Council, Santa Fe, NM. May.
(https://www.wrapair2.org/pdf/NM_OAI_Work_Plan_v2.pdf).
- RAQC and CDPHE. 2016. State Implementation Plan for the 2008 8-Hour Ozone National Ambient Air Quality Standard. Regional Air Quality Council and Colorado Department of Health and Environment, Air Pollution Control Division. Approved by the Colorado Air Quality Control Commission on November 17, 2018.
(https://raqc.egnyte.com/dl/q5zyuX9QC1/FinalModerateOzoneSIP_2016-11-29.pdf).
- Reddy, P.J. and G.G. Pfister. 2016. Meteorological factors contributing to the interannual variability of midsummer surface ozone in Colorado, Utah, and other western U.S. states. *J. Geo. Res.: Atmospheres* (JGR). 10.1002/2015JD023840. March.
(<https://agupubs.onlinelibrary.wiley.com/doi/epdf/10.1002/2015JD023840>).
- Sakulyanontvittaya, T., G. Yarwood and A. Guenther. 2012. Improved Biogenic Emission Inventories across the West. ENVIRON International Corporation, Novato, CA. March 19.
(http://www.wrapair2.org/pdf/WGA_BiogEmisInv_FinalReport_March20_2012.pdf).
- Simon, H., K. Baker and S. Phillips. 2012. Compilations and Interpretation of Photochemical Model Performance Statistics Published between 2006 and 2012. *Atmos. Env.* 61 (2012) 124-139. December.
(<http://www.sciencedirect.com/science/article/pii/S135223101200684X>).
- Skamarock, W. C. 2004. Evaluating Mesoscale NWP Models Using Kinetic Energy Spectra. *Mon. Wea. Rev.*, Volume 132, pp. 3019-3032. December.
(http://www.mmm.ucar.edu/individual/skamarock/spectra_mwr_2004.pdf).
- Skamarock, W. C., J. B. Klemp, J. Dudhia, D. O. Gill, D. M. Barker, W. Wang and J. G. Powers. 2005. A Description of the Advanced Research WRF Version 2. National Center for Atmospheric Research (NCAR), Boulder, CO. June.
(http://www.mmm.ucar.edu/wrf/users/docs/arw_v2.pdf)
- Skamarock, W. C., J. B. Klemp, J. Dudhia, D. O. Gill, D. M. Barker, M. G. Duda, X-Y. Huang, W. Wang and J. G. Powers. 2008. A Description of the Advanced Research WRF Version 3. National Center for Atmospheric Research (NCAR), Boulder, CO. June.
(<https://opensky.ucar.edu/islandora/object/technotes%3A500/datastream/PDF/view>)
- Skamarock, W. C., J. B. Klemp, J. Dudhia, D. O. Gill, Z. Liu, J. Berner, W. Wang, J. G. Powers, M. G. Duda, D. M. Barker and X-Y. Huang. 2019. A Description of the Advanced Research WRF Model Version 4 (No. NCAR/TN-556+STR). doi:10.5065/1dfh-6p97
(<https://opensky.ucar.edu/islandora/object/technotes%3A576/datastream/PDF/download/citation.pdf>)
- Skamarock, W. C. 2006. Positive-Definite and Monotonic Limiters for Unrestricted-Time-Step Transport Schemes. *Mon. Wea. Rev.*, Volume 134, pp. 2241-2242. June. (http://www.mmm.ucar.edu/individual/skamarock/advect3d_mwr.pdf).
- Stoeckenius, T.E., C.A. Emery, T.P. Shah, J.R. Johnson, L.K. Parker, A.K. Pollack. 2009. Air Quality Modeling Study for the Four Corners Region; Prepared by ENVIRON

- International Corporation, Novato, CA. Prepared for the New Mexico Environment Department, Air Quality Bureau, Santa Fe, NM.
- Stoeckenius, T., T. Olevski and M. Zatkan. 2018. Representativeness of Candidate Modeling Years for the Western U.S. Ramboll, Novato, California. July. (https://www.wrapair2.org/pdf/WESTAR_RTOWG_Representativeness_final.pdf)
- UNC. 2008. Atmospheric Model Evaluation Tool (AMET) User's Guide. Institute for the Environment, University of North Carolina at Chapel Hill. May 30. (https://www.cmascenter.org/amet/documentation/1.1/AMET_Users_Guide_V1.1.pdf).
- UNC. 2018. SMOKE v4.6 User's Manual. University of North Carolina at Chapel Hill, Institute for the Environment. Chapel Hill, North Carolina. September 24. (https://www.cmascenter.org/smoke/documentation/4.6/manual_smokev46.pdf)
- .
- Wesely, M.L. 1989. Parameterization of Surface Resistances to Gaseous Dry Deposition in Regional-Scale Numerical Models. *Atmos. Environ.*, 23, 1293-1304.
- Wiedinmyer, C., T. Sakulyanontvittaya and A. Guenther. 2007. MEGAN FORTRAN code V2.04 User Guide. NCAR, Boulder, CO. October 29. (<http://acd.ucar.edu/~guenther/MEGAN/MEGANguideFORTRAN204.pdf>).
- Yarwood, G., J. Jung, G. Z. Whitten, G. Heo, J. Mellberg and M. Estes. 2010. Updates to the Carbon Bond Mechanism for Version 6 (CB6). 2010 CMAS Conference, Chapel Hill, NC. October. (http://www.cmascenter.org/conference/2010/abstracts/emery_updates_carbon_2010.pdf)
- Zhang, L., S. Gong, J. Padro, L. Barrie. 2001. A size-segregated particle dry deposition scheme for an atmospheric aerosol module. *Atmos. Environ.*, **35**, 549-560.
- Zhang, L., J. R. Brook, and R. Vet. 2003. A revised parameterization for gaseous dry deposition in air-quality models. *Atmos. Chem. Phys.*, **3**, 2067-2082.

Appendix A

Time Series of Predicted and Observed MDA8 Ozone Concentrations at Sites in New Mexico

